ANALYSIS OF THE AUTOMATIC CONTROL OF A PRESSURIZED WATER REACTOR

by

MICHELE MUSCETTOLA

Laurea in Ingegneria Elettrotecnica
Universita' di Napoli
(1959)

SUBMITTED IN PARTIAL FULFILLMENT
OF THE REQUIREMENTS FOR THE
DEGREE OF MASTER OF
SCIENCE

at the

MASSACHUSETTS INSTITUTE OF TECHNOLOGY
February, 1961

Signature of Author .....
Department of Electrical Engineering, December 12, 1960

Certified by .....
Thesis Supervisor

Accepted by .....
Chairman, Departmental Committee on Graduate Students

ABSTRACT

Analysis of the Automatic Control of a Pressurized Water Reactor
by
Michele Muscettola

Submitted to the Department of Electrical Engineering on December 12, 1960, in partial fulfillment of the requirements for the degree of Master of Science.

The object of this thesis is to make a preliminary analysis of the stability of a P.W.R. through a combined analytical and graphical approach.

This method is applied to the study of an actual reactor, the Yankee Reactor.

The procedure used involves 1) making a model for the different components and deriving the transfer function of the linear parts, 2) studying the stability (absolute and relative) by the describing function method since the system is non-linear and of high order.

For the example considered, the system made up of only the essential components is unstable. For this the necessary compensation is derived.

The block diagram of the whole system is quite complex. It is shown however that by the use of reasonable approximations the block diagram can be reduced, making possible the use of a simple graphical method.

There are two advantages to such an approach: 1) it gives a good insight into the dynamic behavior of the system, the elements which influence its stability and the type of compensation required for stabilization or improvement of performance; 2) it can be used in connection with an experimental or analog computer study.

It's disadvantage lies mainly in the limited accuracy of the results due to approximation introduced.

Thesis Supervisor: Elias P. Gyftopoulos
Assistant Professor of Nuclear Engineering

ACKNOWLEDGEMENT

I wish to express my gratitude to Professor Elias P. Gyftopoulos for his suggestions and encouragement during the preparation of this thesis and for supervising it.

I am indebted to Mr. Roger J. Coe, Vice President of the Yankee Atomic Electric Company of Boston for allowing the use of the data of the Yankee Reactor for this thesis and to Mr. John W. Lebourveau and Mr. Lawrence E. Minnick for helping in obtaining the data.

I thank Miss Joan E. Fisher for her typing.

TABLE OF CONTENTS

INTRODUCTION

The object of this thesis is a preliminary analysis of the stability of a pressurized water reactor with automatic feedback control.

This analysis is carried out through a combined analytical and graphical approach. Data obtained from an actual reactor, the Yankee Reactor, were used.

The approach to the problem is: First making a model for the different components and deriving the transfer function for the linear part. Second, studying the stability with the method suggested by Kochenburger[7] since the system considered is quite non-linear and of high degree.

A preliminary analytic study is useful for two reasons.

First, it is possible to have through such a study a greater insight into the dynamic behavior of the system and into the factors which have more influence over its performance.

Second, it gives an indication of what direction has to be followed for the compensation or improvement of the system.

In this thesis the frequency responses of individual or groups of components are the final form in which data are utilized. These frequency responses can be obtained experimentally from the system. The method employed is hence useful whether or not a model of the system is available.

The general block diagram of the system however is so complex that approximations were made. The method of analysis of non-linear systems used yields information on the absolute and relative stability. An analysis of the transient response would involve very cumbersome calculations. Additional information could be obtained much more readily through an analog simulation.

The pressurized water reactors built so far and about which descriptions and data are available, can be divided in two groups: small power (few Mw) and large power (more than 100 Mw) reactors.

The small power reactors have no automatic control at all. As will be shown, PWR's can be built inherently stable and exhibiting

a constant average temperature behavior so that for small power a manual control is satisfactory. On the other hand, all the large power PWR's already constructed or in advanced stage of design are automatically controlled at least at full power.

The two completed units, the Shippingport and the Yankee Reactors, both use a constant average temperature program for the automatic control. In the Shippingport Reactor a damping signal from the neutron flux is also added to the temperature error.

Because of the lack of data and the very small number of units built up to the present it is difficult to assume values of the parameters of the reactor, heat utilizer and control system, which can be considered as really standard, so that the results would have a general character. For this reason the data of only one reactor are used: the Yankee Reactor of the Yankee Atomic Electric Company of Boston. It was preferred to the Shippingport Reactor for its later construction and because no study of its automatic control has been published yet.

This thesis is divided into four chapters. In the first chapter a brief description of the plant is given and the transfer functions of the reactor and heat exchanger reviewed. In the second chapter, models of the automatic control loop components are derived and the complete block diagram of the system drawn. In the third chapter the stability of the reactor with the automatic control loop is investigated. And finally, since the system with only the essential components is unstable, the necessary compensation is considered in the fourth chapter.

CHAPTER I

1.1 Description of the Power Plant[1]

The Yankee Reactor is a heterogeneous slightly enriched (3.4 wt %), pressurized, light water moderated and cooled power reactor. It will produce 480 Mw of heat and 135 Mw of net electrical power. A simplified schematic diagram of the plant is shown in Fig. 1.

The water of the primary coolant system is maintained at the pressure of 2000 psi gauge. The temperature at the inlet in the reactor is 499°F and at the outlet 532°F. These conditions yield 525 psi gauge saturated steam at the outlet of the steam generator.

The core contains 76 assemblies of fuel elements. Each assembly contains 304 or 305 rods made of stainless steel tubes filled with UO_2 pellets. It also contains 24 control rods of Ag-In-Cd alloy and 8 shim rods of boron stainless steel.

The light water circulates in four identical loops. Each loop includes a pipe from the reactor outlet to the steam generator (hot leg), a steam generator, a main coolant pump and a pipe back to the reactor core. Valves are provided to isolate individual loops from the reactor.

To allow variation of volume of the primary loop water, due to changes in the average temperature during load transients, a pressurizer is connected to the four main coolant loops. To maintain the variation of pressure in an acceptable range, a heating system and a spray are located inside the pressurizer.

The steam generators are of the shell and U-tube evaporators type together with three-stage moisture separating equipment.

The pumps are centrifugal and are driven by cammed motors. These pumps are designed to a simple speed operation.

The steam produced in the boilers is sent through adequate piping to the throttle valves of a 145 Mw tandem compound steam turbine with three points of automatic extraction for feed water heating. The steam exhausts to an 85,000 sq. ft. single pass, divided water box condenser. The condensate water from the condenser,

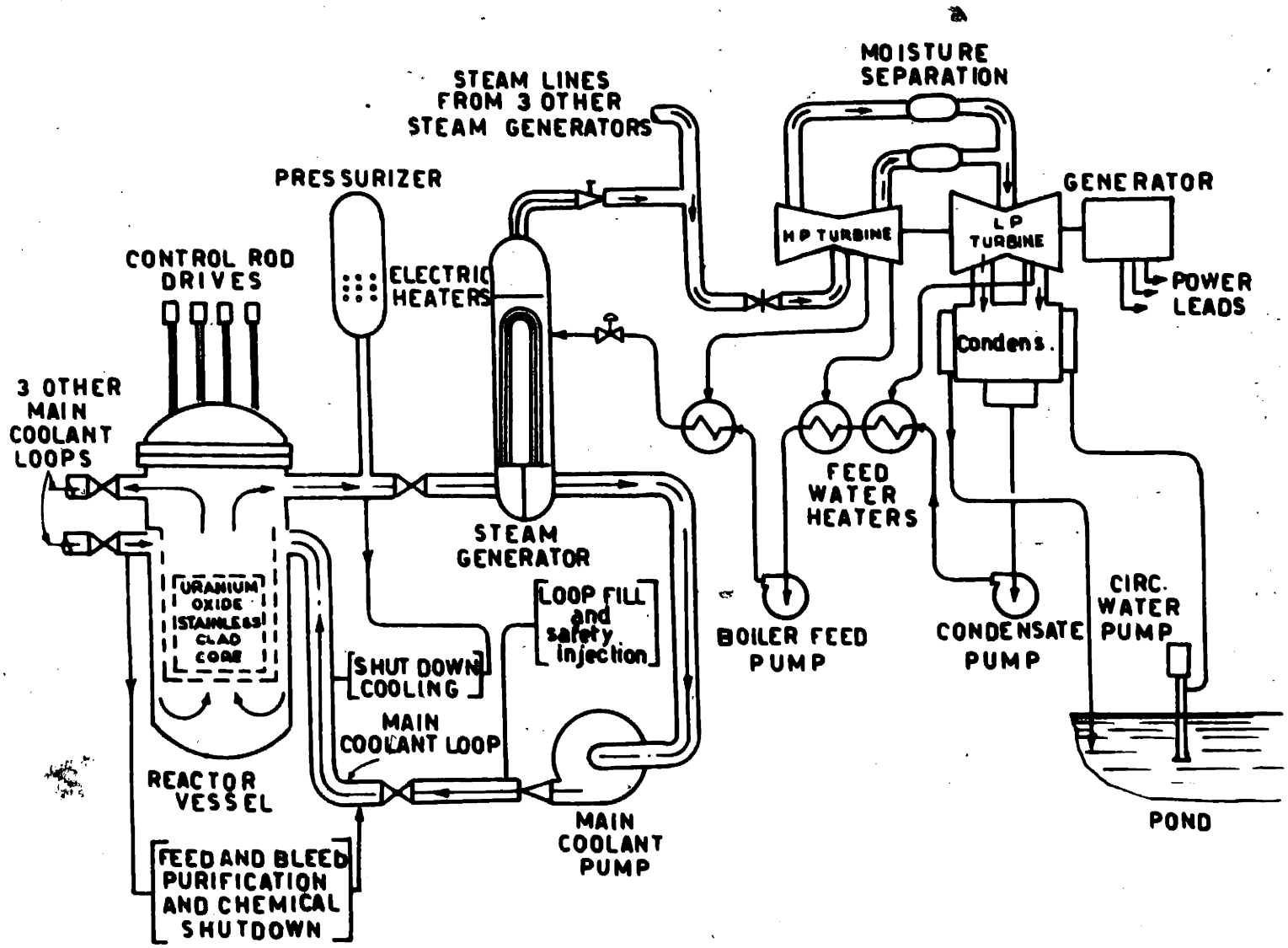

SIMPLIFIELD FLOW DIAGRAM
PRIMARY AND SECONDARY SYSTEMS

FIG. 1

turbine moisture separators, and feed water heaters is sent back to the steam generator by means of pumps through the feed water heaters.

The throttle valves (two single seated, oil operated, spring closing valves) can be operated either manually or by a motor for remote operation. Each of these throttle valves feed two control valves (hydraulically operated, single seated, plug type valves) which are operated in sequence to control steam admission and are actuated either by the turbine speed governor or by throttle pressure regulator.

The turbine drives a 160 KVA, three phase, 60 cycle, 18 KV generator coupled directly to the turbine.

A large complex of apparatus is provided for all the secondary operations necessary both for the nuclear and the conventional section of the plant.

1.2 General Plant Scheme

For the dynamic study, the pressurized water reactor plant can be schematized in its essential elements as in Fig. 2.

Around the reactor core the primary coolant system and the steam generators, two feedback loops (the temperature coefficient feedback and the control system feedback) are closed. The first, due to the temperature reactivity dependence, is an inherent phenomenon in the core. The second is built for regulation purposes. We shall examine them successively in more detail.

1.3 Stability of the Plant Without Control

1.3.1 The temperature reactivity dependence

The temperature dependence of the reactivity in a PWR is characterized through the introduction of two coefficients.

a. The Doppler temperature coefficient which is related to the broadening or narrowing, as the case may be, of the neutron resonance absorption by U-235, U-238 and Pu-239 as the temperature changes. For the Yankee Reactor, it was calculated to be always negative during the core life for the low initial enrichment of the fuel. The calculated

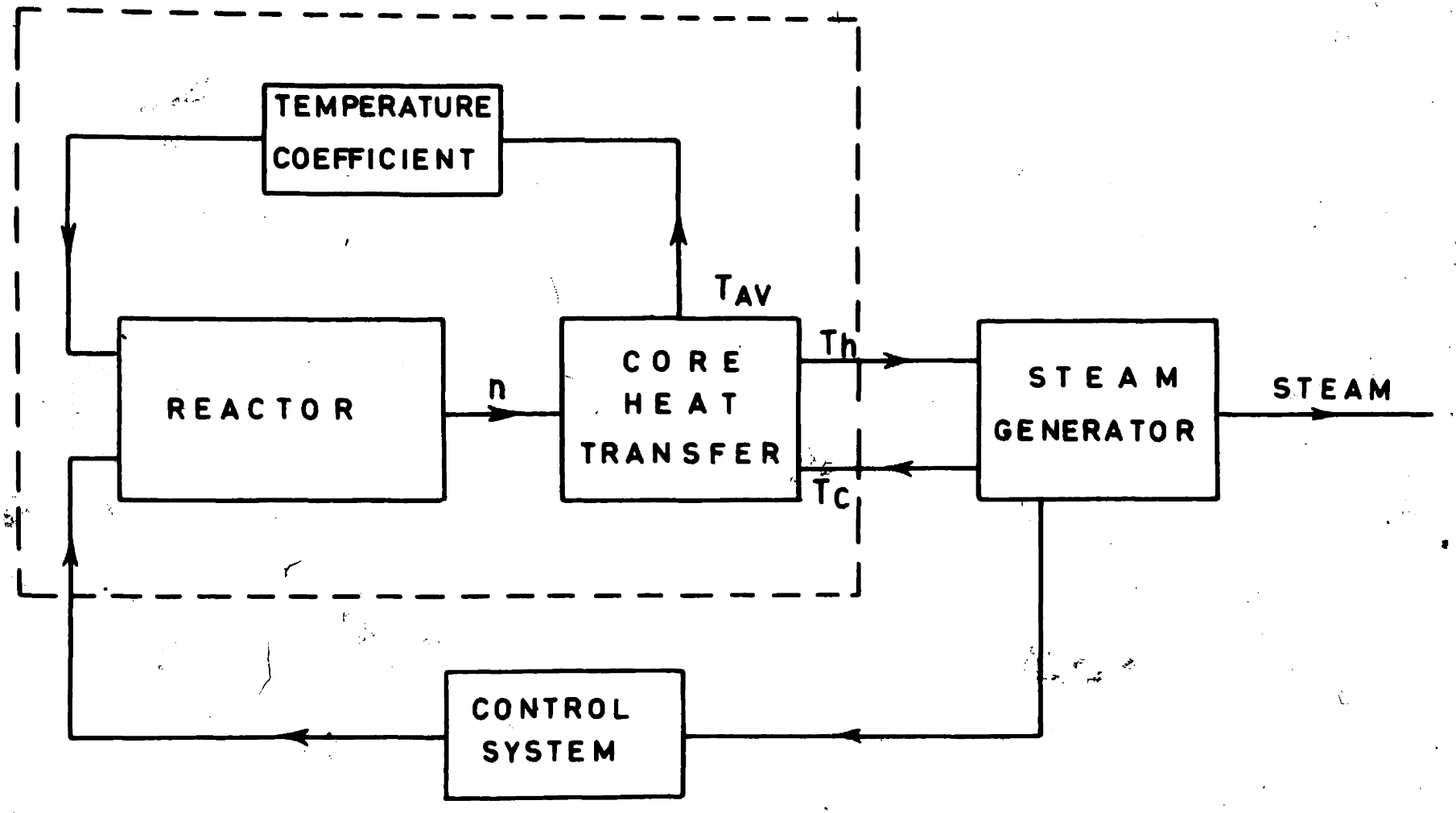
TEMPERATURE
COEFFICIENT
T_{AV}
REACTOR
n
CORE
HEAT
TRANSFER
Th
Tc
STEAM
GENERATOR
STEAM
CONTROL
SYSTEM

FIG. 2

value is

Doppler temperature coefficient

$$\frac{1}{k}\frac{\partial k}{\partial T} = -2.3 \times 10^{-5}/°F \quad \text{(moderator temperature: 516°F)}$$

where T is the temperature of the fuel material where U-235, U-238, and Pu-239 are intimately mixed.

b. The moderator temperature coefficient which is related with the change in density and in nuclear properties of the moderator when its temperature varies.

The following values have been calculated for the Yankee Reactor:

Moderator temperature coefficient (without control rods)

$$\frac{1}{k}\frac{\partial k}{\partial T} \quad (1/°F)$$

Temperature of the moderator	Beginning of the life	End of the life
68	-0.35×10^{-4}	-0.10×10^{-4}
250	-0.98×10^{-4}	-0.80×10^{-4}
516 (full power)	-2.9×10^{-4}	-2.8×10^{-4}

From these values it can be seen that the moderator temperature coefficient varies in magnitude both with the temperature of the moderator and with the operation of the reactor※. These variations affect the dynamics of the system and hence have to be considered in the study of the stability.

1.3.2 The pressure dependence of reactivity

A change of the average temperature of the core will produce another indirect effect which will influence the multiplication factor. A variation of the average temperature determines a change of the volume of water in the primary loop which in turn produces a surge in the pressurizer and therefore a change of pressure in the primary loop.

※ This reduction is due to the plutonium buildup.

The pressure variation introduces a change of density of the moderator and hence of the multiplication factor. This effect can be taken into account through the introduction of a pressure coefficient of reactivity.

For the Yankee Reactor it was calculated to be:

Pressure coefficient of reactivity

$$\frac{1}{k}\frac{\partial k}{\partial p} = + 2.6 \times 10^{-6}/\text{psi}$$

(water temperature: 516°F, system pressure: 2000 psig)

This pressure coefficient is positive and hence tends to oppose the temperature coefficient (temperature and pressure surges occur simultaneously).

1.3.3 The overall temperature coefficient

For the purpose of this study, which is concerned solely with the full power operation, only one reactivity temperature coefficient will be assumed. The overall temperature dependence will be taken into account through the introduction of a temperature coefficient related to the average temperature of the moderator and equal to

Temperature coefficient of reactivity:

$$K_{TC} = \frac{1}{k}\frac{\partial k}{\partial T} = - 2.7 \times 10^{-4}/°F$$

The reactivity dependence with changes in pressure and for the Doppler effect will be disregarded assuming that their influence is negligible with respect to that of the strong negative moderator temperature coefficient.

1.3.4 Influence of the temperature coefficient feedback

The negative temperature coefficient feedback exerts a favorable effect on the dynamic behavior of the reactor operated without control since it stabilizes the reactor in the sense that it removes the pole

in the origin from the transfer function of the nuclear chain reaction. With such a feedback the reactor displays a constant average temperature behavior. However, if the neutron level is too high or the magnitude of the temperature coefficient too large, while long heat transfer time delays are involved, the system can become unstable.

The investigation of the stability of the Yankee Reactor without automatic control was made by C. F. Obermesser in a USAEC REport[2]*.

While no attempt is made here to rewrite the complete calculations, the block diagram and the related transfer functions derived in this paper are reported in detail, since these data are necessary for the analysis developed in this thesis.

1.3.5 System block diagram and transfer functions

From the general simplified scheme of Fig. 1 a block diagram of the reactor and cooling system can be derived as in Fig. 3, where the four loops are substituted by an equivalent one. Each block will be examined in detail and the associated transfer function derived.

a. Reactor neutron chain reaction dynamics

The kinetic equation of the reactor, assuming only one group of delayed neutrons and small variations around an equilibrium point, can be written in the form

$$\frac{\delta n(s)}{\delta k(s)} = \frac{n_o \lambda_{av} \tau_2 (1 + \tau_1 s)}{1' \cdot s(1 + \tau_2 s)} = K_r G_r(s) \qquad **$$

where

n_o = average equilibrium neutron density, neutrons/cm^3

λ_{av} = average decay constant of the six radioactive decay processes, sec^{-1}

---

* In this report the author has followed the procedure described by M. A. Schultz[3].

** Bonilla: Nuclear Engineering, p 668 [4].

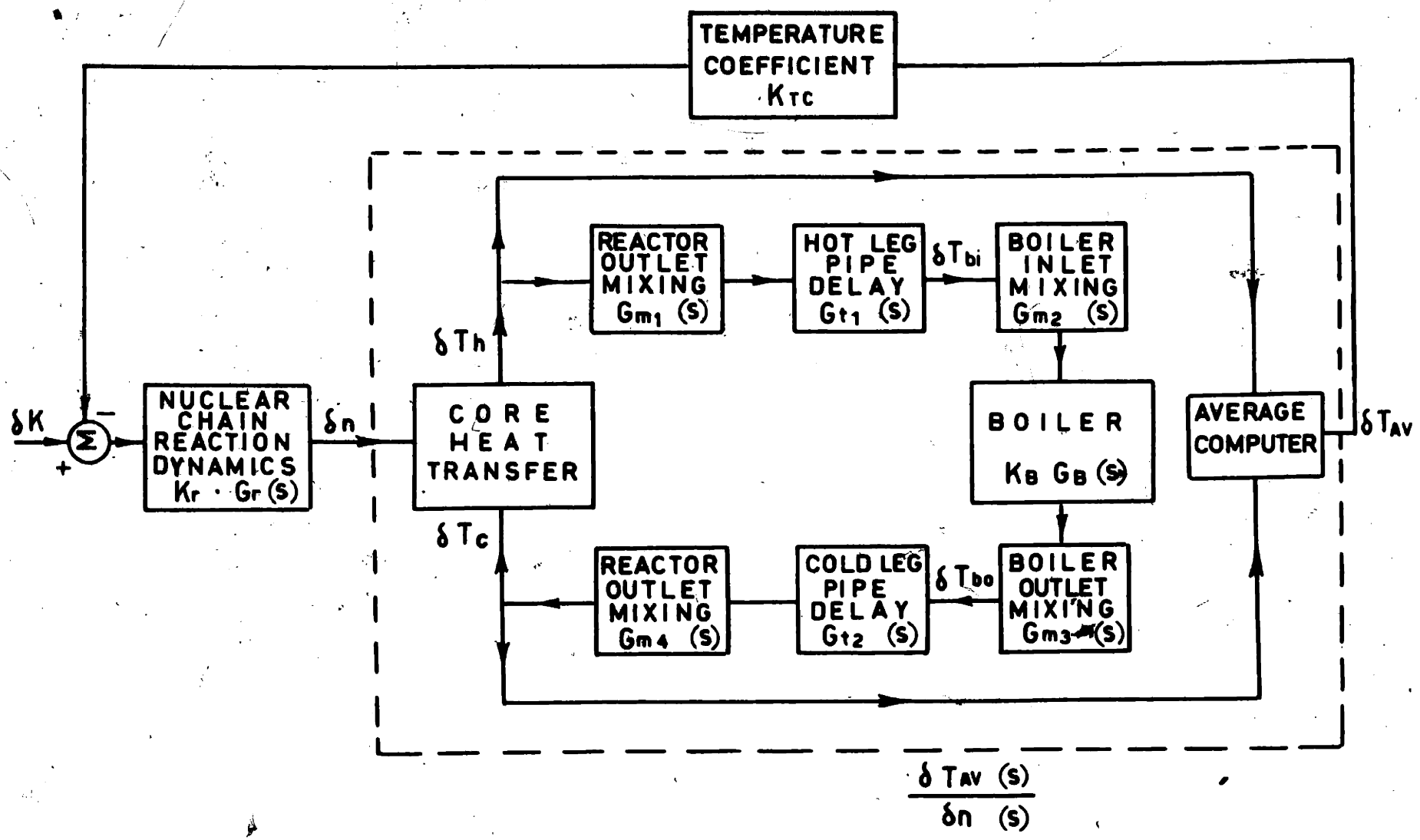
TEMPERATURE COEFFICIENT K_{TC}
REACTOR OUTLET MIXING G_{m_1} (S)
HOT LEG PIPE DELAY G_{t_1} (S)
δT_{bi}
BOILER INLET MIXING G_{m_2} (S)
δT_h
δK
NUCLEAR CHAIN REACTION DYNAMICS $K_r \cdot G_r(s)$
δn
CORE HEAT TRANSFER
BOILER $K_B G_B$ (S)
AVERAGE COMPUTER
δT_{AV}
δT_c
REACTOR OUTLET MIXING G_{m_4} (S)
COLD LEG PIPE DELAY G_{t_2} (S)
δT_{bo}
BOILER OUTLET MIXING G_{m_3} (S)
$\frac{\delta T_{AV}(s)}{\delta n(s)}$

FIG. 3

l' = prompt neutrons lifetime, sec

$\tau_1 = 1/\lambda_{av}$; $\tau_2 = l'/(l'\lambda_{av} + \beta)$

For the Yankee Reactor the following values are assumed for the full power operation:

$n_o = 875 \times 10^5$ neutrons/cm^3

$\lambda_{av} = 0.080$ sec^{-1}

$\tau_1 = 12.50$ sec

$\tau_2 = 0.1245$ sec

Substituting and rearranging

$$K_r G_r(s) = 1.5 \times 10^{10} \frac{(1 + 12.50s)}{s(1 + 0.1245s)}$$

b. Reactor heat transfer to the coolant

The reactor is assumed to be divided in three sections in the direction of the coolant flow (which is single pass), so that the block diagram of the heat transfer is as in Fig. 4* where the meaning of the symbols is:

$$\gamma = \frac{1}{Rc}$$

R = flow rate through the reactor, ft^3/sec

c = heat capacity of the coolant per unit volume, BTU/ft^3·°F

R and c are evaulated in each section assuming linear variation of the temperature

$\alpha = \dfrac{\text{heat generated}}{\text{average neutron density}}$ evaluated on the basis of the axial flux distribution

$$G_c(s) = (1 - \tau_r s)$$

$$G_h(s) = \frac{1}{1 + \tau_r s}$$

---

* For the simplifications involved in this transfer function see Obermesser[2] p 16.

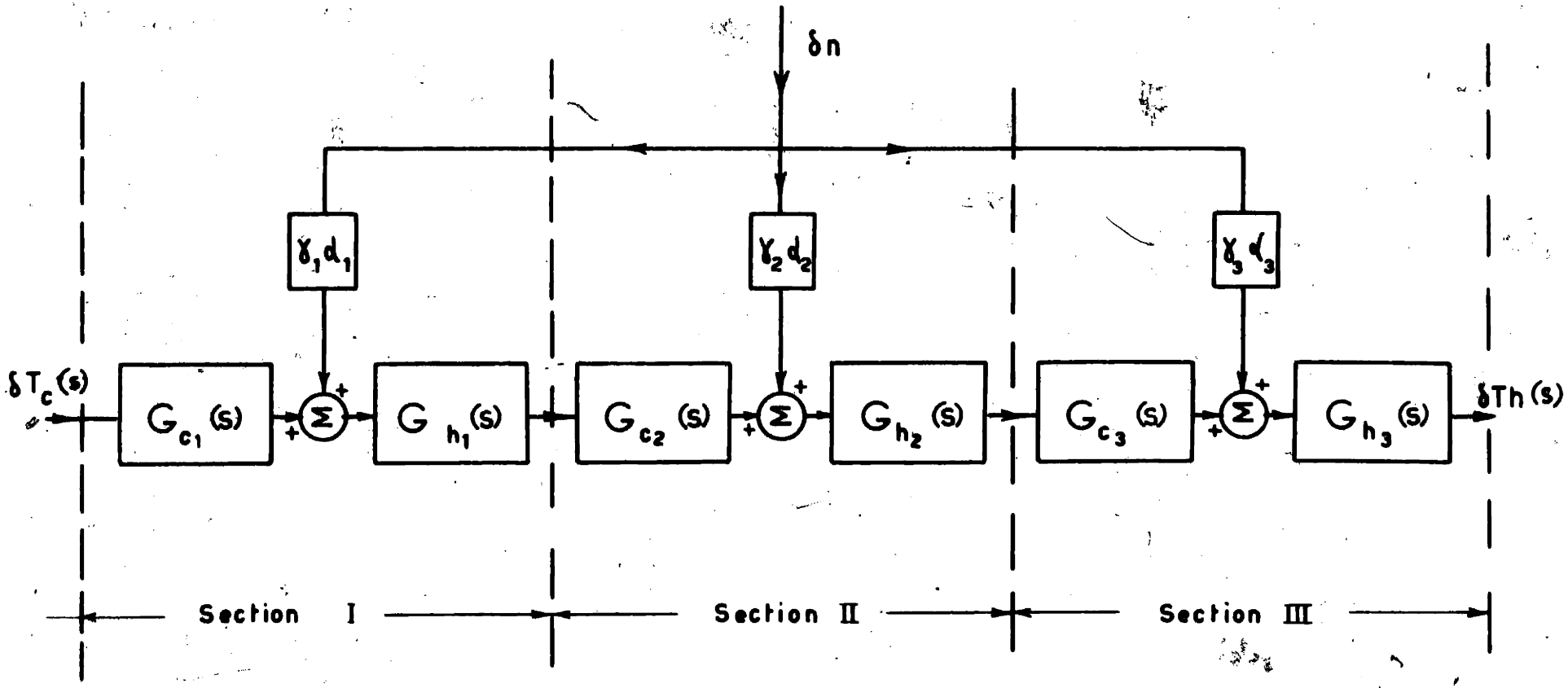
δn
γ1d1
γ2d2
γ3d3
δTc(s)
Gc1(s)
Σ
Gh1(s)
Gc2(s)
Σ
Gh2(s)
Gc3(s)
Σ
Gh3(s)
δTh(s)
Section I
Section II
Section III

FIG. 4

$$\tau_r = \frac{C_r}{2Rc}$$

C_r = total heat capacity of the reactor fuel including the cladding stainless steel and the rod follower zirconium, BTU/lb.·°F, evaluated as a weighed value in each section.

For the Yankee Reactor the following values were calculated:

$$\alpha_1\gamma_1 = \alpha_2\gamma_2 = \alpha_3\gamma_3 = 40.25 \times 10^{-8}$$

$$G_{c1}(s) = (1 - 0.09s) \qquad G_{h1}(s) = \frac{1}{(1 + 0.09s)}$$

$$G_{c2}(s) = (1 - 0.905s) \qquad G_{h2}(s) = \frac{1}{(1 + 0.0905s)}$$

$$G_{c3}(s) = (1 - 0.09s) \qquad G_{h3}(s) = \frac{1}{(1 + 0.09s)}$$

c. Mixing transfer functions

Complete mixing is assumed in each of the reactor and boiler headers. The general mixing transfer function is of the form

$$\frac{T_{out}(s)}{T_{in}(s)} = \frac{1}{1 + \frac{V}{F}s}$$

where V = the mixing volume, ft^3

F = the flow rate, ft^3/sec

For the Yankee Reactor the mixing transfer functions are:

$$G_{m_1}(s) = \frac{1}{1 + 0.37s}$$ reactor outlet mixing

$$G_{m_2}(s) = \frac{1}{1 + 0.66s}$$ boiler inlet mixing

$$G_{m_3}(s) = \frac{1}{1 + 0.70s}$$ boiler outlet mixing

$$G_{m_4}(s) = \frac{1}{1 + 0.33s}$$ reactor inlet mixing

d. Pipe transport delay

An approximate transfer function for the pipe transport delay was assumed of the form:

$$\frac{T_{out}(s)}{T_{in}(s)} = \frac{1}{1 + ts}$$

where t = the transit time, i. e., the ratio

$$t = \frac{\text{volume of the pipe, ft}^3}{\text{flow rate, ft}^3/\text{sec}}$$

In the Yankee Reactor for the two main pipes from the reactor to the boiler (hot leg) and from the boiler back to the reactor (cold leg) the following values were found

$$G_{t_1}(s) = \frac{1}{1 + 2.4s} \qquad \text{hot leg}$$

$$G_{t_2}(s) = \frac{1}{1 + 2.92s} \qquad \text{cold leg}$$

e. Boiler transfer function

The four steam generators are considered lumped together. As derived in the Appendix, the transfer function of the boiler is (throttle in fixed position):

$$K_B G_B(s) = K_B \frac{1 + \tau_{bi} s}{1 + \tau_{bo} s} \quad \text{※}$$

For the Yankee Reactor the following values were derived:
$K_B = 0.680$; $\tau_{bi} = -0.195$; $\tau_{bo} = 13.25$
(the throttle is assumed full open)
Hence

$$K_B G_B(s) = 0.680 \frac{1 - 0.195s}{1 + 13.25s}$$

※ For the meaning of the symbols see the Appendix.

1.3.6 Open loop transfer function

Performing the necessary mathematical manipulations* the open loop transfer function of the reactor, the cooling system and the temperature coefficient feedback, i.e.,

$$K_T G_T(s) = K_{TC} \frac{\delta n(s)}{\delta k(s)} \cdot \frac{T_{av}(s)}{\delta n(s)}$$

where K_{TC} is the temperature coefficient, is:

$$K_T G_T(s) = 36.34 \times 10^{-3} \cdot \frac{(s^2 + 0.186s + 0.021)}{s(1 + 0.1145s)} \cdot$$

$$\cdot \frac{(1 + 0.15s)(s^2 + 0.404s + 0.073)(s^2 - 1.50s + 2.92)(1 + 12.5s)}{(1 + 0.1245s)(1 + 0.33s)(s^2 + 0.50s + 0.110)(s^2 + 2.71s + 1.88)} \cdot$$

$$\cdot \frac{(s^2 + 0.244s + 384.16)}{(1 + 1.46s)(s^2 + 24.1s + 151.29)(1 + 67.5s)}$$

The Bode diagram of this open loop transfer function is in Diagram I**. Correction at the break points for the amplitude, and the phase were calculated.

1.3.7 Stability considerations

From the Bode diagram we see that the phase margin is more than 85°. For the examined condition of full power, the system is very stable and over damped. It is interesting to observe at this point that the stability of the system is insured also for disturbances originating from changes of the throttle valve opening, resulting from variation of the load at the turbine. This is true for the following reason.

---

* For details, see Obermesser, p 29 and seg.

** The calculations of the Obermesser report end with the straight line approximation for the Bode diagram.

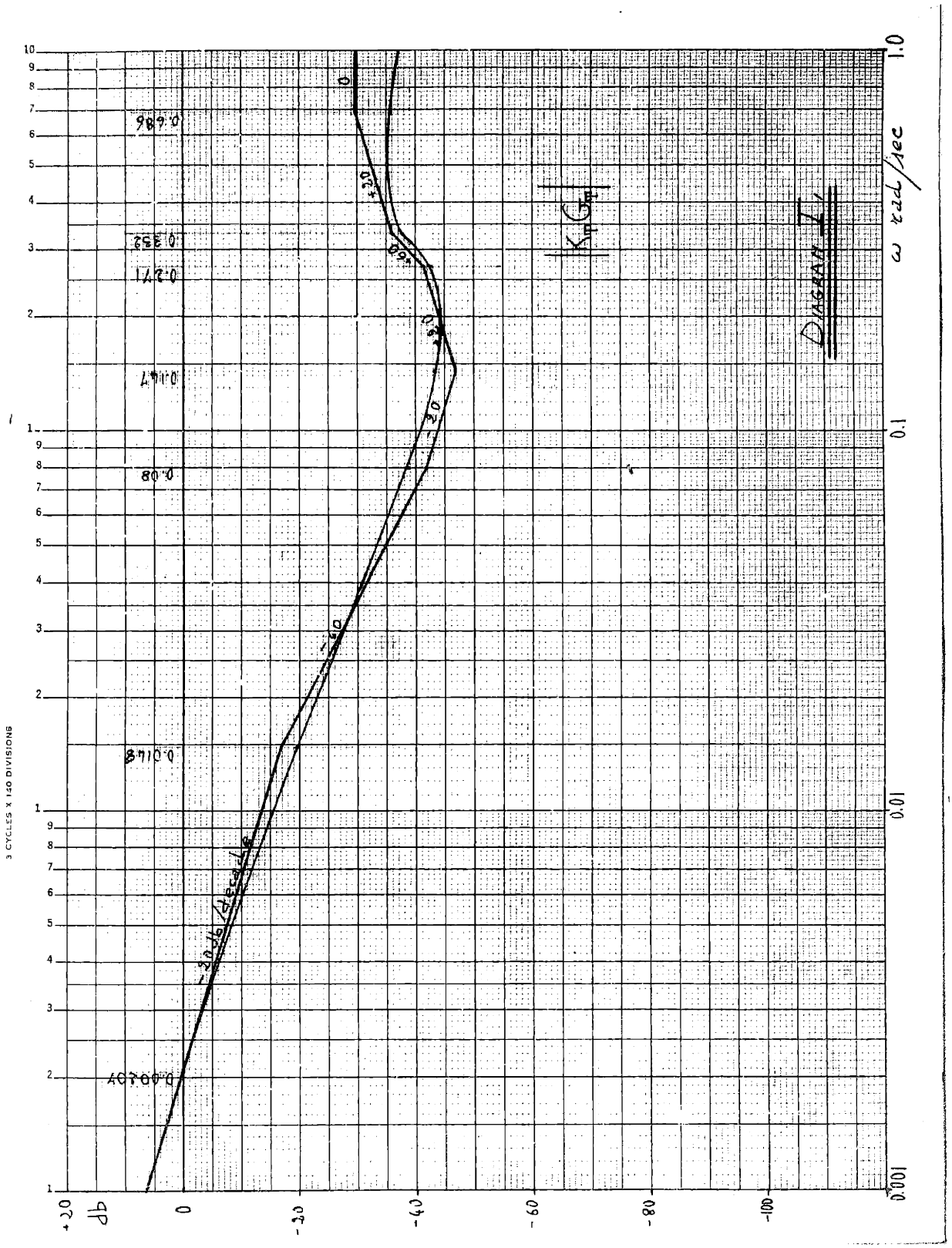
DIAGRAM 1
$K_m G_m$
ω rad/sec
1.0
0.1
0.01
0.001
dB
+20
0
-20
-40
-60
-80
-100
0
+30
+60
+90
-30
-60
-90
-20db/decade
0.0425
0.0178
0.08
0.147
0.271
0.352
0.636
3 CYCLES X 140 DIVISIONS

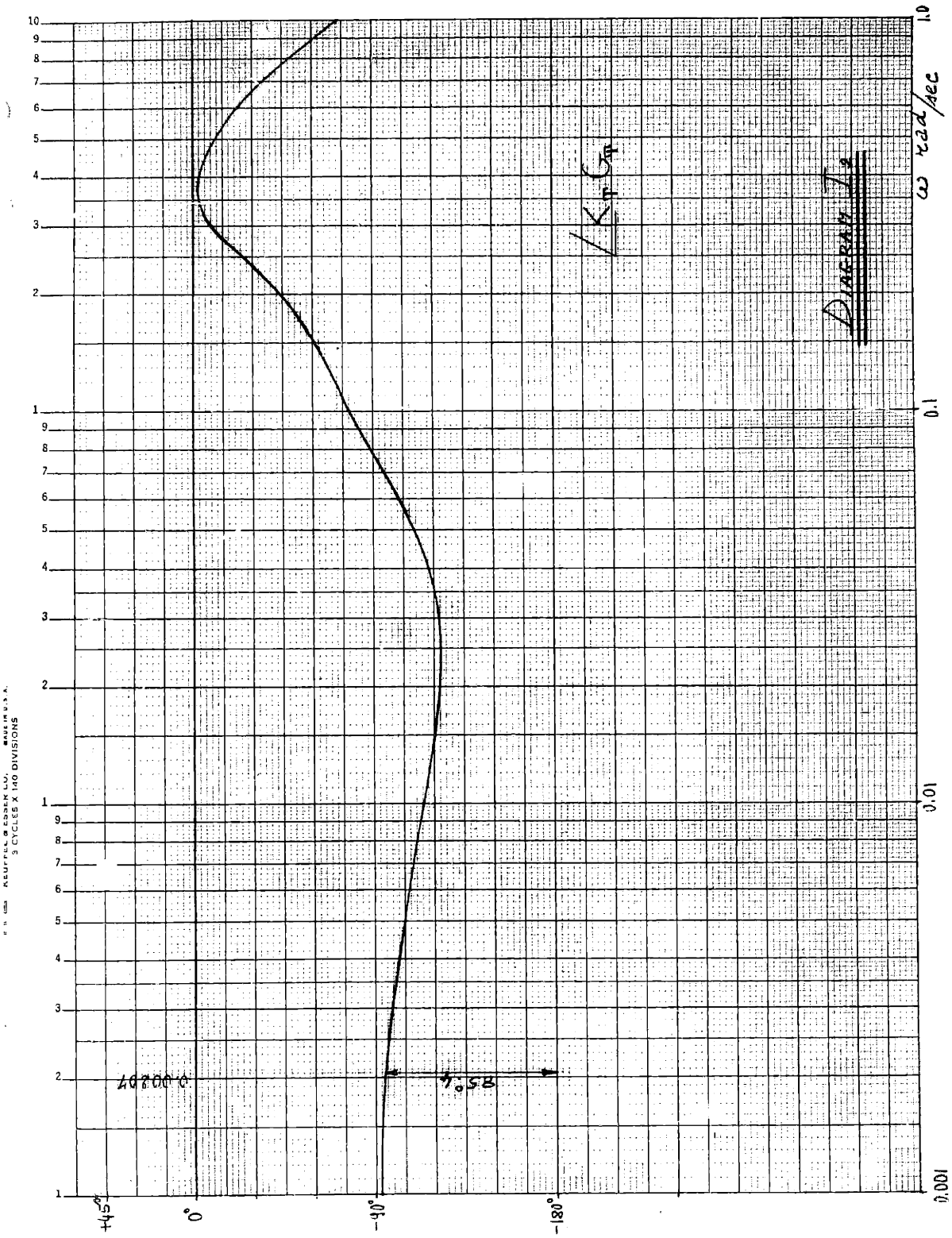
Diagram 7a
ω rad/sec
1.0
0.1
0.01
0.001
$\angle K_f G_m$
+45°
0°
-90°
-180°
85°
0.00207
KEUFFEL & ESSER CO. MADE IN U.S.A.
3 CYCLES X 140 DIVISIONS

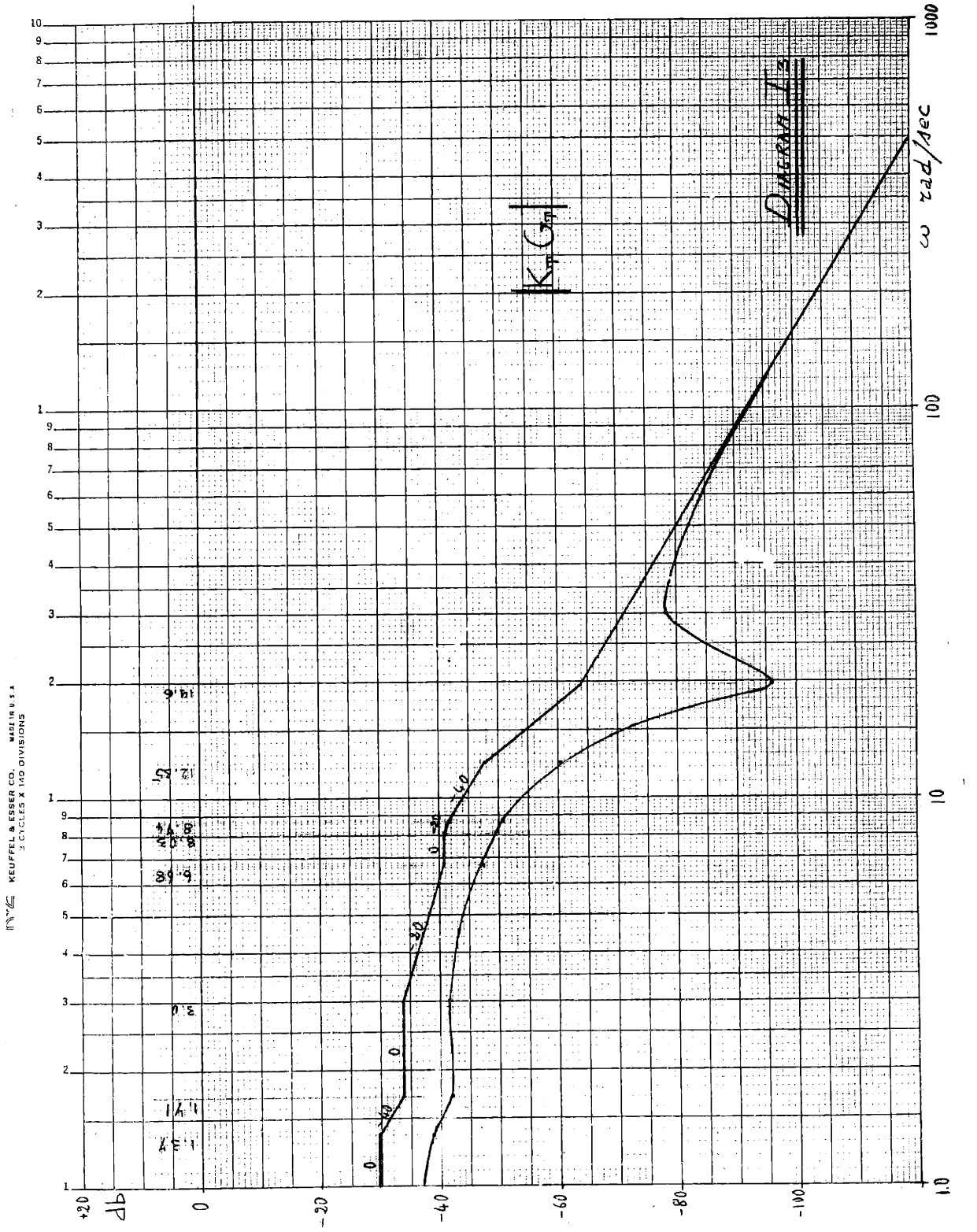
DIAGRAMA DE BODE
$K_m G_{fp}$
ω rad/seg
dB
+20
0
-20
-40
-60
-80
-100
1000
100
10
1.0
KEUFFEL & ESSER CO. MADE IN U.S.A.
2 CYCLES X 140 DIVISIONS

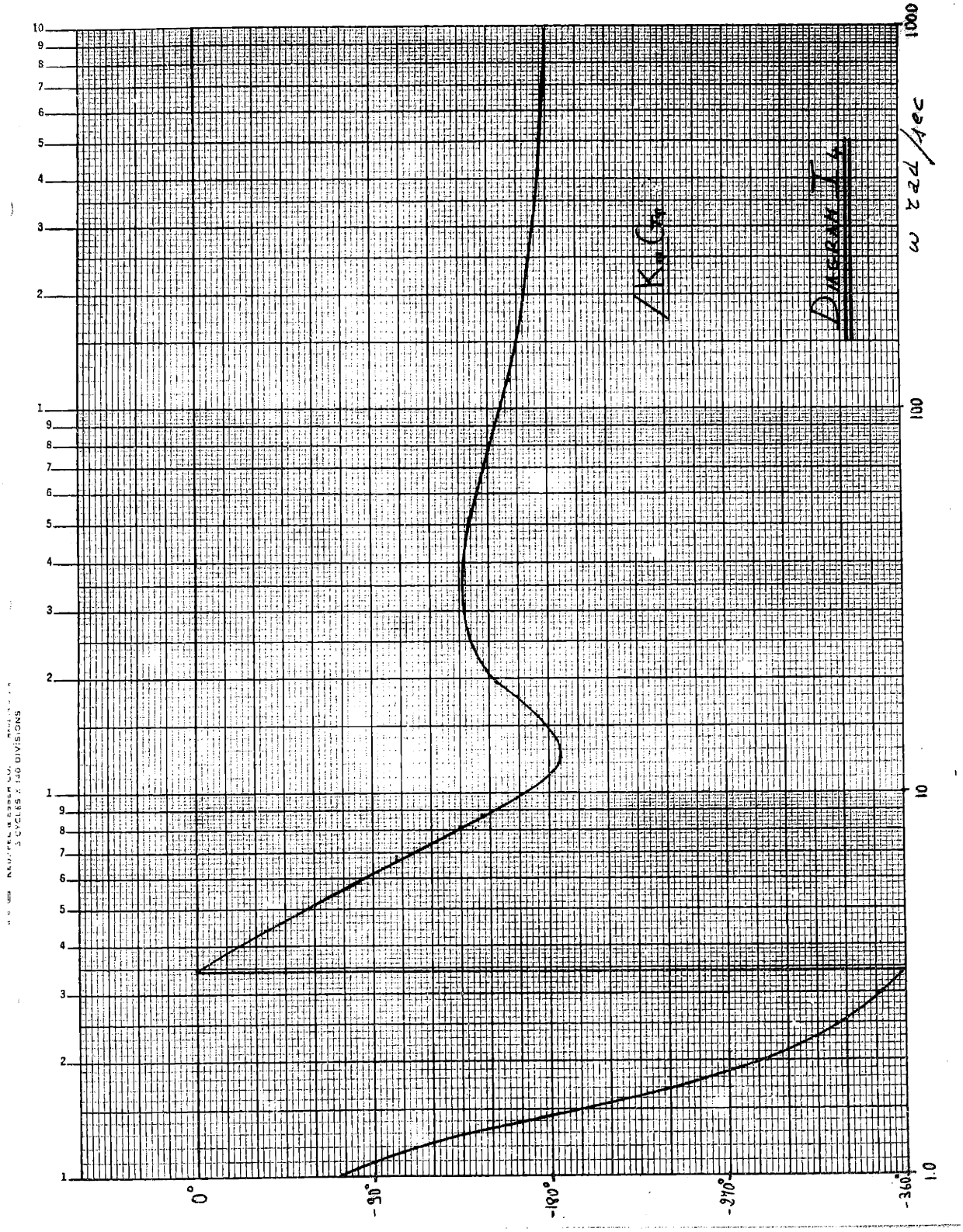
10000
1000
100
10
1.0
0°
-90°
-180°
-270°
-360°
Data/Phase
Magnitude

As it is derived in the Appendix, if the setting of the throttle valve is assumed variable, the transfer function of the boiler, for small variations around an equilibrium point, differs from that with fixed setting only through the addition of another input. The system is left unaltered.

Since a linear system (and ours was assumed as such) is stable if all its poles (natural frequencies) are in the left half plane, and since the natural frequencies are independent of the point of excitation when the system is not altered, we can conclude that the Yankee Reactor is stable also for disturbances due to load variations.

CHAPTER II

2.1 The Control of the Core

Even though the reactor and the steam generator complex, for the negative temperature feedback displays a very stable behavior, a means to control the reactivity of the core must be provided for many reasons.

1. To start up and to shut down or to change the power level it is necessary to vary the reactivity of the core.

2. During operation there is a reduction of reactivity due to the increase of temperature from cold to full power, to the fuel burn-up, and to the poisons production.

3. And finally when shut-off, the reactor must be maintained largely subcritical for safety.

It is hence necessary to build in the core a certain initial excess of reactivity. For the Yankee Reactor it was calculated to be, for the clean cold core, around 25% δk/k. To compensate for this excess of reactivity and for control purposes, 24 cruciform rods are located in the core. Furthermore there are eight fixed shim rods* for adjusting the initial reactivity**.

The control rods are distributed on four concentric rings and are symmetrically distributed in six groups. These groups are operated successively. The rods are moved by individual drive mechanisms, but the mechanisms of the rods of the same group are operated by a unique control device so that all the rods of the same group move simultaneously.

The distribution of rods in the groups and the sequence with which these groups are operated is such as to minimize flux non-uniformity.

---

* These rods can be moved only with the vessel head removed.

** To alleviate the task of the control rods, a chemical reduction of reactivity through the addition of boric acid in the cooling water is provided when the reactor is shut off.

2.2. Control Rod Drive Mechanism

The drive mechanism which moves each individual rod is a positive-grip modification of the magnetic jack type. A schematic view of the drive mechanism itself and of its control apparatus is in Figs. 5 and 6. The choice of a drive mechanism for a pressurized water reactor is strongly influenced by the necessity of operating it in a high pressure vessel and by safety considerations.

The positive-grip, magnetic jack mechanism is composed of two main parts: the mechanical jack mechanism inside the pressure housing, and the electromagnetic coils situated outside. The jack mechanism moves a grooved cylindrical shaft connected to the control rod.

2.2.1 Drive mechanism principle of operation

The mechanism operates in the following manner:

a. Rod withdrawal

1. Initially the stationary gripper latches are engaged and are supporting the rod weight. The stationary gripper magnet coil and the transfer magnet coil are energized.

2. The movable gripper magnet coil is energized, causing the movable gripper latches to engage the drive rod.

3. The load transfer magnet coil is de-energized so that the load is transferred from the stationary gripper assembly to the movable gripper latches.

4. The stationary gripper magnet coil is de-energized, the stationary gripper latches disengage the drive rod.

5. The lift magnet coil is energized. This raises the movable gripper assembly and the drive rod one step: 3/8 in.

6. The stationary gripper magnet coil is energized, causing the stationary gripper latches to engage the drive rod.

7. The load transfer magnet coil is energized unloading the movable gripper latches.

8. The movable gripper magnet coil is de-energized so

2.2. Control Rod Drive Mechanism

The drive mechanism which moves each individual rod is a positive-grip modification of the magnetic jack type. A schematic view of the drive mechanism itself and of its control apparatus is in Figs. 5 and 6. The choice of a drive mechanism for a pressurized water reactor is strongly influenced by the necessity of operating it in a high pressure vessel and by safety considerations.

The positive-grip, magnetic jack mechanism is composed of two main parts: the mechanical jack mechanism inside the pressure housing, and the electromagnetic coils situated outside. The jack mechanism moves a grooved cylindrical shaft connected to the control rod.

2.2.1 Drive mechanism principle of operation

The mechanism operates in the following manner:

a. Rod withdrawal

1. Initially the stationary gripper latches are engaged and are supporting the rod weight. The stationary gripper magnet coil and the transfer magnet coil are energized.

2. The movable gripper magnet coil is energized, causing the movable gripper latches to engage the drive rod.

3. The load transfer magnet coil is de-energized so that the load is transferred from the stationary gripper assembly to the movable gripper latches.

4. The stationary gripper magnet coil is de-energized, the stationary gripper latches disengage the drive rod.

5. The lift magnet coil is energized. This raises the movable gripper assembly and the drive rod one step: 3/8 in.

6. The stationary gripper magnet coil is energized, causing the stationary gripper latches to engage the drive rod.

7. The load transfer magnet coil is energized unloading the movable gripper latches.

8. The movable gripper magnet coil is de-energized so

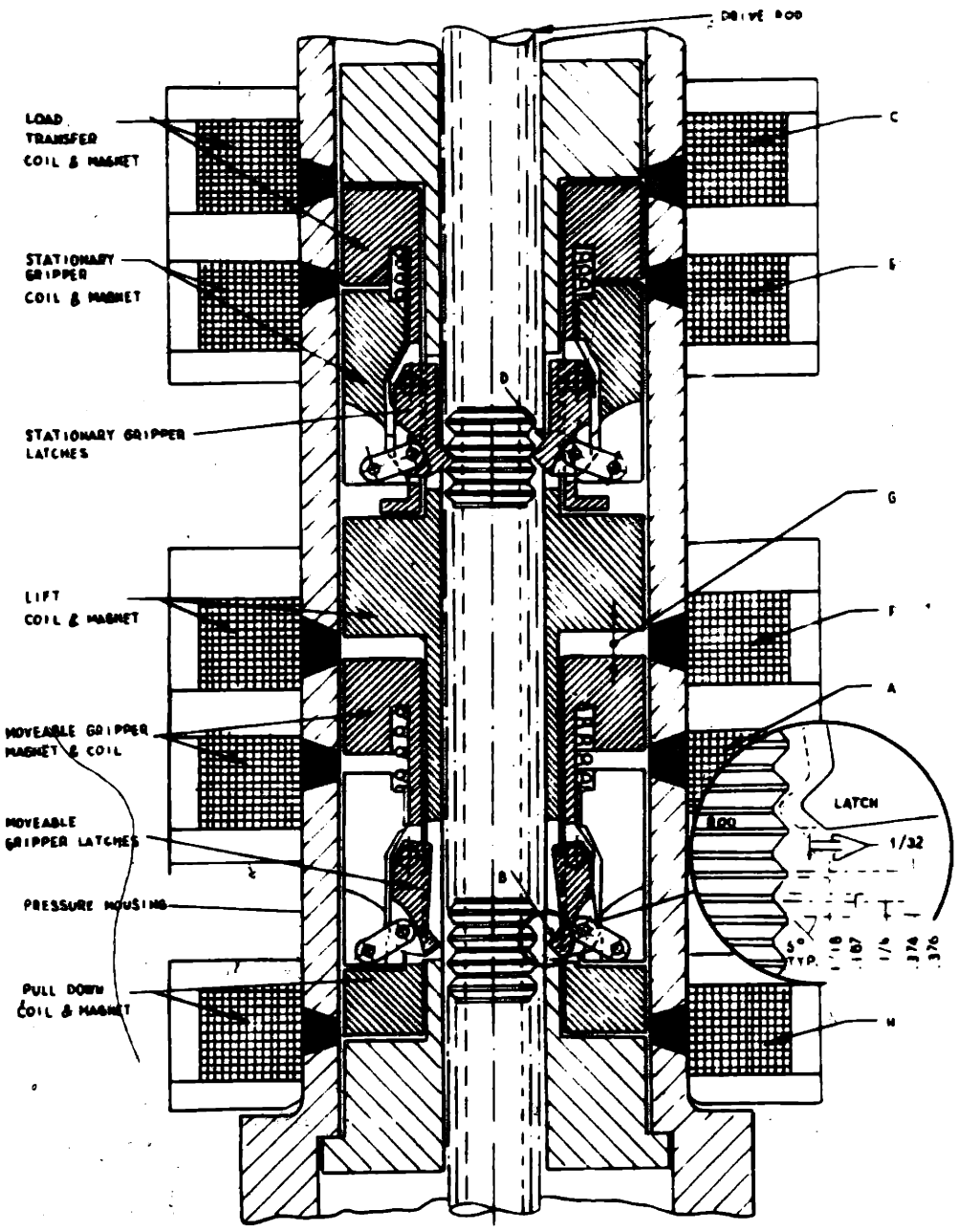

MECHANISM SCHEMATIC DIAGRAM

MAGNETIC JACK LATCH TYPE CONTROL ROD DRIVE MECHANISM

FIG. 5

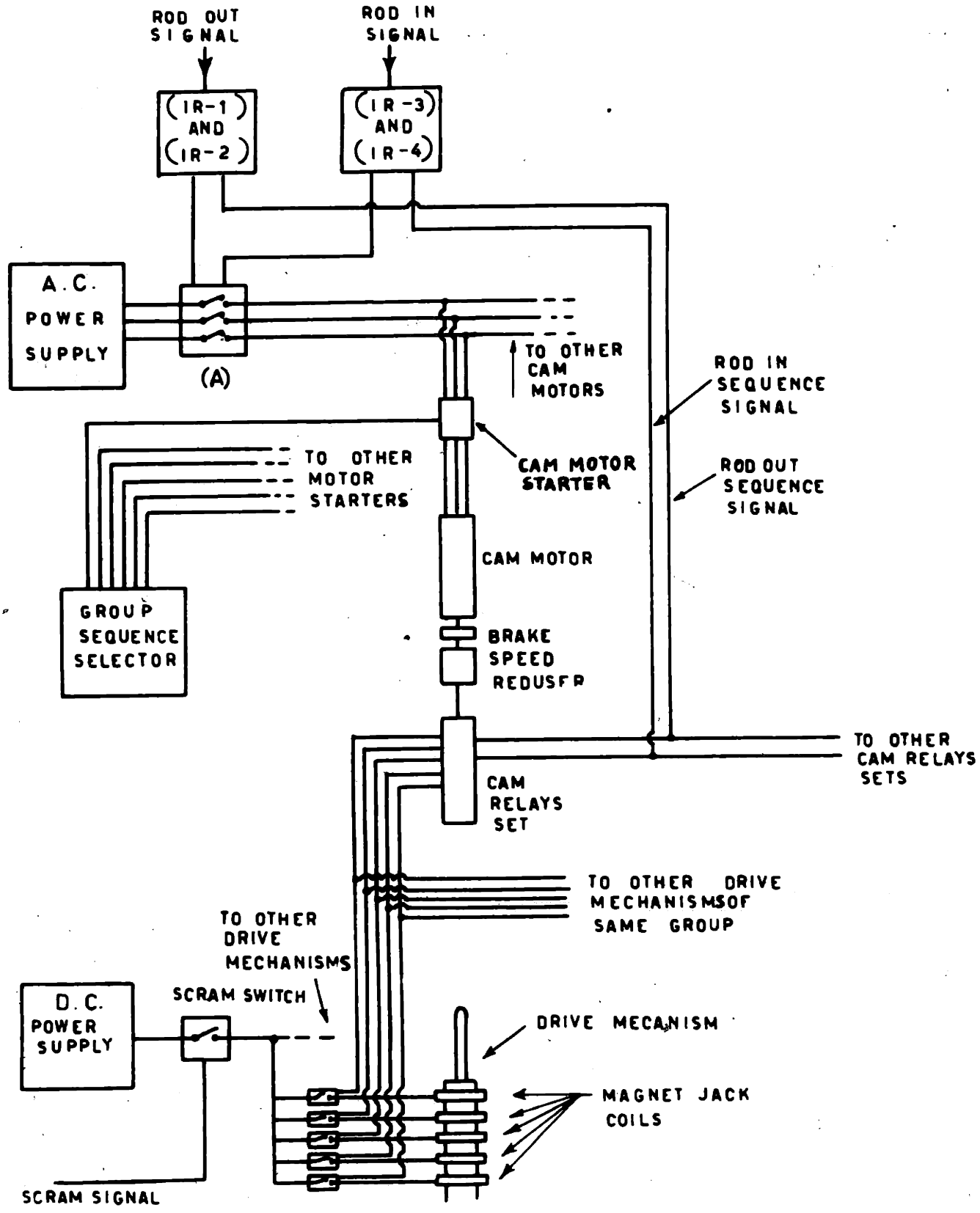
ROD OUT SIGNAL
ROD IN SIGNAL
(IR-1) AND (IR-2)
(IR-3) AND (IR-4)
A.C. POWER SUPPLY
(A)
TO OTHER CAM MOTORS
ROD IN SEQUENCE SIGNAL
ROD OUT SEQUENCE SIGNAL
CAM MOTOR STARTER
TO OTHER MOTOR STARTERS
CAM MOTOR
GROUP SEQUENCE SELECTOR
BRAKE SPEED REDUSER
TO OTHER CAM RELAYS SETS
CAM RELAYS SET
TO OTHER DRIVE MECHANISMSOF SAME GROUP
TO OTHER DRIVE MECHANISMS
SCRAM SWITCH
D.C. POWER SUPPLY
DRIVE MECANISM
MAGNET JACK COILS
SCRAM SIGNAL

FIG. 6

that the movable gripper latches disengage the drive rod.

9. The pull down magnet coil is energized and the lift magnetic coil is de-energized: the movable gripper assembly is brought back to its initial position ready for the next cycle.

b. Rod insertion

To lower the drive rod the order of the operations of rod withdrawal are reversed except for the pull down magnet coil which is disconnected since the drive rod, dropping by gravity, lowers also the movable gripper assembly[※].

c. Scram

To scram, the whole system is de-energized: the drive rod is disengaged and drops by gravity in the core.

2.2.2 Power supplies and control apparatus (Fig. 6)

All the coils are fed by a 125 V D.C. common power supply through individual contactors. These contactors are open and closed in the proper sequence by a set of cam operated relays. The unique cam shaft is moved at a constant speed by a three phase induction motor through a speed reducer.

The speed of withdrawal and insertion (except for scram) is fixed and cannot be changed. Its value was chosen (for mechanical and electric limitation) as 30 complete cycles per minute, i.e., the rods are moved in steps of 3/8 in., 30 steps per minute (11.25 in/min). Each group of control rods has its own induction motor - cam relays set so that each group can be operated independently and in the proper sequence. Each induction motor receives power from a common bus through a starter relay.

The chosen sequence for the control rod groups operation is obtained by energizing and de-energizing these starter relays with

---

※ An opportune small clearance between drive rod and latches is provided during engagement and disengagement which happen hence without friction. The whole system is lubricated by the main cooling system water.

the desired succession. The common bus for the cam-motors supply is connected to the source through a normally-open, relay-operated contactor (A).

The Rod-In sequence for the magnet coils of the drives is determined by energizing two relays (IR-1 and IR-2) while the Rod-Out sequence is determined by energizing two other relays (IR-3 and IR-4).

2.2.3 Operation of the drive mechanism

a. Rod-Out — When a rod-out signal is applied to the system relays (IR-1) and (IR-2) are energized determining the rod-out sequence combination for the cam switches. (IR-1) and (IR-2) also energize the contactor (A), which closes and feed the cam-motors bus. Previous selection of the control rod group which has to be moved, was obtained by closing the starter relay for the cam-motor of the chosen group. Hence as (A) is closed, the selected cam-motor starts closing and opening the magnet coil contactors, determining the withdrawal of the rods of the chosen group.

b. Rod-In — When a rod-in signal is applied to the system, relays (IR-3) and (IR-4) are energized determining the rod-in sequence combination for the cam-switches. At the same time (IR-3) and (IR-4) close contactors (A) determining the excitation of the selected cam-motor. The chosen rod group is so inserted.

When the excitation signal ends, an interlock holds the system moving until the cam-motor returns to the initial position of the cycle where it is held "as is" by a brake. Then the relays are de-energized and the system returns to the normal position, ready for a new operation. A complete set of other interlocks is also provided for safety considerations but does not interfere with the normal operation.

The sequence of events which take place during the rod movement are pictured in Scheme I.

SCHEME I

Control Rod Drive Mechanism Operation Sequences

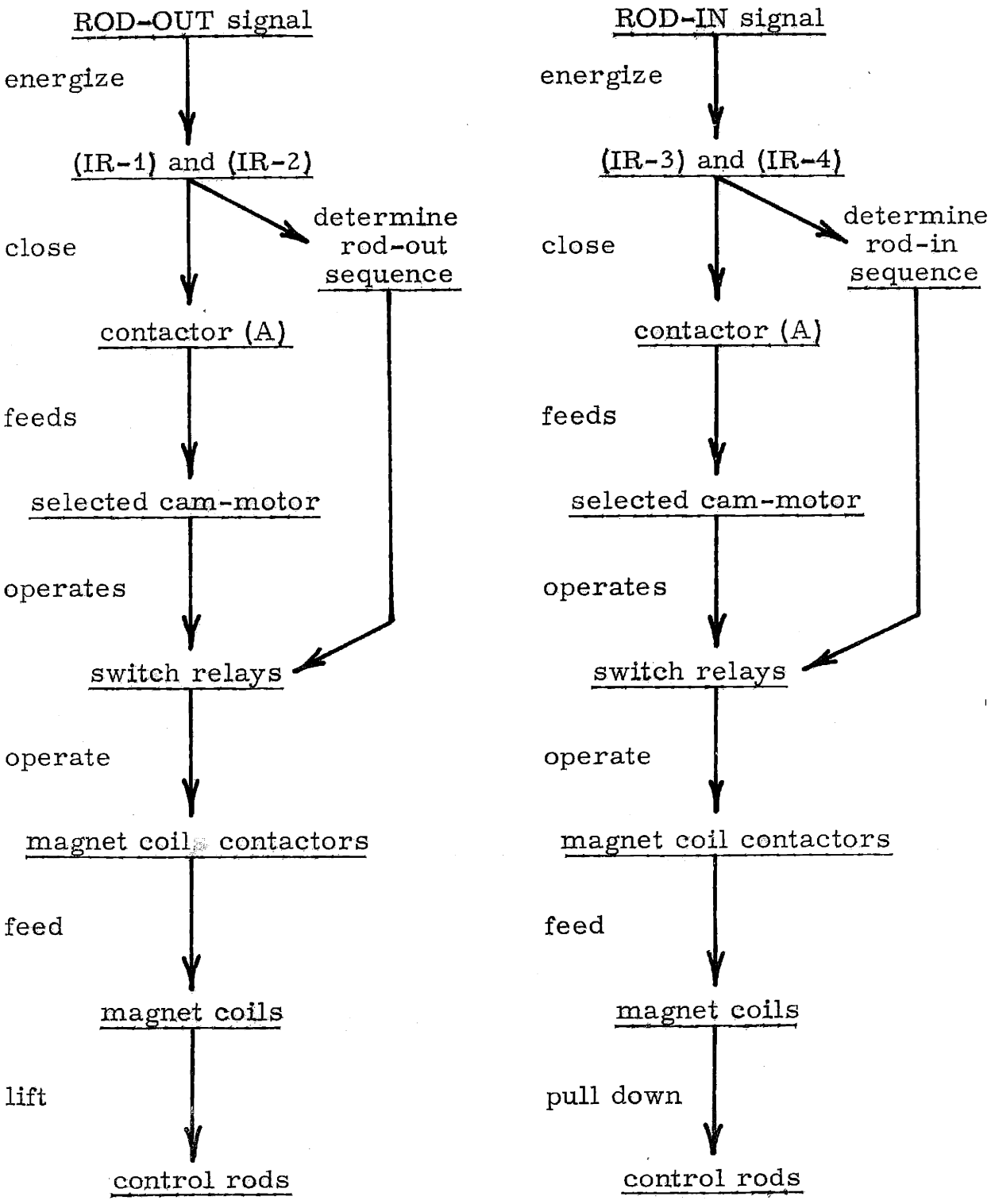

2.2.4 Delay times involved

As was determined in the testing program[5] the lifting period of the rod starts 0.65 seconds after the beginning of each cycle and lasts for 0.55 seconds (since there are 30 cycles per minute, each cycle requires 2 seconds).

The falling down period during rod-in operation starts after a longer time from the beginning of the cycle and lasts for less than 0.55 seconds. However the two movements will be assumed to be equal※.

No exact values were available for the delays involved in the operation of each relay and contactor and in the starting time of the induction motors, so that values derived by similar apparatus in the literature were assumed as follows:

Relays and contactors delay times:

(IR-1), (IR-2), (IR-3), and (IR-4) ≅ 0.1 sec.

cam-switches relays ≅ 0 (can be disregarded)

Contactor(A) ≅ 1 sec

Motor starting time, including break relief, ≅ 1 sec.

The total time delay between application of the signal (either rod-in or rod-out signal) and the beginning of the first operating cycle will be assumed to be ≅ 2.0 sec.

The displacement of the rod versus time is drawn in Fig. 7, where $t = 0$ is the time at which the signal is applied to the system. In the figure the movement of the rod is assumed to happen at constant speed. The actual type of movement effects in a negligible way only the initial delay time.

From this figure it is evident how the motion of the rod can be fairly well approximated with a constant velocity movement of 0.1875 in. per second, starting with 1.60 seconds of delay from the application

---

※ Exact data concerning the insertion movement were not available, however the only difference with the withdrawal movement may be in the initial delay time which is already an approximate value.

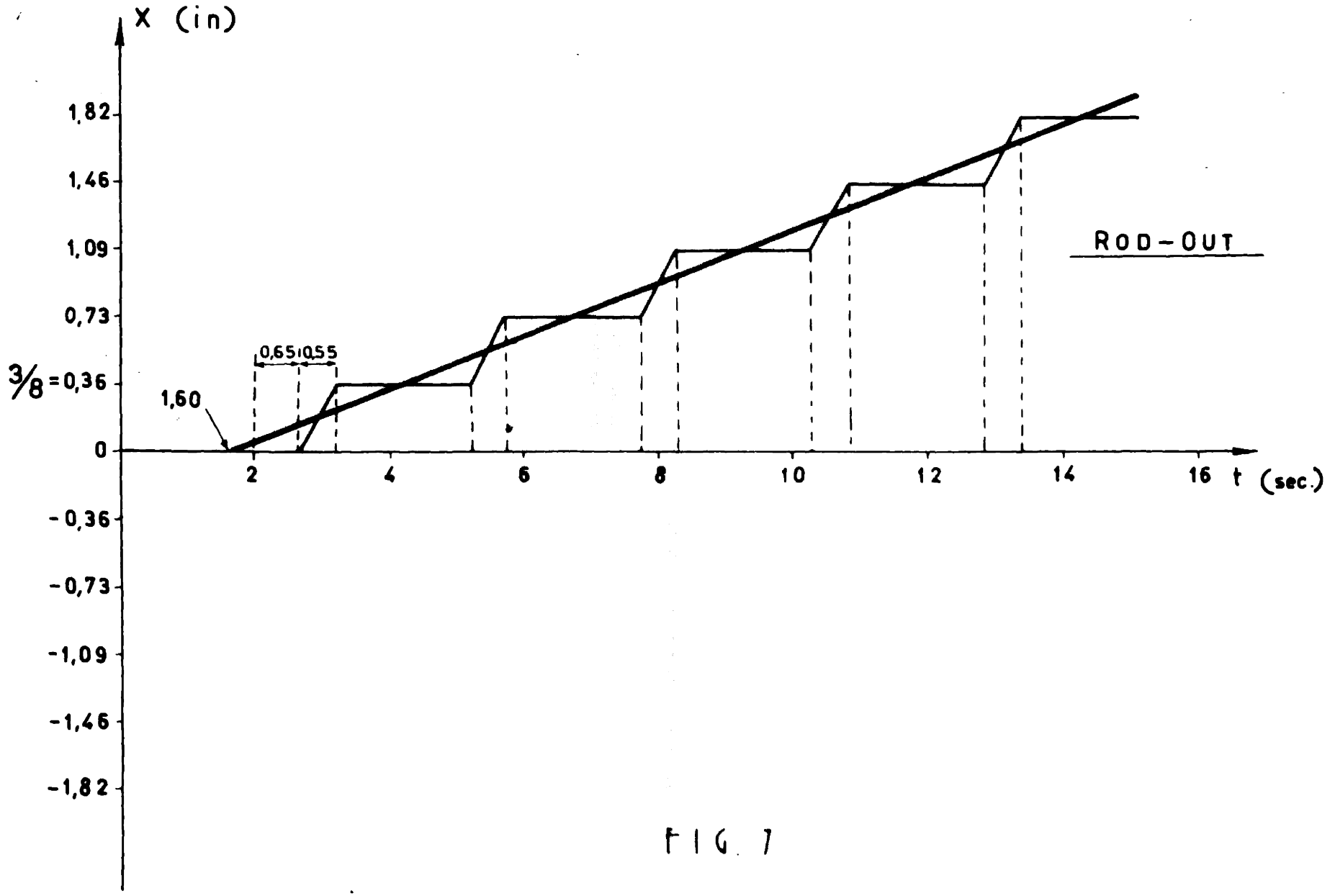
X (in)
1,82
1,46
1,09
0,73
3/8 = 0,36
0
-0,36
-0,73
-1,09
-1,46
-1,82
1,60
0,65
0,55
2
4
6
8
10
12
14
16
t (sec.)
ROD-OUT

FIG. 7

of an operation signal. Both speed and delays are constant and independent of the input signal in so far as it is large enough to trigger the first relay.

2.2.5 Change of reactivity introduced

It was concluded from the "Technical Informations and Final Hazard Summary Report"[1] for the Yankee Reactor that the average reactivity worth for each group of control rods is around 0.028 δk. Since the rod total travel is 90 in., the change of reactivity introduced on the average by each group per inch of movement is

$$\cong 3.10^{-4}\ \delta k/in.$$

2.2.6 Summary

Combining the derived data we can conclude that the control drive mechanism and the associated control rod constitute a highly non-linear complex which operates in the following way.

When a signal is applied to the input of the driving system, after a time delay of 1.60 seconds, a constant change of reactivity at the rate of

$$3 \times 10^{-4}(\delta k/in.) \times 0.187\ (in/sec) \approx 0.55 \times 10^{-4}\ \delta k/sec.$$

is introduced in the core and it will continue until the input signal is reduced again to zero.

The sign of the change of reactivity depends on the polarity of the input signal.

2.3 Automatic Control Loop

The control rod drive mechanisms of the Yankee Reactor can be operated both manually and through an automatic control system. The starting up and shutting down of the reactor will be always done manually for safety consideration. But for power levels higher than 10% of full power, the reactor may be controlled through the

automatic system.

The control program chosen for the Yankee Reactor is the constant average temperature program. This program is not very satisfactory for the turbine for changing load, but was chosen both for safety, since it seconds the natural behavior of the reactor and heat exchanger, and because the plant is scheduled to operate as a base plant with an almost constant power output.

For such a program the actual average temperature is measured and is compared with the reference value, so that the error signal is obtained. This error after amplification is applied to the drive mechanisms input.

The component elements will now be considered in more detail. A general schematic drawing of the automatic control system is in Fig. 8.

2.3.1 The average temperature measurement and error computation

In the Yankee Reactor the measurement of the average temperature and error computation is obtained through the following steps:

1. by measuring the temperature at the inlet of the four heat exchangers with a resistance temperature detector, and choosing the highest value of the four through an auctioneer circuit.

2. measuring the temperature at the outlet of the four heat exchangers with a resistance temperature detector, and choosing the highest value of the four through an auctioneer circuit.

3. making the average of the highest inlet and outlet temperature and subtracting the reference temperature.

We first observe that instead of measuring the temperature at the inlet and outlet of the core, they are measured at the boiler[*]. In steady state conditions, if the losses of heat along the pipes are negligible or assumed to be equal in the hot and cold legs, there will be no difference between the two average temperatures. It will not be so under transient conditions and this will be considered later

---

[*] Probably for simplicity of installation.

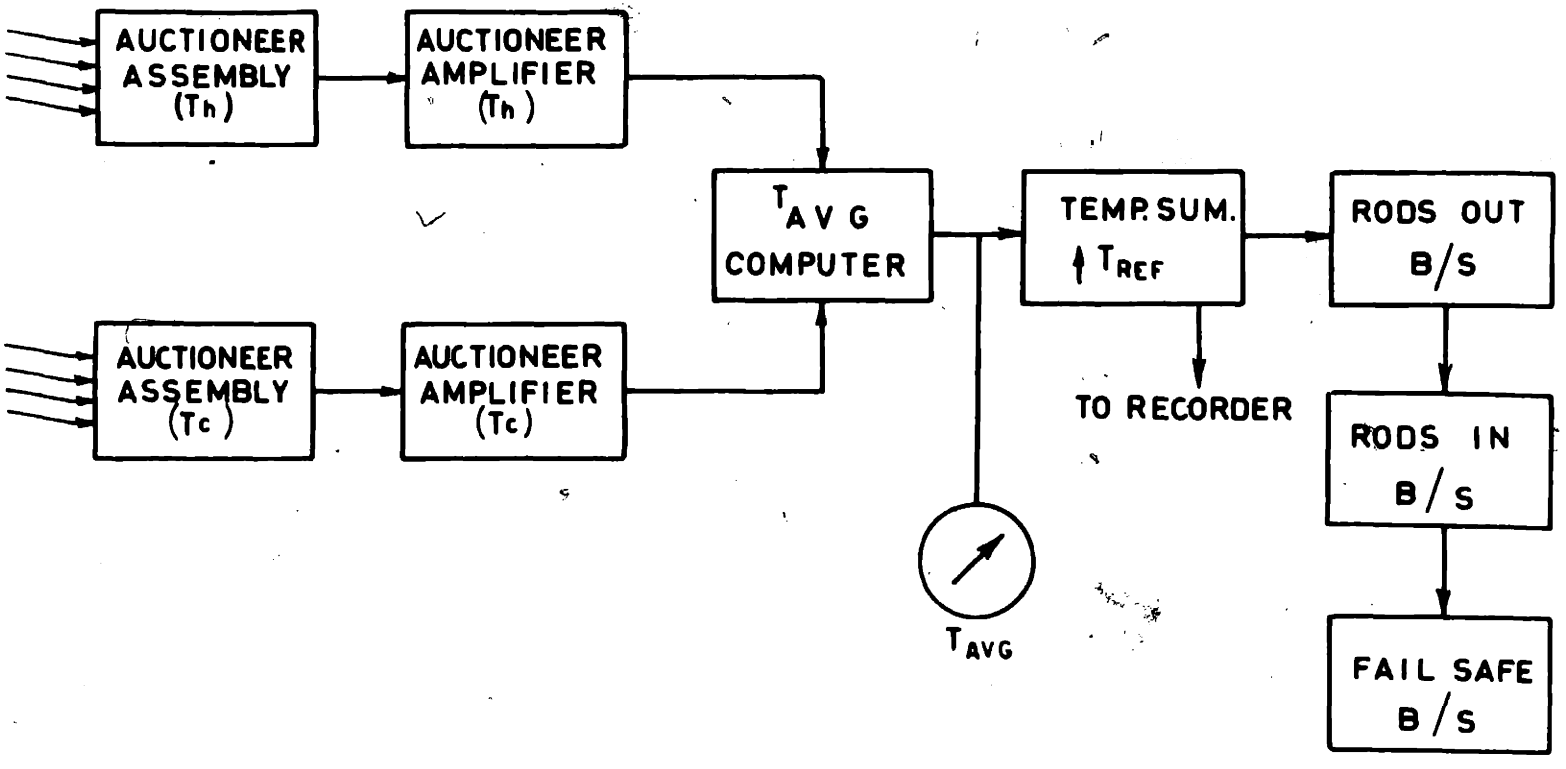

REACTOR SERVO CONTROL

FIG. 8

in this study.

The auctioneer circuits are introduced for safety. In this way the highest value of the average temperature is measured.

The temperature detectors are high speed resistance thermometers (Bailey Meter Co.). The constant of the detecting element is

$$\frac{dR}{dT^\circ} = 0.0333\,\Omega/^\circ F$$

in the range $0 \div 700^\circ F$. The characteristic curve is linear within $\pm 0.5^\circ F$.

The speed of response, defined as the time necessary to reach the 63.2% of a step change in water flowing at 3 ft/sec, is 2.5 secs.

The transfer function for the temperature detector will be assumed to be

$$\frac{V(s)}{T(s)} = \frac{k}{1 + 2.5s}$$

where V is the output voltage of the detector, volts
T is the measured temperature, °F
k is a constant of which it is not necessary to know the actual value, as it will be shown later.

In writing this expression for the transfer function of the temperature detector, it was assumed implicitly that the only significant time constant involved was that of the resistance element, and that the associated bridge and amplifying system have flat response. This simplification is justified by the fact that, as will be seen later, time constants less than 0.1 seconds do not influence the dynamic behavior of the system .

The auctioneer and the average temperature and error computer are realized with static components (junction diodes and resistances) for safety and for the same reason indicated above their transfer functions can be assumed to be frequency independent pure gains. The same will be said of the auctioneer amplifier which will be represented by a constant. As already mentioned, the knowledge of

the actual values of such constants is not necessary.

2.3.2 The amplification

As was written in the description of the control rod drive mechanism, the input of this device, which is a highly nonlinear element, is a relay. Furthermore the reactor and the steam generator complex alone, for the strong negative temperature coefficient was shown to be highly stable. These two considerations and the necessity of insuring great dependability have suggested the use of two bistable magnetic amplifiers to operate the rods-in and rods-out relays. The first (rods-in) switches-on when the average temperature error exceeds +3°F and switches-off when it is reduced to +2.5°F. The second (rods-out) switches-on for an error of -3°F and off for -2.5°F.

The idea of exploiting as much as possible the inherent stability of the reactor and steam generator alone for small disturbances would have suggested a larger dead zone, but the specifications for a satisfactory performance of the turbine had limited the value of the admissible error[※].

On the basis of the values of the switching currents and of the hysteresis of the magnetic amplifiers, their bias voltage and the value of the gain of the temperature detector were settled so that the indicated dead zone and hysteresis amplitude were realized. This explains why it was written before that the knowledge of the values of the gain of the temperature detector, of the auctioneer amplifier and of the average and error temperature computer were not actually necessary.

Since the specifications on the dead zone and on the hysteresis value are known directly in degrees of temperature error, we can consider that it is this temperature error which directly operates the bistable-magnetic amplifier while the overall gain between this error and the amplifier is one.

※ It is possible however to change those values.

The switching event in a bistable magnetic amplifier does not appear instantaneously.

The value of this switching time for the amplifier used in the Yankee Reactor was not available so that data given in the literature will be used.

In a study done by L. A. Finzi and G. C. Feth[6] it was derived that the time necessary to pass from one state to the other in a bistable magnetic amplifier is inversely proportional to the input signal and ranges between 1 and 10 seconds. This is a further non linearity in the system. However for our calculation this delay time will be assumed to be constant and equal to 2 seconds[※]. The output of the bistable amplifier is chosen large enough to operate the input relays of the control drive mechanisms.

2.4 Control Loop Block Diagram

On the basis of the previous conclusions it is now possible to resume, as in Fig. 9, the information necessary for the study of the dynamic behavior of the control loop of the Yankee Reactor. Only one equivalent loop is considered and the auctioneer circuits are disregarded.

The scheme includes two pure time delays and two nonlinear elements which make the study very complicated. The system, however, can be fairly well approximated through the following steps:

1. The two pure time delays are added and transferred before the bistable magnetic amplifier. This approximation is justified by the consideration of the actual physical system. Since all the operations are switching events, it does not matter when the delay appears, before or after the switch.

2. The second step is to approximate the total time delay (3.6 seconds) with a tranfer functio[n] of the form

$$\frac{1}{1 + 3.6s}$$

※ The exciting signal will always be larger than a certain minimum necessary to trigger the amplifier and, for our study where only small variations are considered, never too large.

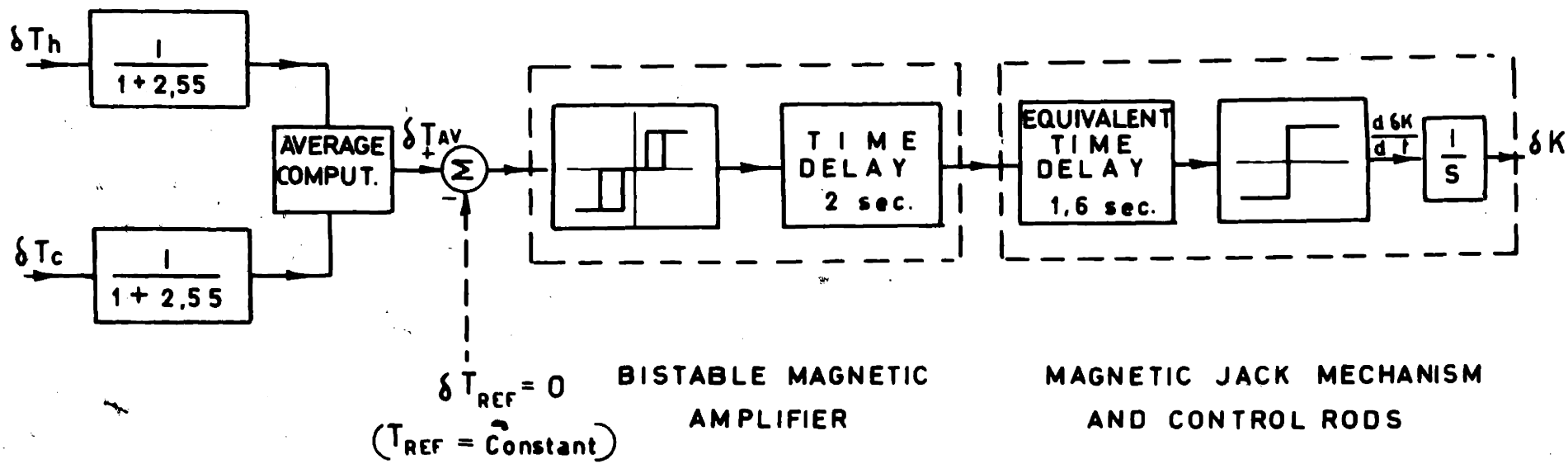
δTh
1 / 1+2,55
δTc
1 / 1+2,55
AVERAGE COMPUT.
δTAV
Σ
+
−
δTREF = 0
(TREF = Constant)
TIME DELAY 2 sec.
EQUIVALENT TIME DELAY 1,6 sec.
d δK / d t
1 / S
δK
BISTABLE MAGNETIC AMPLIFIER
MAGNETIC JACK MECHANISM AND CONTROL RODS

FIG. 9

3. The third step is to combine the two non-linearities: the bistable magnetic amplifier, and the magnetic jack drive and the control rods in only one non linear element with a characteristic function as in Fig. 10.

Though this third step is self evident, it can be easily understood if the blocks of Fig. 11 are considered. We observe that, since the output of the first non-linear element is the input of the second, when the first switches — on or off the second does the same without any delay.

The overall system from the error signal to the reactivity variation can be, hence, represented by the block diagram of Fig. 12.

As a conclusive observation it will be noted that the only real approximation done so far in the representation of the automatic control loop is that involved with the pure time delays, both for the uncertainty on the actual values of such time delays and for the approximation made in the derivation of their transfer function.

2.5 The Complete Block Diagram

It is possible now to draw the complete block diagram for the reactor, heat exchangers, and automatic control system, as in Fig. 13.

The resulting block diagram is too complicated for a direct analytical approach, and the necessity of approximating it appears evident.

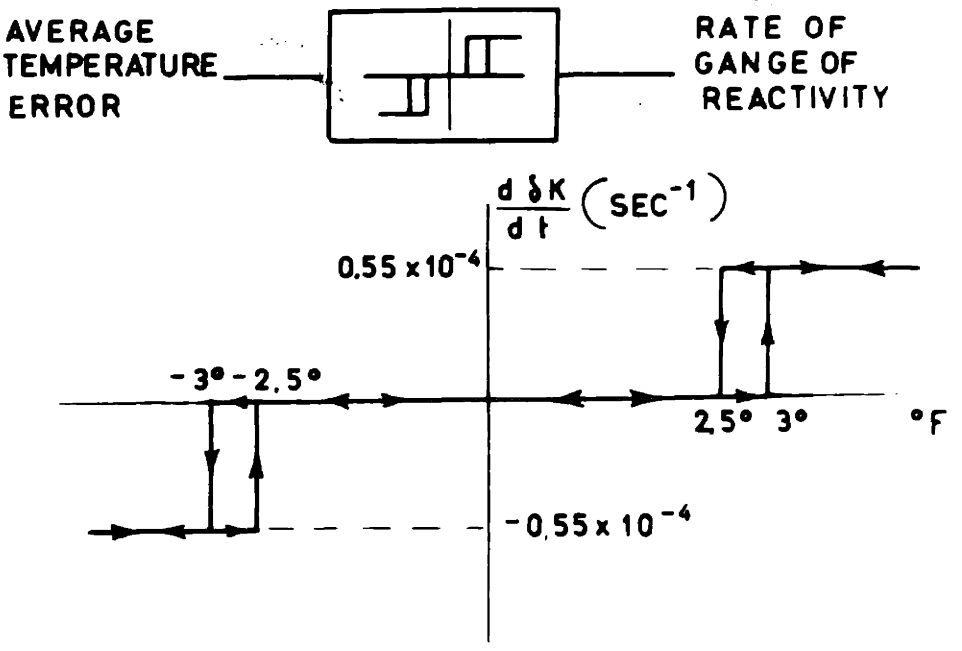
AVERAGE
TEMPERATURE
ERROR
RATE OF
GANGE OF
REACTIVITY
$\frac{d\,\delta K}{d\,t}$ (SEC^{-1})
0.55 x 10^{-4}
-3° -2.5°
2.5° 3°
°F
-0.55 x 10^{-4}

FIG. 10

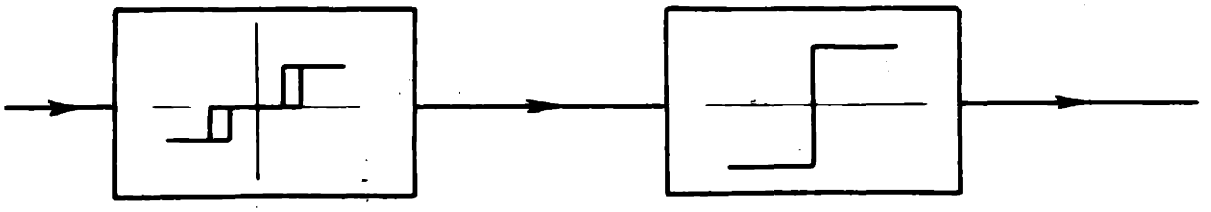

FIG. 11

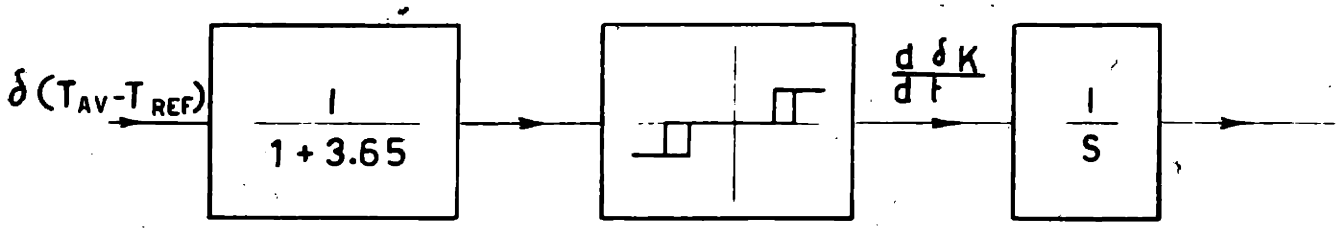

FIG. 12

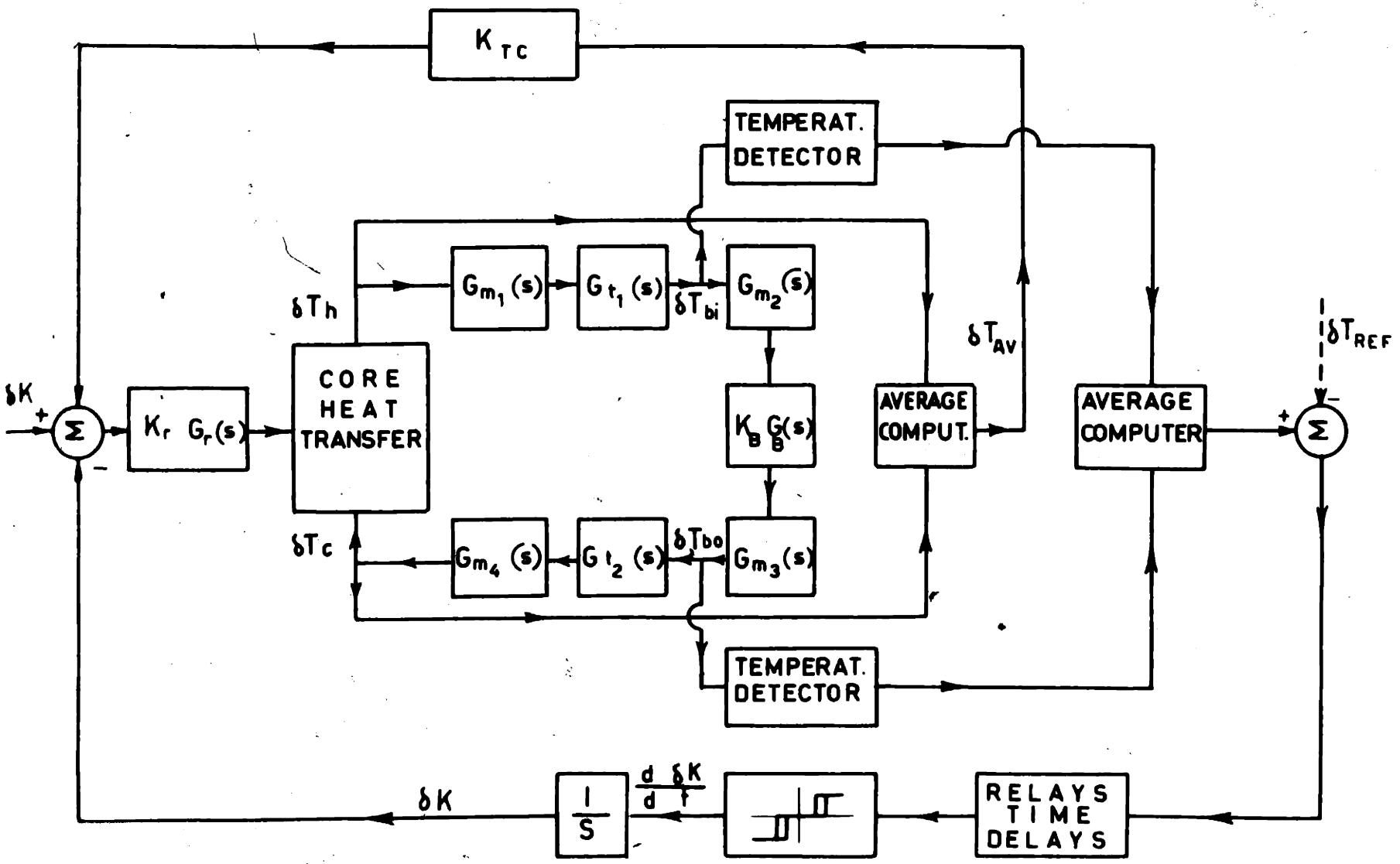
K TC
TEMPERAT. DETECTOR
δTh
Gm1 (s)
Gt1 (s)
δTbi
Gm2 (s)
δTAV
δTREF
δK
Σ
Kr Gr(s)
CORE HEAT TRANSFER
KB GB(s)
AVERAGE COMPUT.
AVERAGE COMPUTER
Σ
δTc
Gm4 (s)
Gt2 (s)
δTbo
Gm3 (s)
TEMPERAT. DETECTOR
δK
1/S
d δK / d t
RELAYS TIME DELAYS

FIG. 13

CHAPTER III

3.1 Approximation of the Block Diagram

As was written before, the block diagram derived is too complicated for an analytic study. This is true because the system has many elements and more than one feedback loop, with a non linear element in one of the loops. However, if a simplification is introduced the block diagram can be reduced to a form that may be studied in a fairly simple way. The simplification that will be assumed is that the temperature detectors, instead of measuring the inlet and outlet temperatures at the boilers, as they actually do, they measure the inlet and outlet temperature at the core.

This approximation can be interpreted on the block diagram through the following steps. First, rearrange the block diagram as in Fig. 14. Second, the time delays $G_{m_1}(s)$ and $G_{t_1}(s)$ in branch $A-B$ and the time lead $1/G_{m_4}(s)$ and $1/G_{t_2}(s)$ in branch $C-B$ are disregarded. Physically this amounts to disregarding the effect of pipe transport time and of the mixing in the inlet and outlet of the reactor, in so far as the measurements of the temperatures for the automatic control are concerned. With this simplification, branch $A-B$ and branch $C-D$ in Fig. 14 become identical since the temperature detectors are equal.

The block diagram between points ABEDC can be redrawn as in Fig. 15, where the temperature detector block is passed after the average temperature computer. Doing this we simply rearrange the block diagram because the operation of average is merely an addition of halves.

The complete block diagram can now be drawn as in Fig. 16. In this form the reactor and the heat exchanger have both temperature coefficient feedback and automatic control feedback in parallel.

From the Bode diagram of the open loop transfer function of the reactor, heat exchanger and temperature coefficient feedback, the

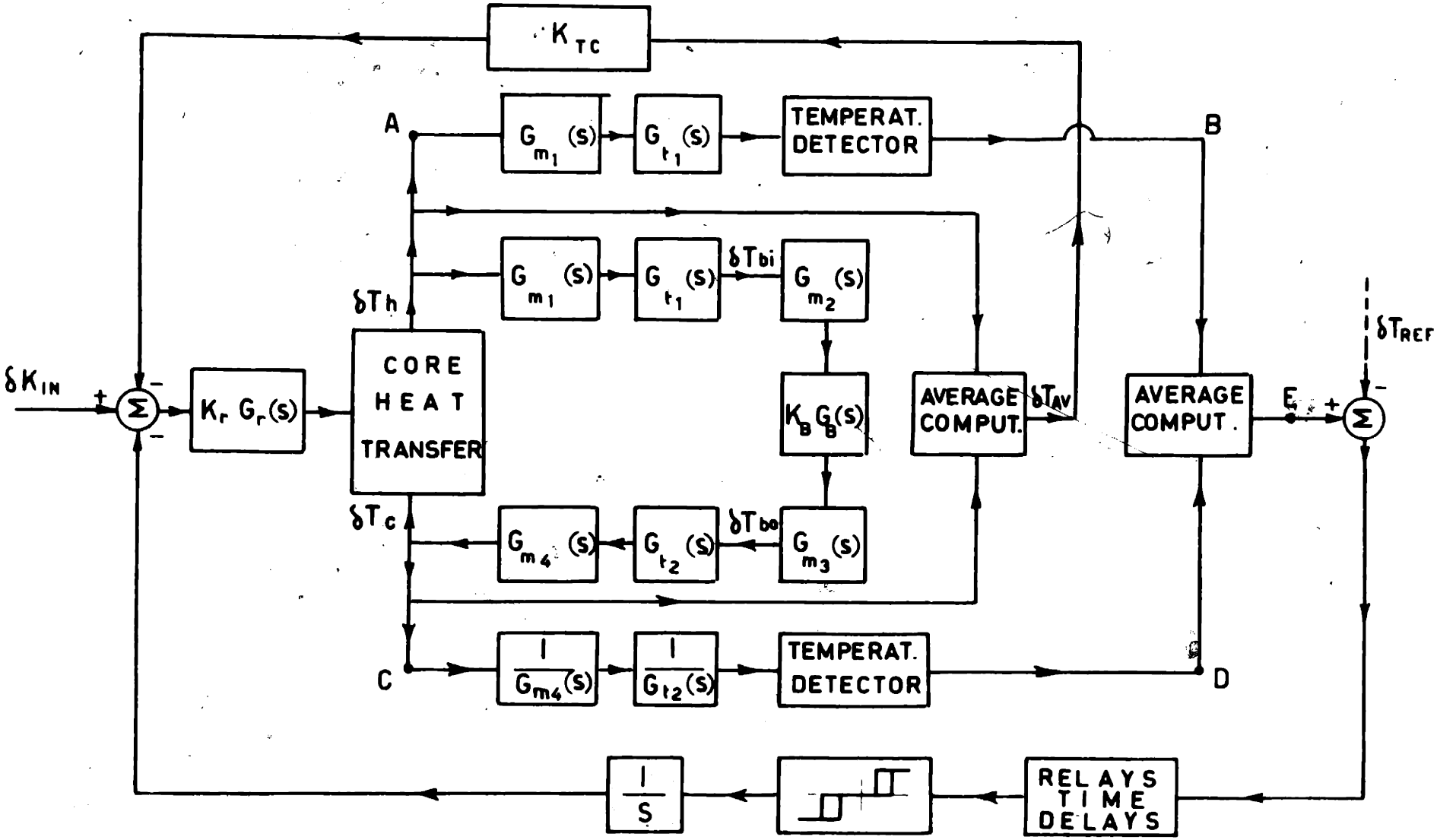
K_{TC}
A
$G_{m_1}(s)$
$G_{t_1}(s)$
TEMPERAT. DETECTOR
B
δT_{bi}
$G_{m_2}(s)$
δT_h
δK_{IN}
$K_r G_r(s)$
CORE HEAT TRANSFER
$K_B G_B(s)$
AVERAGE COMPUT.
δT_{AV}
AVERAGE COMPUT.
E
δT_{REF}
δT_c
δT_{bo}
$G_{m_4}(s)$
$G_{t_2}(s)$
$G_{m_3}(s)$
C
$\frac{1}{G_{m_4}(s)}$
$\frac{1}{G_{t_2}(s)}$
TEMPERAT. DETECTOR
D
$\frac{1}{S}$
RELAYS TIME DELAYS

FIG. 14

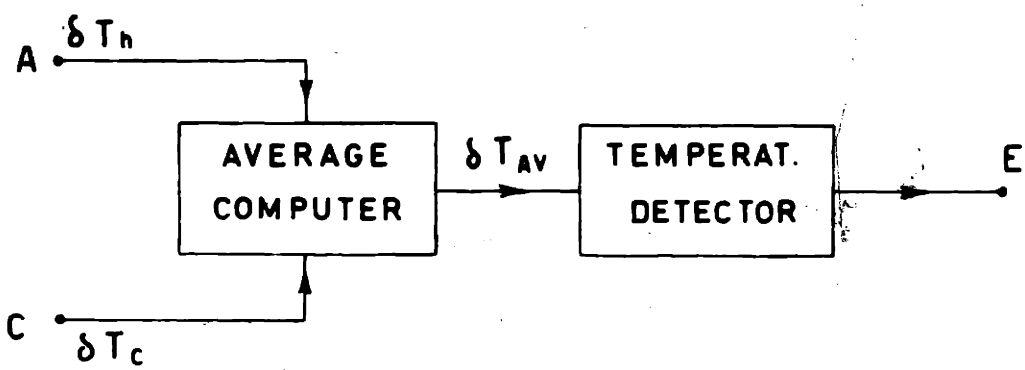

FIG. 15

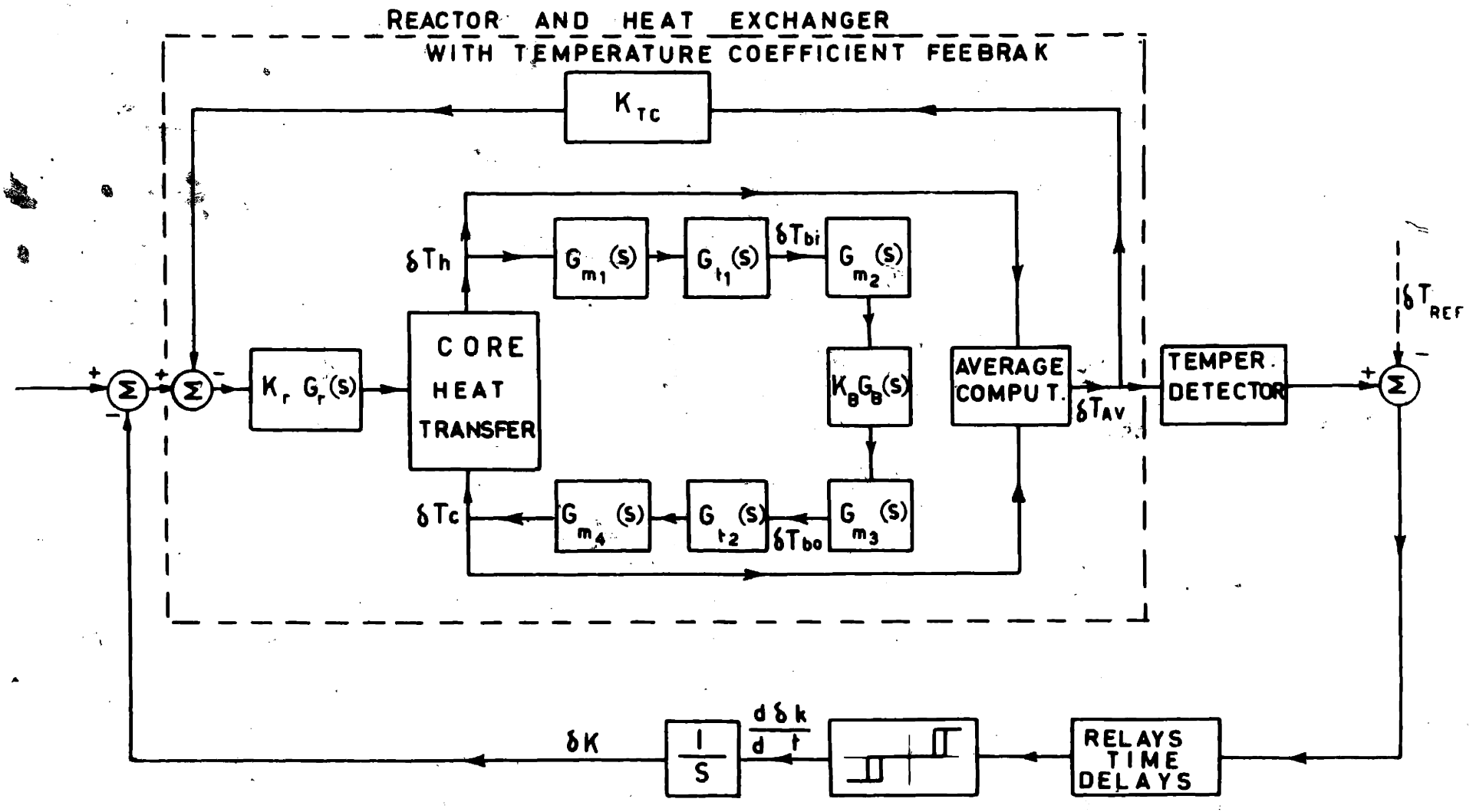
REACTOR AND HEAT EXCHANGER
WITH TEMPERATURE COEFFICIENT FEEBRAK
K_{TC}
δT_h
$G_{m_1}(s)$
$G_{t_1}(s)$
δT_{bi}
$G_{m_2}(s)$
δT_{REF}
$K_r G_r(s)$
CORE HEAT TRANSFER
$K_B G_B(s)$
AVERAGE COMPUT.
δT_{AV}
TEMPER. DETECTOR
δT_c
$G_{m_4}(s)$
$G_{t_2}(s)$
δT_{bo}
$G_{m_3}(s)$
δK
$\frac{1}{S}$
$\frac{d\delta k}{dt}$
RELAYS TIME DELAYS

FIG. 16

closed loop transfer function Bode diagram can be obtained very easily, with the help of Nichol's chart.

The overall block diagram is reduced to only one loop (Fig. 17) where all the elements but one are assumed linear. Since the system is of high degree, its stability and its dynamic behavior can be very well studied following the method suggested by Kochenburger[7]: the describing function approach.

Because of the complexity of the block diagram it is impossible to determine intuitively how the assumed simplification will affect the system, that is, whether the system will be improved or not. However it will be shown later that the range of frequencies which are relevant for the stability lies below $\omega = 0.1$ rad/sec. Hence, disregarding time constants smaller than 10 seconds will not appreciably affect the results.

3.2 Study of the Stability of the Reactor with the Automatic Control Feedback, by Means of the Describing Function Method

3.2.1 The describing function method

The idea at the basis of describing function technique, for the study of a non-linear system, is to linearize the input-output relation of the non-linear component in such a way that criteria of the frequency response method can be applied.

If a sinusoidal excitation is applied at the input of a non-linear element the output is not a pure sinusoid, but contains a fundamental of the same frequency of the input signal and high frequency components. The amplitude and the phase of the fundamental and of the harmonics are functions of the amplitude of the input signal but, in general, not of its frequency.

The approximation made in the describing function method is in considering only the fundamental and in disregarding the higher harmonics. This approximation is justified by two considerations:

1. The fundamental is in general predominant in amplitude,
2. This method is adopted only for systems in which the amplitude of the remaining open loop transfer function decrease rapidly with increasing frequency, so that the higher components are filtered.

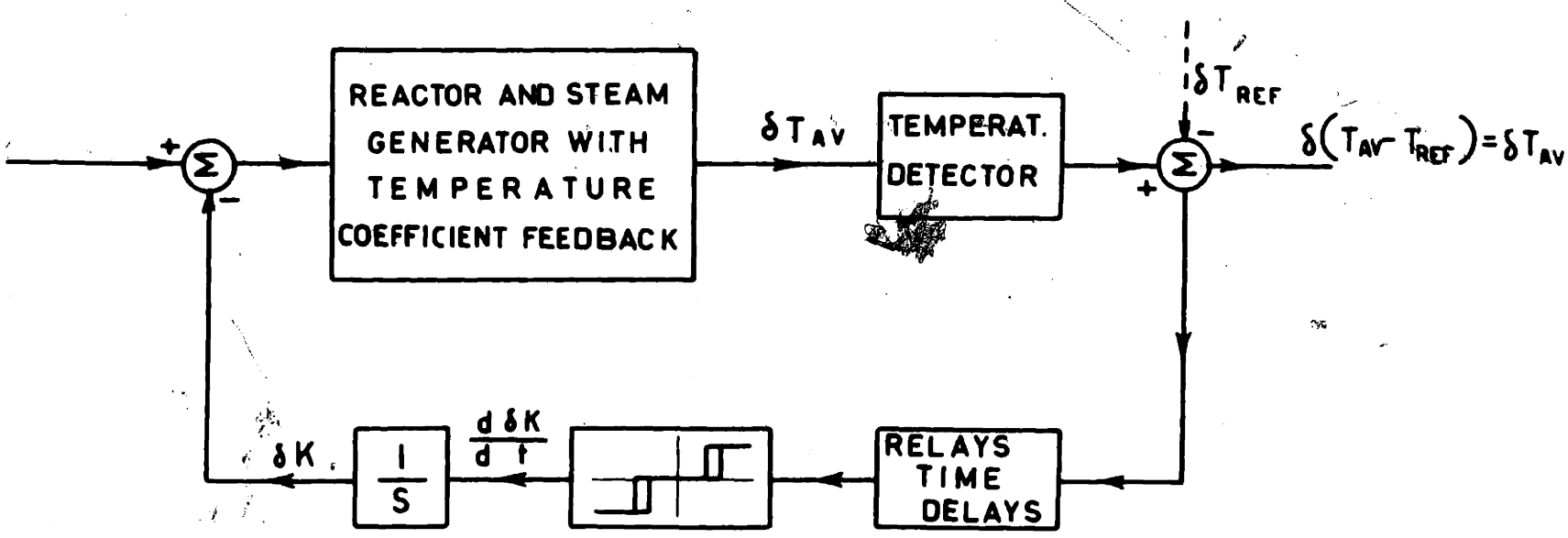
REACTOR AND STEAM GENERATOR WITH TEMPERATURE COEFFICIENT FEEDBACK
δT AV
TEMPERAT. DETECTOR
δT REF
δ(T AV - T REF) = δT AV
RELAYS TIME DELAYS
d δK / d t
δK
1/S

FIG. 17

The relation between amplitude of the input signal and amplitude and phase of the fundamental of the output signal is defined as the describing function of the non-linear element.

The reason for such an approximation is that through the describing function it is possible to extend to non-linear systems criteria of the linear ones as the Nyquist criterion. This method is however limited to systems with only one non-linearity and with an open loop transfer function for the linear elements with amplitudes rapidly decreasing with frequency (the denominator of higher degree than the numerator).

While for the general discussion of such methods we refer to the original paper of Kochenburger[7], the conditions of stability of our system will be discussed in detail, observing that it differs from the general case considered by Kochenburger, both because the non-linear element is in the feedback loop and because the open-loop transfer function of the linear part has two zeros in the right half plane.

3.2.2 The stability conditions

Say $K_T G_T$ — the open loop transfer function of the reactor, heat exchanger and temperature coefficient feedback (as on page 15)

K_{TC} — the temperature coefficient

$H(s)$ — the transfer function of the frequency dependent part of the automatic control feedback

$g(|c|)$ — the describing function of the non-linear element (it is function only of the amplitude, not of the frequency)

From the previous calculation it was found that

$$K_T G_T(s) = \frac{\text{tenth order polynomial (two r.h.p. roots)}}{\text{twelfth order polynomial}}$$

K_{TC} = a constant

$$H(s) = \frac{1}{\text{third order polynomial}}$$

The closed loop transfer function of the reactor and boiler with the temperature coefficient feedback is hence

$$G_R(s) = \frac{1}{K_{TC}} \cdot \frac{K_T G_T}{1 + K_T G_T} = \frac{\text{tenth order polynomial (two r.h.p. roots)}}{\text{twelfth order polynomial}}$$

The transfer function of the frequency dependent part of the control open loop is:

$$G_L(s) = G_R(s) \cdot H(s) = \frac{\text{tenth order polynomial (two r.h.p. roots)}}{\text{fifteenth order polynomial}}$$

and hence:

$$\frac{1}{G_L(s)} = \frac{\text{fifteenth order polynomial}}{\text{tenth order polynomial (two r.h.p. roots)}}$$

The closed loop transfer function for the reactor with automatic control feedback, introducing the describing function, is:

$$\frac{T_{av}(s)}{k(s)} = \frac{G_R(s)}{1 + H(s)\, G_R(s)\, g(|c|)} = G(s, |c|)$$

which can be also written

$$G(s, |c|) = \frac{\frac{1}{H(s)}}{\frac{1}{G_L(s)} + g(|c|)}$$

The system will be stable if, for all the values of the signal amplitude at the input of the non-linear element, the expression $\frac{1}{G_L(s)} + g(|c|)$ has no right half-plane zeros.

This condition can be investigated by means of the Nyquist criterion, in the following manner.

$1/G_L(s)$ is plotted on the s-plane, with s as parameter varying on the usual contour for Nyquist's plot (on the $j\omega$ axis and on a semi-circle in the r.h.p. with the center in the origin and the radius approaching infinity). On the same diagram $-g(|c|)$ is plotted with $|c|$ as parameter varying from zero to infinity. The plot of $1/G_L(s) + g(|c|)$ for each value of $|c|$ ($g(|c|)$, we recall, is independent of frequency) is obtained simply by transferring (ideally) the origin of the plot of $1/G_L(s)$ in the point $-g(|c|)$.

For the system to be stable no zeros of $1/G_L(s) + g(|c|)$ are allowed in the right half plane. This condition will be satisfied if, for all values of $|c|$, the origin of the plot of $1/G_L(s) + g(|c|)$, i.e., all the points of the plot of $-g(|c|)$, are encircled twice by the plot of $1/G_L(s)$ in the counterclockwise direction, since the function $1/G_L(s)$ has two poles in the right half-plane.

3.2.3 Inverse of the transfer function of the frequency dependent part of the open loop

The automatic control loop includes, as can be seen in Fig. 17, the following linear-element blocks: 1. the reactor and heat exchanger with the temperature coefficient feedback, 2. the temperature detector, 3. the relays time delay, 4. the block corresponding to the integration factor $1/s$.

The amplitude and phase diagram versus frequency of the block including the reactor and the heat exchanger with the temperature coefficient feedback can be easily derived (as already written) from the Bode diagrams of the open loop transfer function included at the beginning of the thesis, using a Nichol's chart. They are plotted in Diagram II.

The transfer function of the remaining linear elements is obtained combining the single transfer functions derived in the previous pages.

For the sake of simplifying the calculation of the describing function for the non-linear element, we will assume that its output

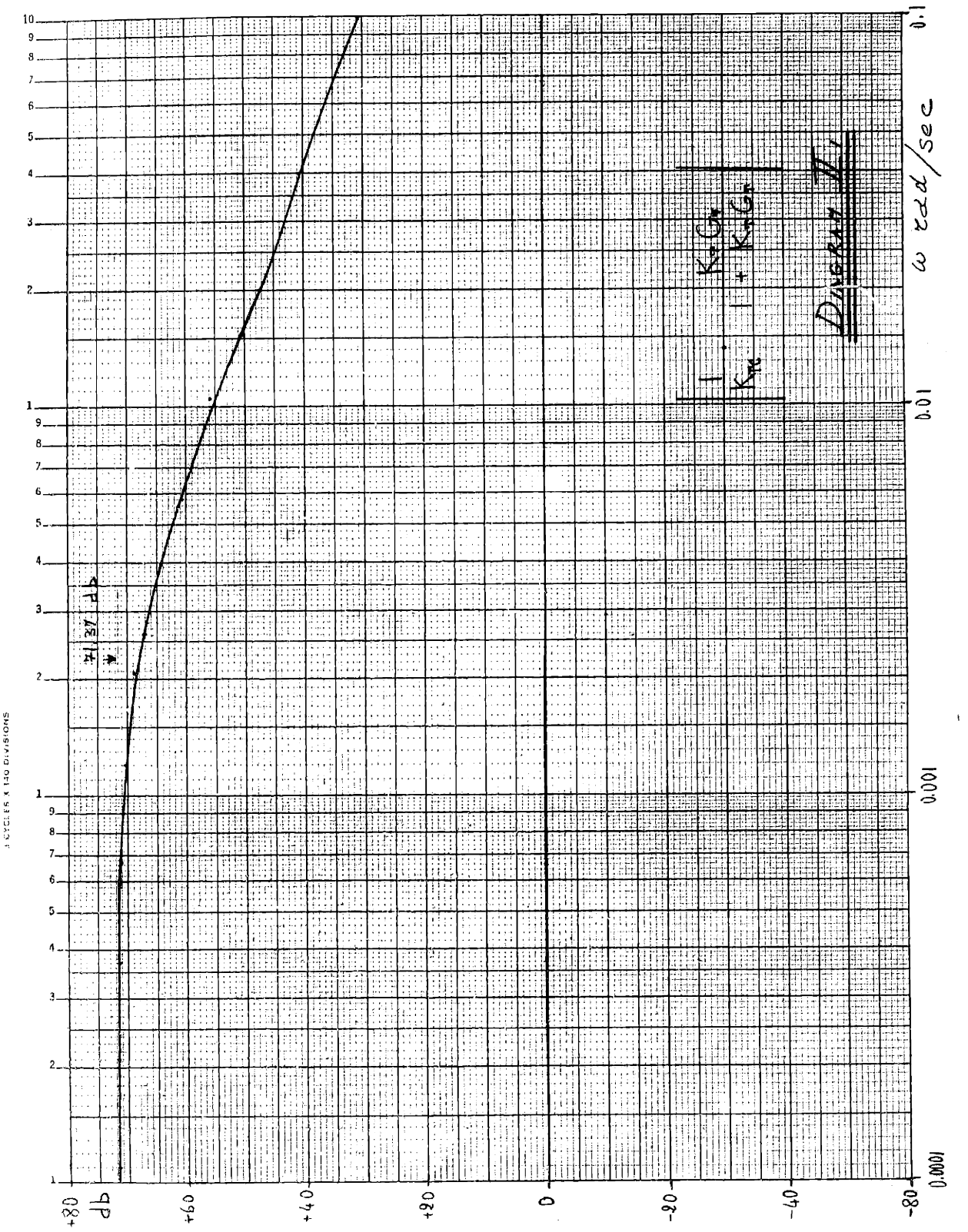
10
9
8
7
6
5
4
3
2
1
9
8
7
6
5
4
3
2
1
9
8
7
6
5
4
3
2
1
+80
+60
+40
+20
0
-20
-40
-80
dB
0.1
0.01
0.001
0.0001
ω rad/sec
Diagram
1 + K₀G₀
1 + K₁G₁
4
<P 45°
CYCLES X 140 DIVISIONS

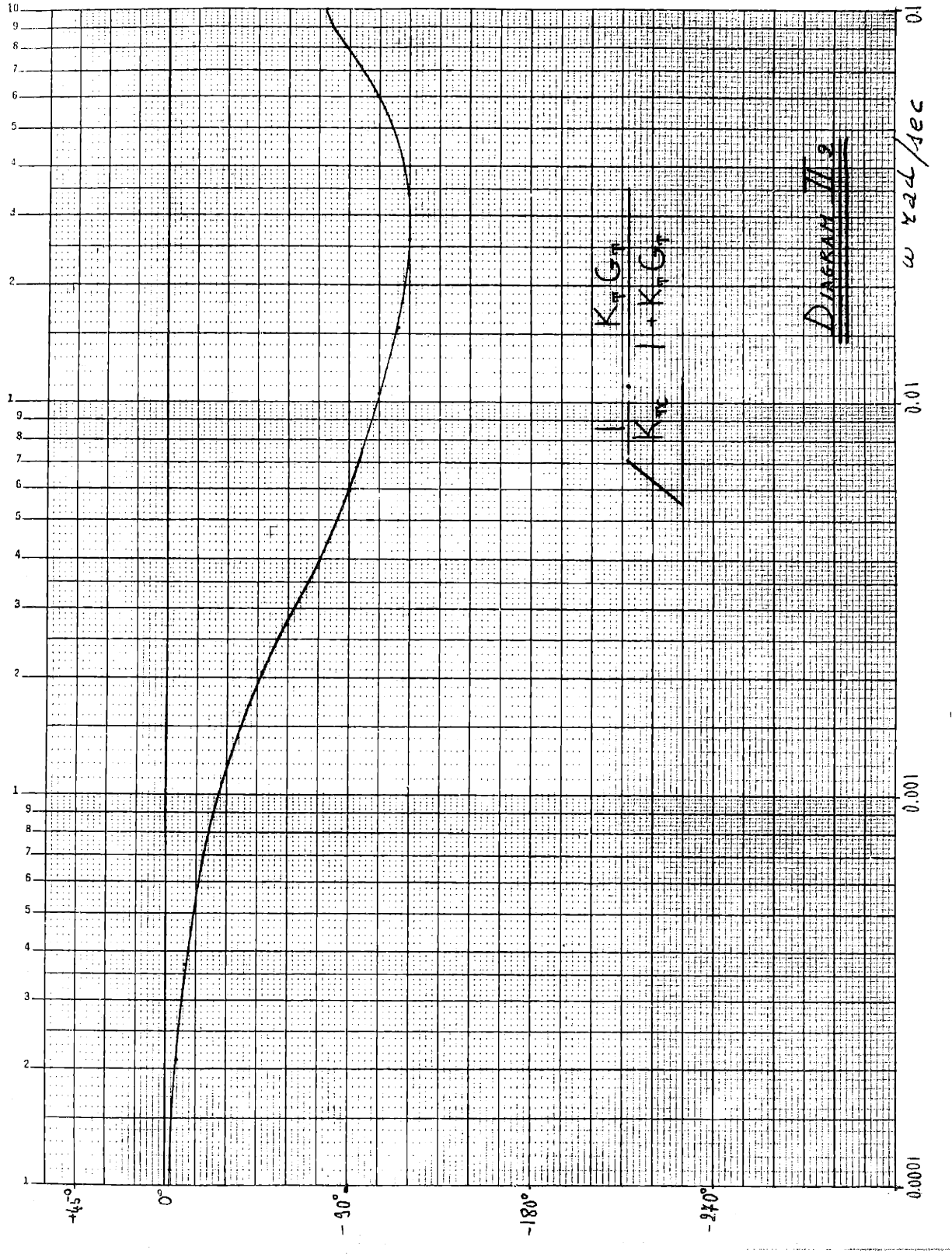
$\frac{1}{K_T}\cdot\frac{K_T G_T}{1+K_T G_T}$
Diagram III-8
rad/sec ω
0.0001
0.001
0.01
0.1
1
10
0°
-90°
-180°
-270°
+45°
-45°
CYCLES X 140 DIVISIONS

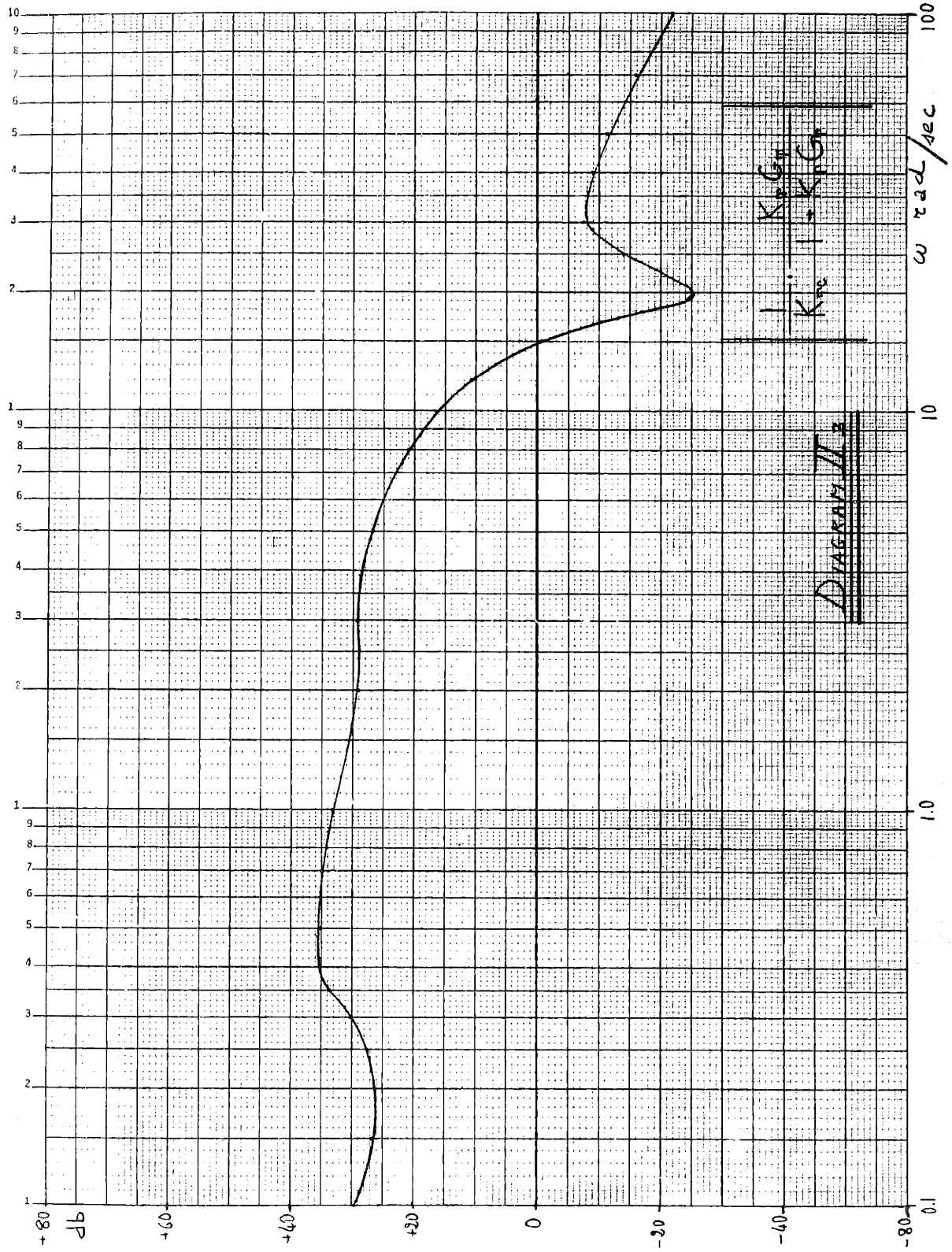
+80
+60
+40
+20
0
-20
-40
-80
dB
100
10
1.0
0.1
ω rad/sec
$\frac{K_P G_H}{1 + K_{FC}}$
Diagram #3

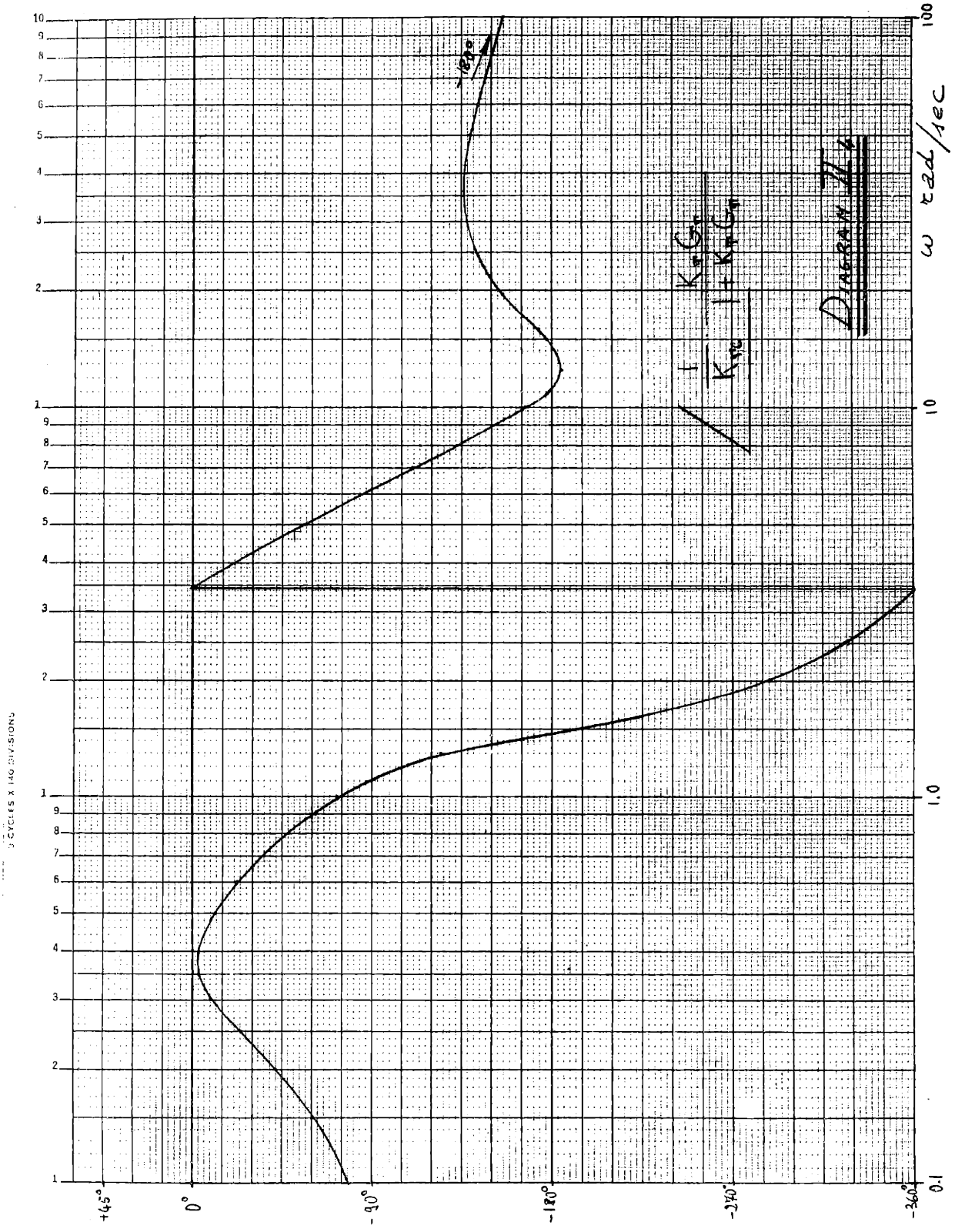
-180°
$\frac{K_a G_s}{1+K_a K_t G_s}$
$\frac{1}{K_t G_s}$
Diagram No. 4
ω rad/sec
100
10
1.0
0.1
+45°
0°
-90°
-180°
-270°
-360°
5 CYCLES X 140 DIVISIONS

is unity and a pure gain equal to 0.55×10^{-4} (the actual value of the constant rate of change of reactivity introduced in the core when rods are moved) is added after the non-linear element itself. Of course, this is a pure mathematical manipulation.

The expression for the transfer function of the frequency dependent part of the automatic control is thus:

$$H(s) = \frac{0.55 \times 10^{-4}}{s(1 + 2.5s)(1 + 3.6s)} \quad \text{※}$$

The Bode diagram of this function is in Diagram III.

By merely adding Diagrams II and III, one obtains the Bode diagram of the transfer function of the frequency dependent part of the open loop. Now it is observed that the magnitudes in the Bode diagrams are in decibels (20 times the logarithm) so that the inverse is simply obtained by changing sign. Likely, the phase of the inverse of a complex number equals the phase of the given number changed of sign.

Hence, to obtain the Bode diagram of the inverse of the transfer function of the frequency dependent part of the open loop, one simply revolves the diagram obtained by adding Diagrams II and III, about the axis of the abscissas. This corresponds to a change of sign. The resulting diagram is plotted directly in Diagram IV. From this diagram it is easy to derive Nyquist's plot of $1/G_L(s)$.

3.2.4 Describing function of the non-linear element

From the calculations and assumptions done in the previous paragraphs, the relation between input and output of the non-linear element is as is shown in Fig. 18.

As derived in Kochenburger[7], the describing function for a contactor type non-linearity, having, as in our case, both an inactive

---

※ This relation was derived assuming: 1. small variation around an equilibrium point, 2. T_{ref} = constant so that $\delta T_{ref} = 0$. Hence T_{ref} does not appear in this transfer function.

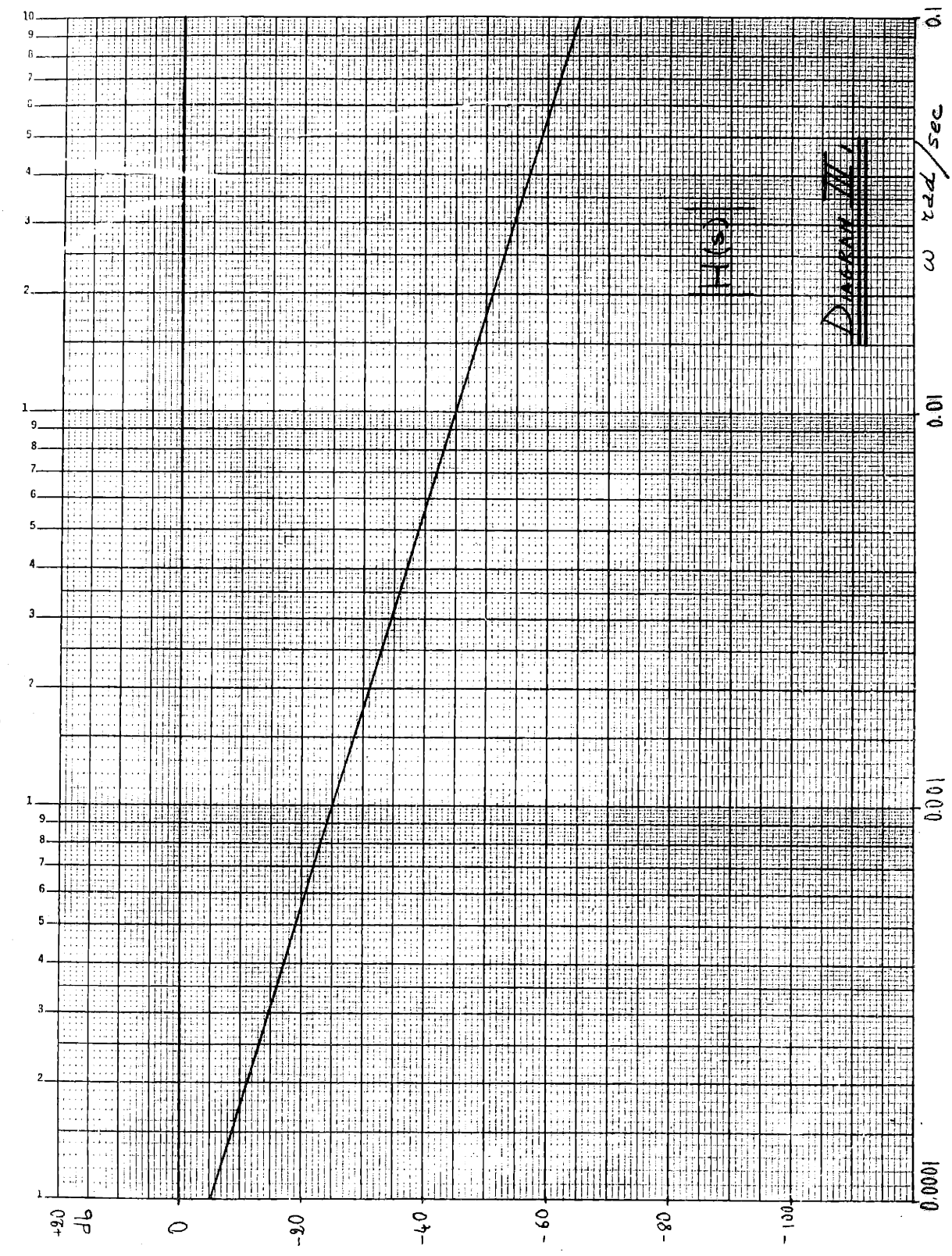
10
9
8
7
6
5
4
3
2
1
9
8
7
6
5
4
3
2
1
9
8
7
6
5
4
3
2
1
0.1
0.01
0.001
0.0001
ω rad/sec
DIAGRAM
H(s)
dB
+6.0
0
-3.0
-4.0
-6.0
-8.0
-10.0
: CYCLES X 140 DIVISIONS

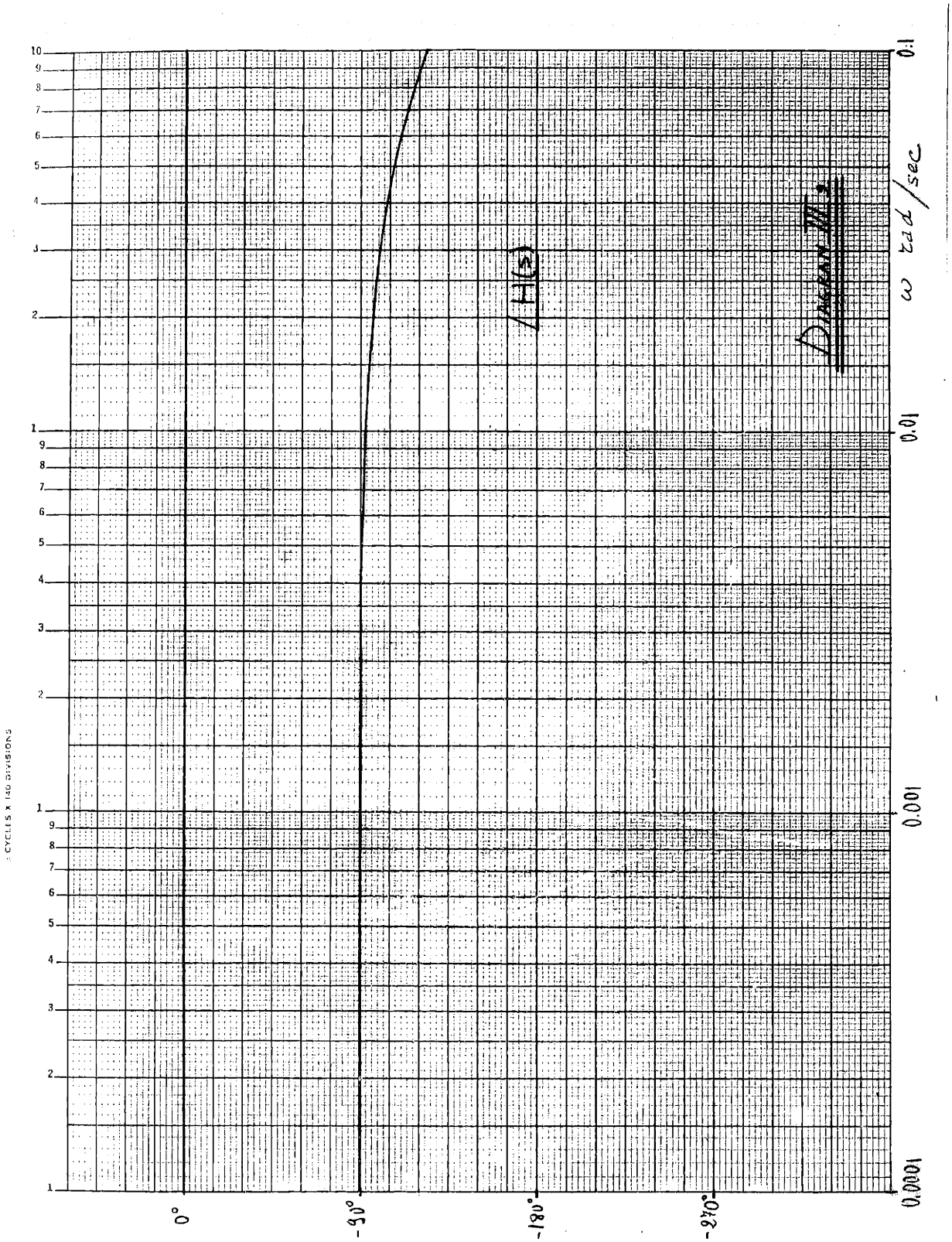
0°
-90°
-180°
-270°
0.1
0.01
0.001
0.0001
ω rad/sec
/F(s)
DIAGRAM III
CYCLES X 140 DIVISIONS

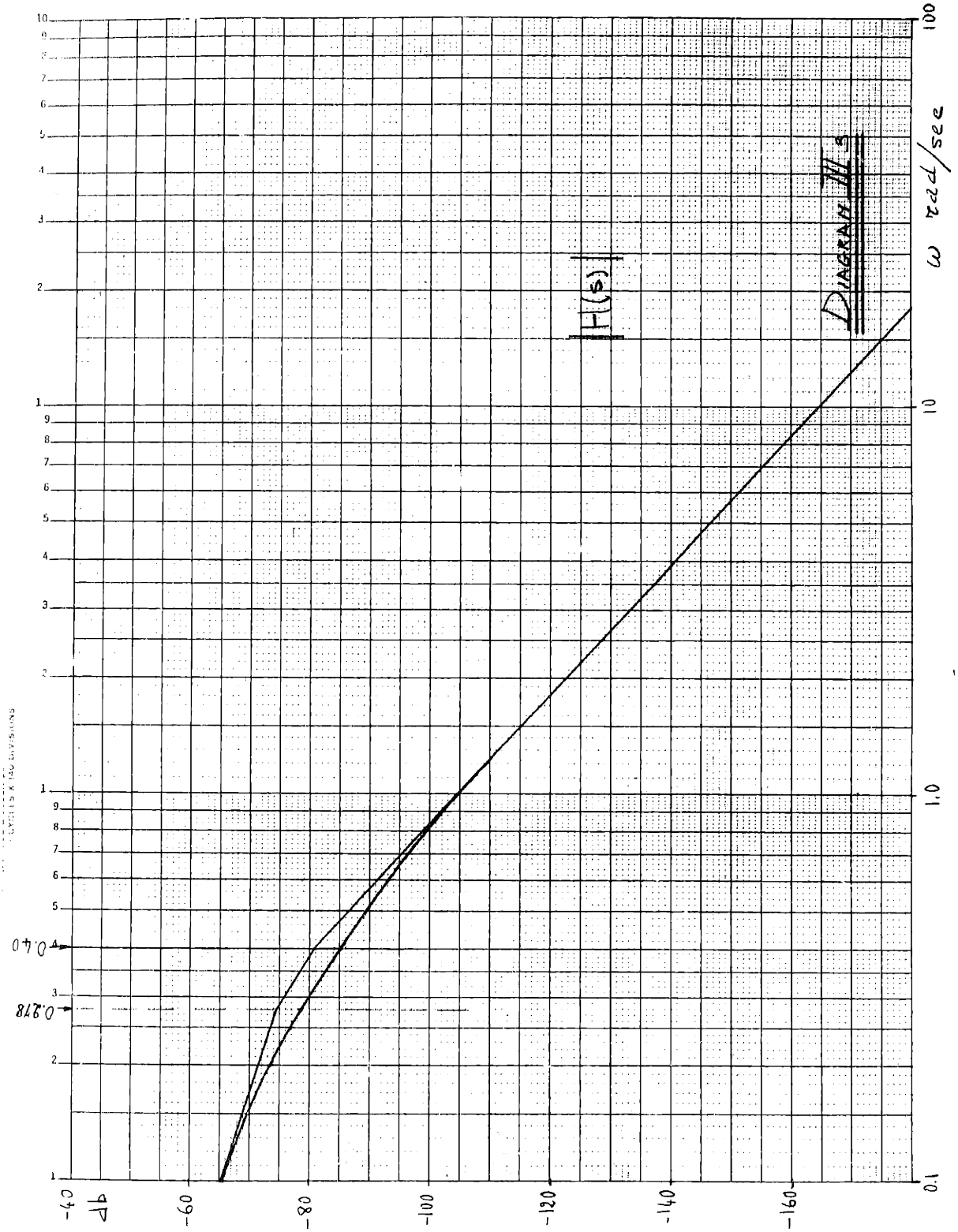
DIAGRAM III 3
|H(s)|
ω rad/sec
0.1
1.0
10
100
0.278
0.40
-40
-60
-80
-100
-120
-140
-160
dB

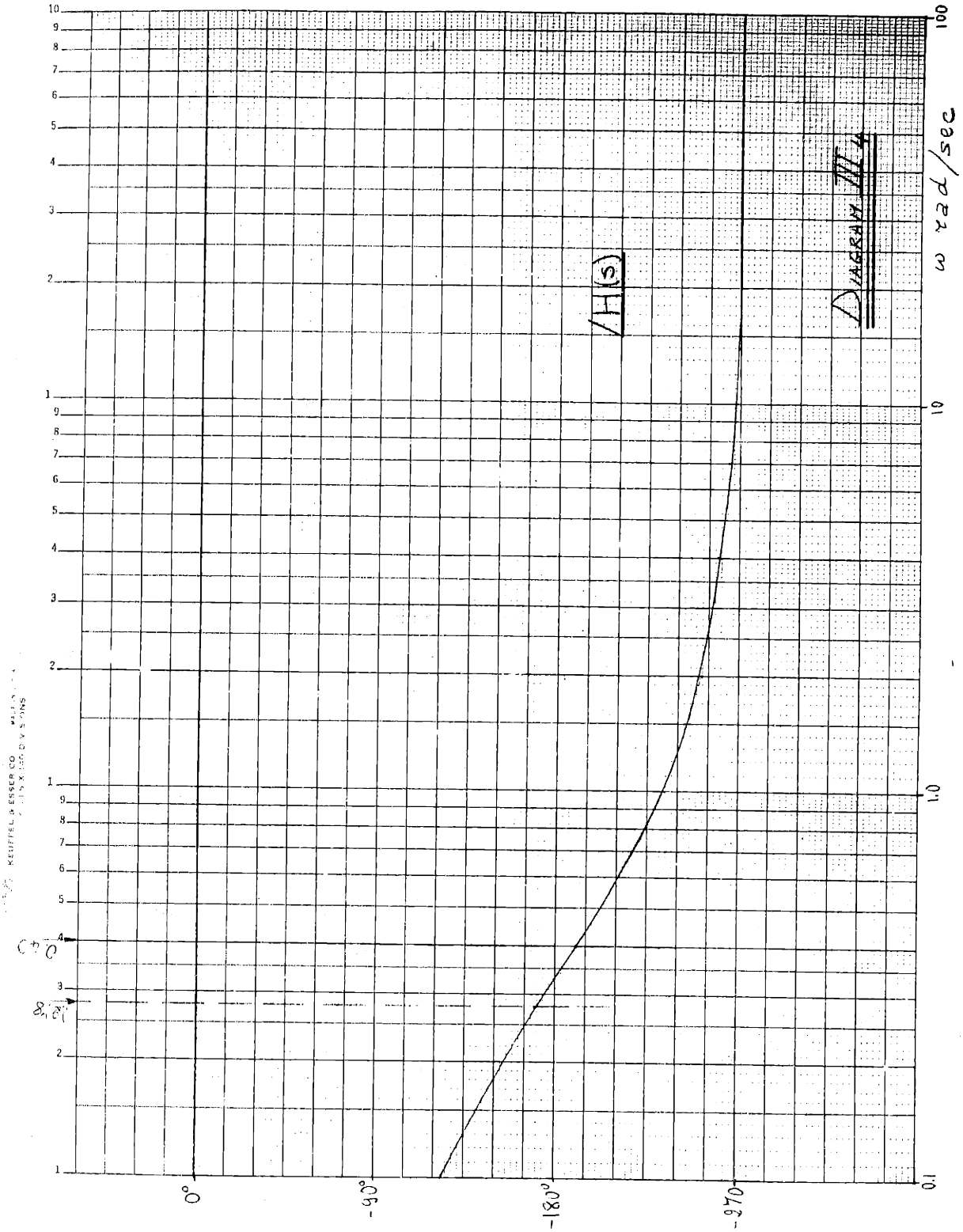
/H(s)
DIAGRAM III 4
rad/sec
0°
-90°
-180°
-270°
100
10
1.0
0.1

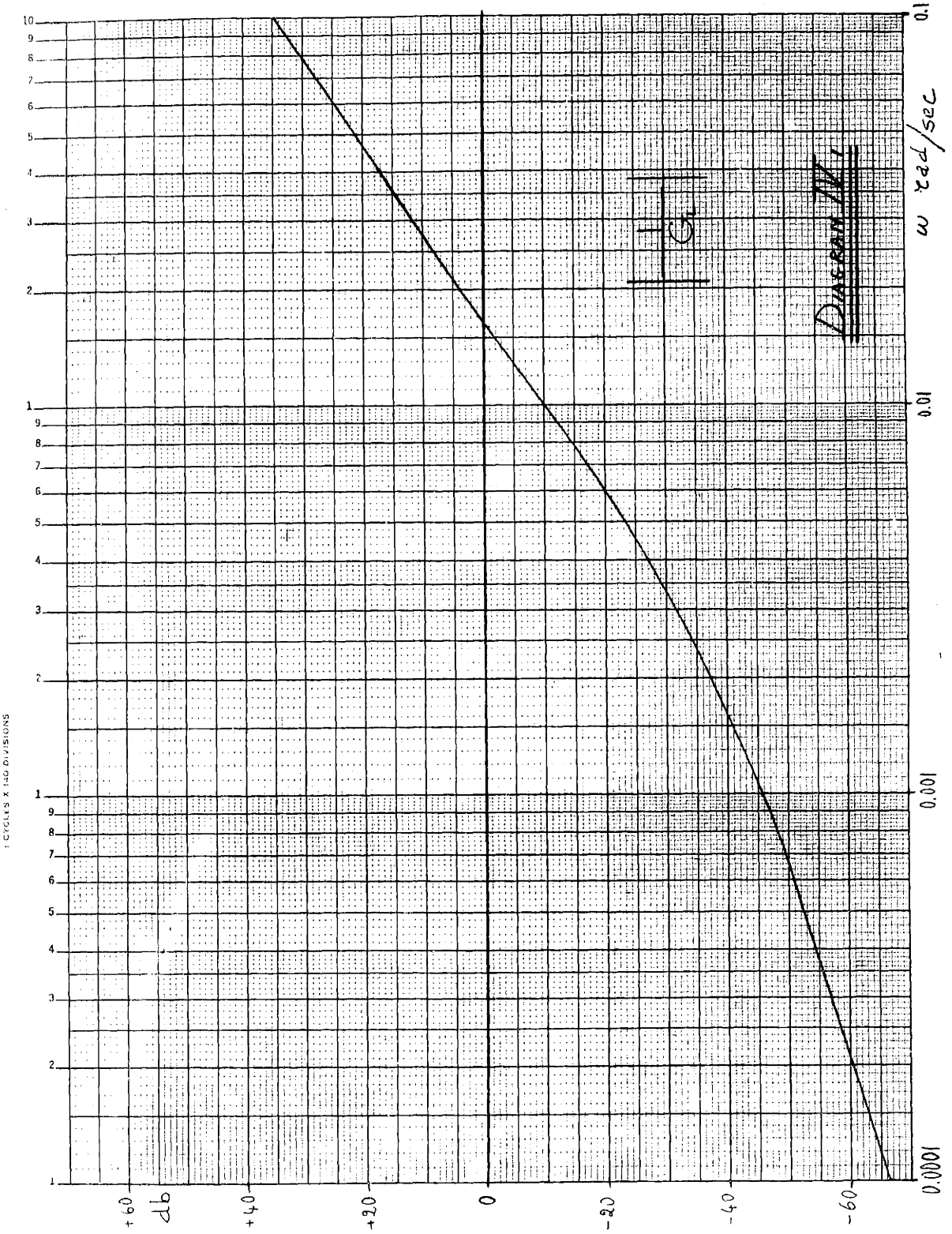
DIAGRAM III
rads/sec
0.1
0.01
0.001
0.0001
db
+60
+40
+20
0
-20
-40
-60
1 CYCLES X 140 DIVISIONS

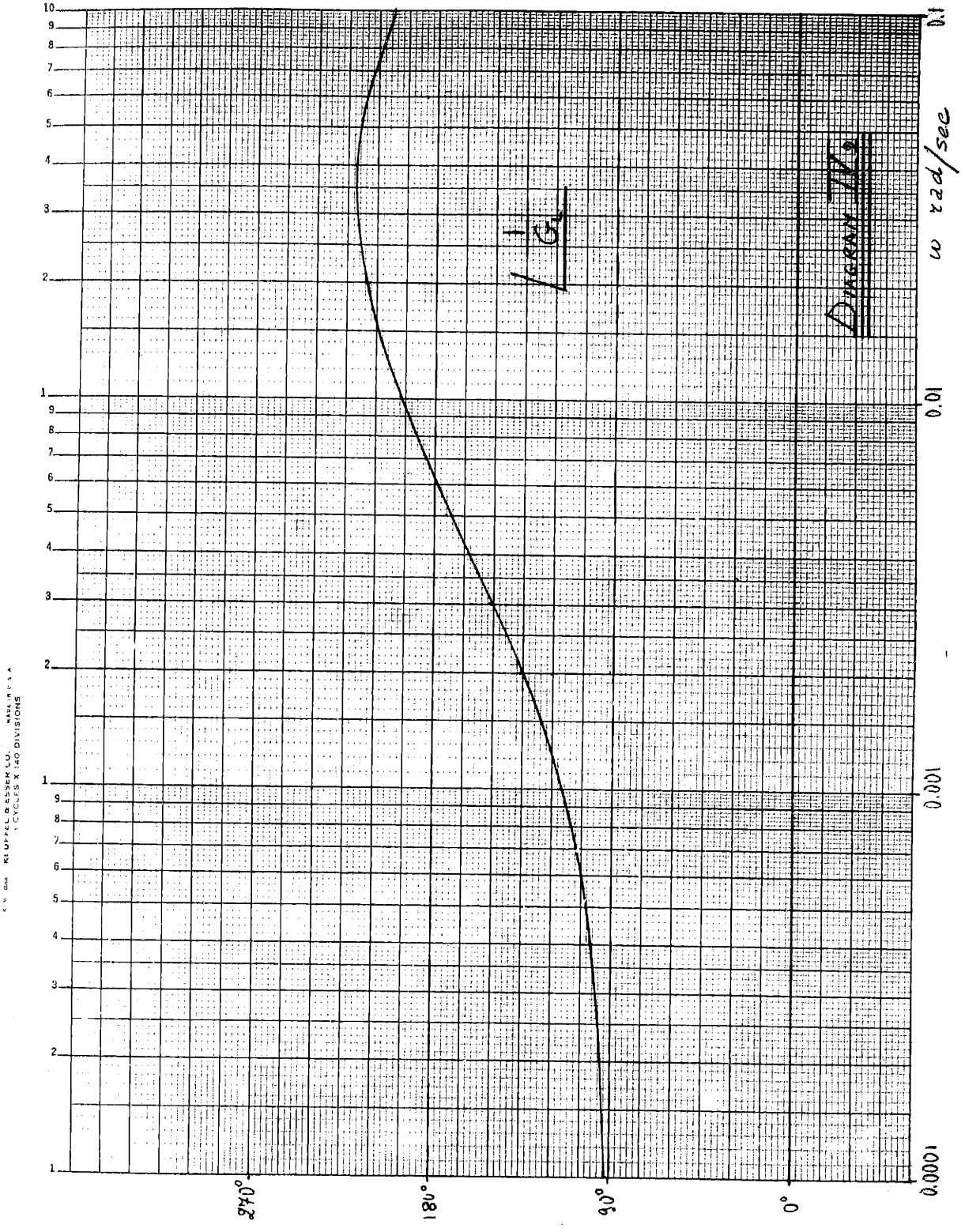
Diagram No. 3
$-G_{jw}$
ω rad/sec
0.0001
0.001
0.01
0.1
0°
90°
180°
270°
KEUFFEL & ESSER CO.
1 CYCLES X 140 DIVISIONS

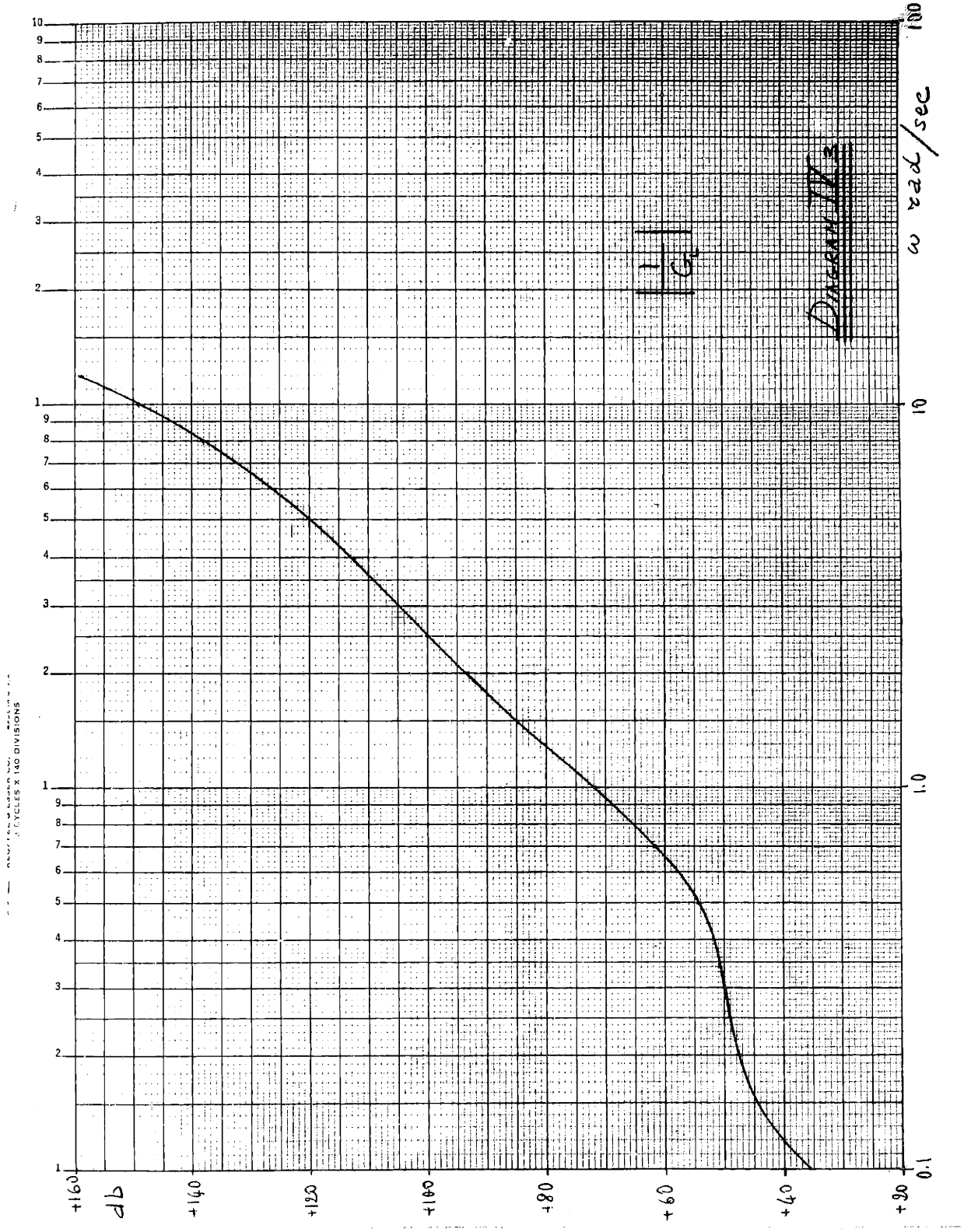
dB
+160
+140
+120
+100
+80
+60
+40
+20
0.1
1.0
10
100
ω rad/sec
Diagram #3
$\frac{1}{1+G}$

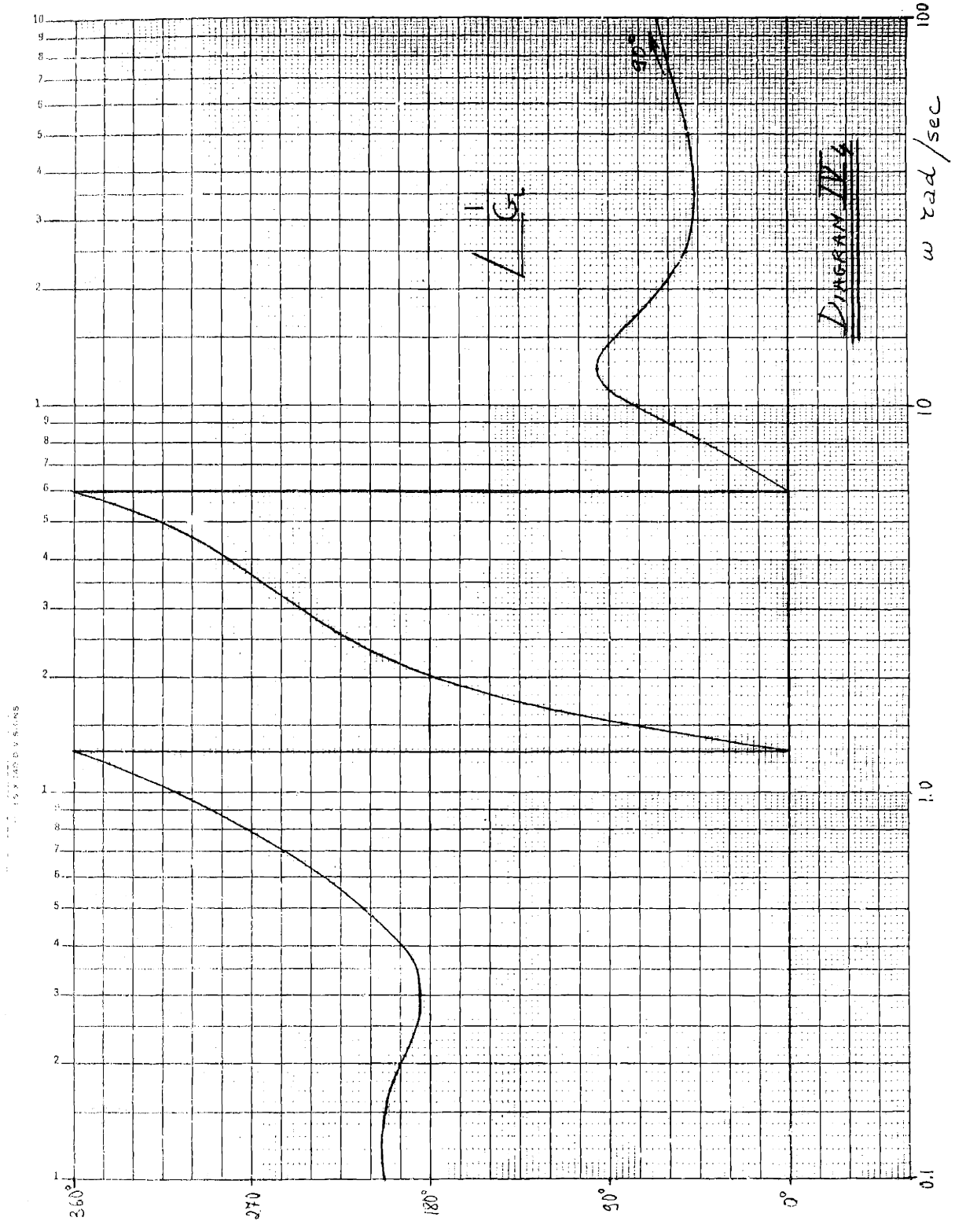
DIAGRAM No. 2
$\frac{1}{1+G}$
-90°
ω rad/sec
0.1
1.0
10
100
360°
270
180°
90°
0°

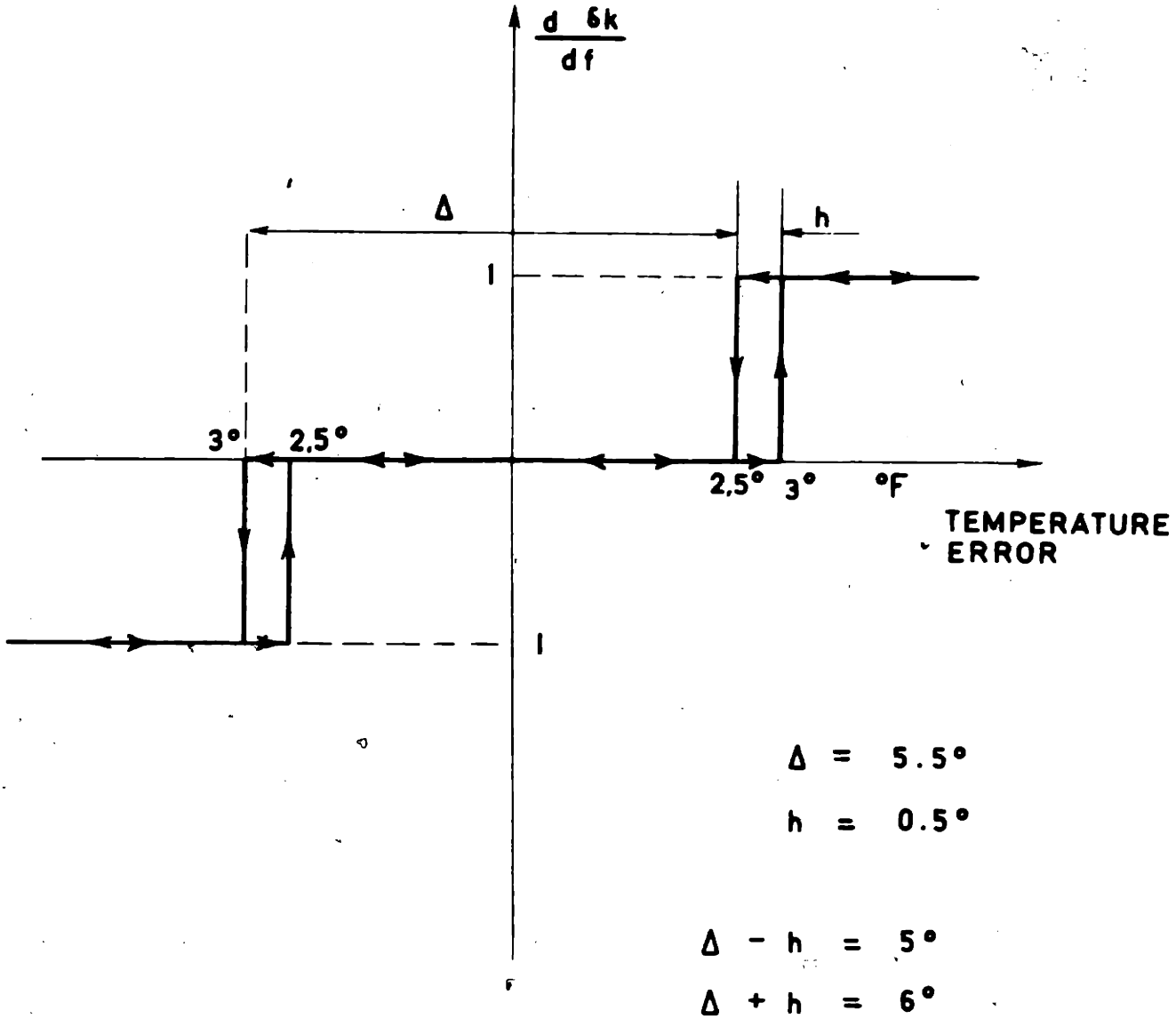

$\Delta = 5.5°$

$h = 0.5°$

$\Delta - h = 5°$

$\Delta + h = 6°$

FIG. 18

zone and hysteresis, is of the form:

$$|g(|c|)| = \frac{4}{\pi} \frac{\sin \beta}{|c|}$$

$$\angle\, g(|c|) = -\alpha$$

where

$|c|$ is the amplitude of the input sinusoidal signal

$$\beta = \frac{1}{2}\left[\cos^{-1} \left(\frac{\Delta - h}{2|c|}\right) + \cos^{-1} \left(\frac{\Delta + h}{2|c|}\right) \right]$$

$$\alpha = \frac{1}{2}\left[\cos^{-1} \left(\frac{\Delta - h}{2|c|}\right) - \cos^{-1} \left(\frac{\Delta + h}{2|c|}\right) \right]$$

Δ is the inactive zone (see Fig. 18)

h is the hysteresis range (see Fig. 18)

Values of β, α, and $|g(|c|)|$ have been calculated for different values of $|c|$ and tabulated in Table I.

3.3 Stability Study

Nyquist's plot is drawn in Diagram V (the diagram is not to scale for containing it in one sheet, but this is immaterial) and details of the region around the origin are shown in Diagram VI.

One first of all observes that the two plots $1/G_L(s)$ and $-g(|c|)$ intersect for $\omega = 0.006$ rad/sec and $|c| = 12°F$. For these conditions the denominator of the closed loop transfer function is zero. The system is therefore unstable.

It can also be seen that the points corresponding to $|c| > 12$ are encircled twice while the points corresponding to $|c| < 12$ are encircled only once. From this it can be said that the system is unstable and hence will oscillate, but these oscillations will be stable in amplitude and frequency. In fact a small increase in amplitude brings the system into the stable region and the oscillations will tend to diminish, while a small reduction in amplitude will bring the system

TABLE I

Numerical Values of the Describing Function for the Non-linear Element

$\lvert c \rvert$	β	α	$\lvert g(\lvert c \rvert) \rvert$	$\angle g(\lvert c \rvert)$
< 3	-	-	0	-
3.0	$16.\overline{75}^\circ$	$16.\overline{75}^\circ$	0.122	$-16.\overline{75}^\circ$
3.2	29.35°	9.15°	0.195	-9.15°
3.4	35.25°	7.45°	0.216	-7.45°
3.6	39.65°	6.15°	0.225	-6.15°
3.8	43.30°	5.50°	0.229	-5.50°
4.0	46.30°	4.95°	0.230	-4.95°
4.5	52.20°	4.10°	0.224	-4.10°
5.0	56.50°	3.50°	0.211	-3.50°
6.0	62.65°	2.65°	0.188	-2.65°
7.0	66.75°	2.25°	0.167	-2.25°
8.0	69.75°	1.95°	0.149	-1.95°
9.0	72.15°	1.75°	0.135	-1.75°
10.0	74.00°	1.50°	0.122	-1.50°
11.0	75.35°	1.35°	0.113	-1.35°
12.0	76.65	1.15°	0.103	-1.15°
$\to \infty$	$\to 90^\circ$	$\to 0^\circ$	$\to 0$	

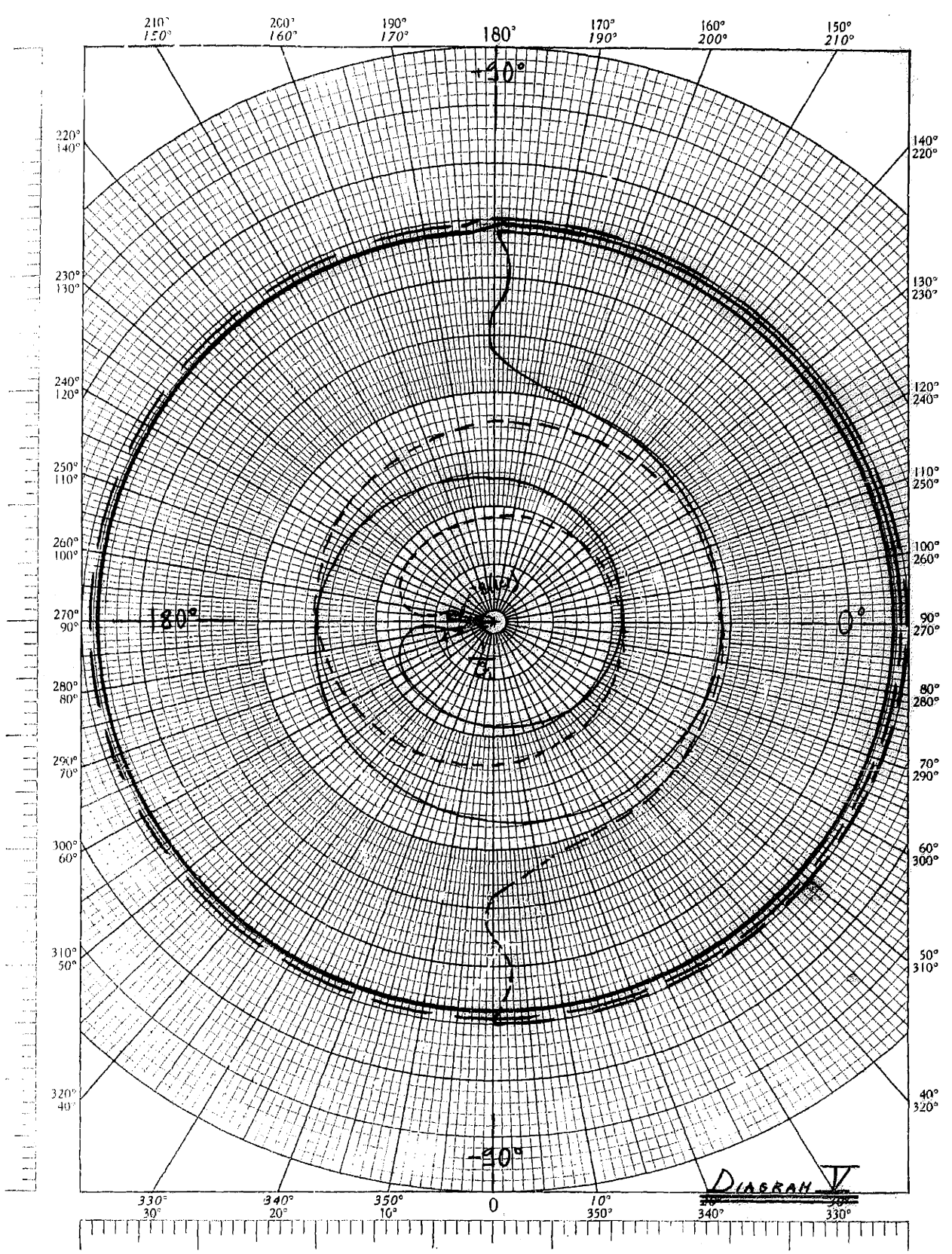
210° 150°
200° 160°
190° 170°
180°
170° 190°
160° 200°
150° 210°
90°
220° 140°
140° 220°
230° 130°
130° 230°
240° 120°
120° 240°
250° 110°
110° 250°
260° 100°
100° 260°
270° 90°
180°
0°
90° 270°
280° 80°
80° 280°
290° 70°
70° 290°
300° 60°
60° 300°
310° 50°
50° 310°
320° 40°
40° 320°
-90°
330° 30°
340° 20°
350° 10°
0
10° 350°
20° 340°
30° 330°
DIAGRAM V

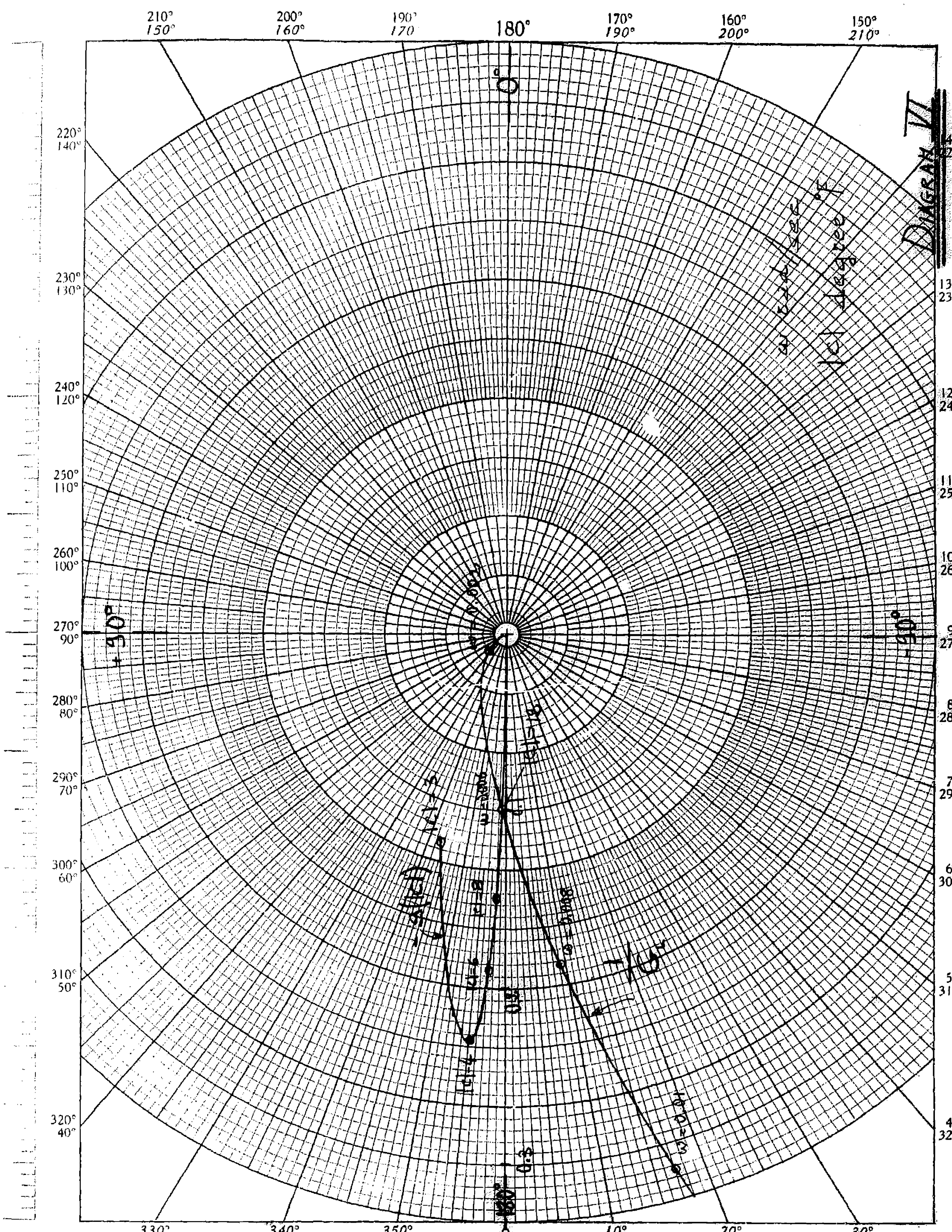
DIAGRAM VI
180°
0°
+90°
-90°
210° 150°
200° 160°
190° 170°
170° 190°
160° 200°
150° 210°
220° 140°
230° 130°
240° 120°
250° 110°
260° 100°
270° 90°
280° 80°
290° 70°
300° 60°
310° 50°
320° 40°
140° 220°
130° 230°
120° 240°
110° 250°
100° 260°
90° 270°
80° 280°
70° 290°
60° 300°
50° 310°
40° 320°
330° 30°
340° 20°
350° 10°
0
10° 350°
20° 340°
30° 330°

into the unstable region and the amplitude of oscillations will tend to increase.

The frequency of such oscillations is very low ($\omega = 0.006$ rad/sec, corresponding to 3.44 cycles/hour), but the amplitude is not so small[※], so that they cannot be allowed and the system must be compensated[※※].

※ An oscillation of the average temperature of 24°F peak to peak corresponds to a variation of the output power of 4.65%.

※※ Examining Diagrams IV and VI it can be seen that the amplitudes and phases of the frequency dependent part of the open loop transfer function for frequencies greater than $\omega = 10$ rad/sec do not influence the stability of the system. This explains why it was written, in the description of the temperature detector, that time constants smaller than 0.1 sec could have been disregarded.

CHAPTER IV

4.1 Compensation of the Automatic Control System

4.1.1 Single phase lead circuit

As can be seen by examining Diagram V, the best compensation for the system would be a passive phase lead circuit in the range of ω between 0.001 rad/sec and 0.01 rad/sec. But since this circuit cannot be inserted in any other place than between the temperature detector resistance and the non-linear element, and since, for the specified conditions on the temperature error, the gain between such elements must be equal to one at zero frequency, the lead network must be active.

With an active lead network the system can be made stable, but the margin of stability is very small.

In Diagram VII the amplitude and phase of an active lead circuit as in Fig. 19, is shown. Using the procedure of trial and error the following values are assumed:

$$\alpha = 10, \quad \frac{1}{\alpha\tau} = 0.0025, \quad \frac{1}{\tau} = 0.025, \quad \tau = 40 \text{ sec.}$$

Bode's diagram of the inverse of the new open loop transfer function ($1/G_{LC}(s)$) is in Diagram VIII and the interesting part of Nyquist's plot in Diagram IX. This diagram shows that the system is stabilized, but the margin of stability is very small. Considering the simplifications done, such compensation cannot be considered satisfactory.

4.1.2 Two phase lead circuit in cascade

Before looking for a new compensation, let us consider what should be the characteristics of the optimum compensation. Since, as said, the gain may not be altered, the compensation network must have a gain of one at zero frequency. The best compensation would be obtained by reducing the gain and advancing the phase in the range

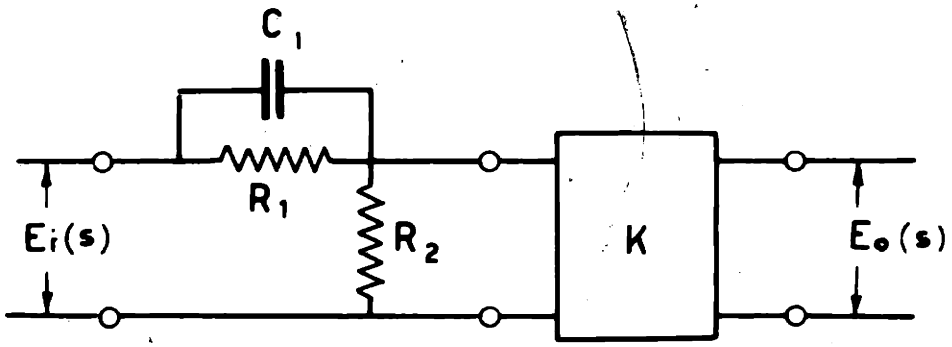

$$\frac{E_o(s)}{E_i(s)} = \frac{1}{\alpha} \quad \frac{\alpha \tau s + 1}{\tau s + 1}$$

$$\tau = \frac{R_1 R_2}{R_1 + R_2} C_1$$

$$\alpha = \frac{R_2}{R_1 + R_2}$$

$$K = \alpha$$

FIG. 19

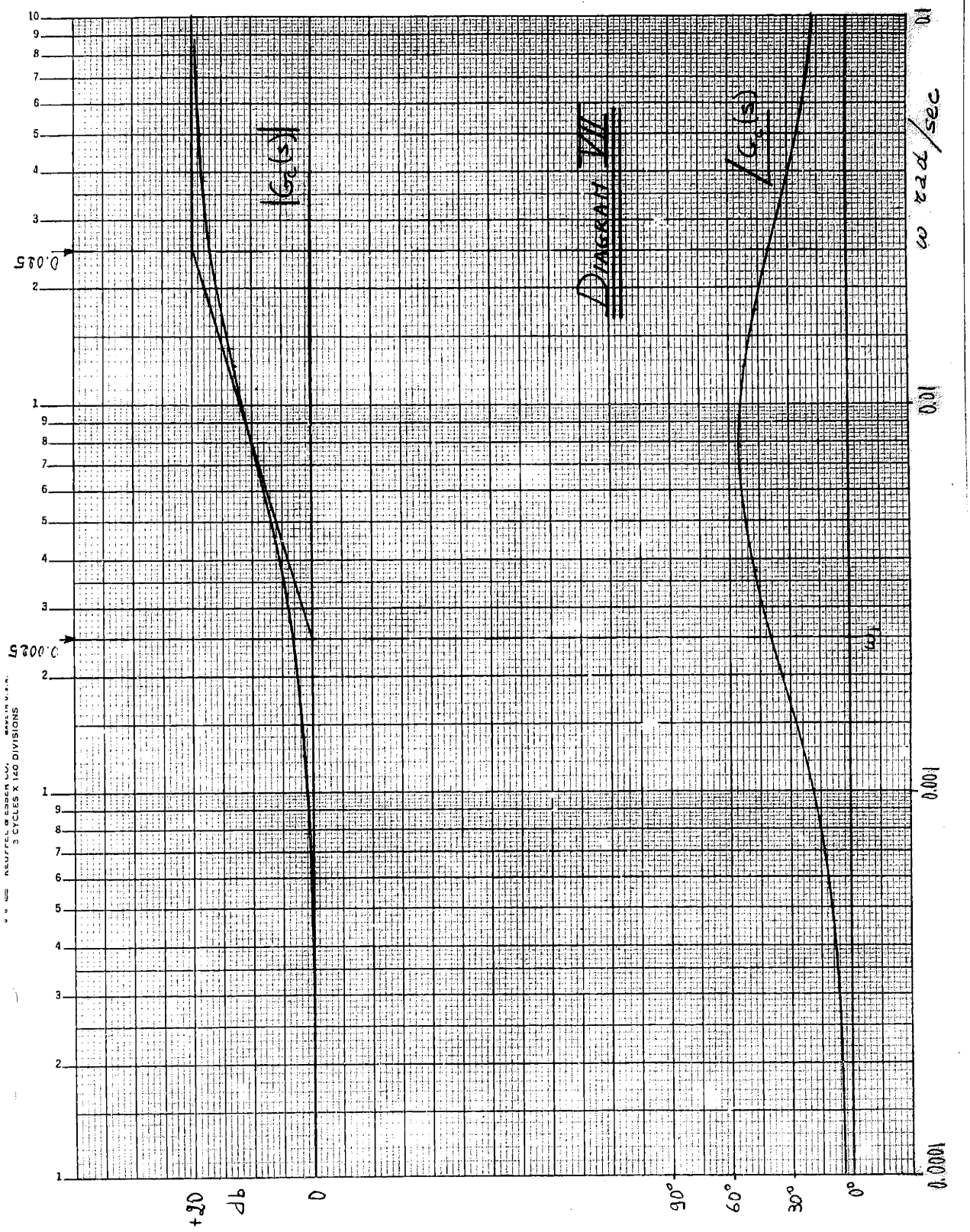
DIAGRAM #1
$|G_c(j\omega)|$
$\angle G_c(j\omega)$
ω rad/sec
0.0085
0.00285
0.1
0.01
0.001
0.0001
+20 dB
0 dB
0
90°
60°
30°
0°
10 CYCLES X 140 DIVISIONS

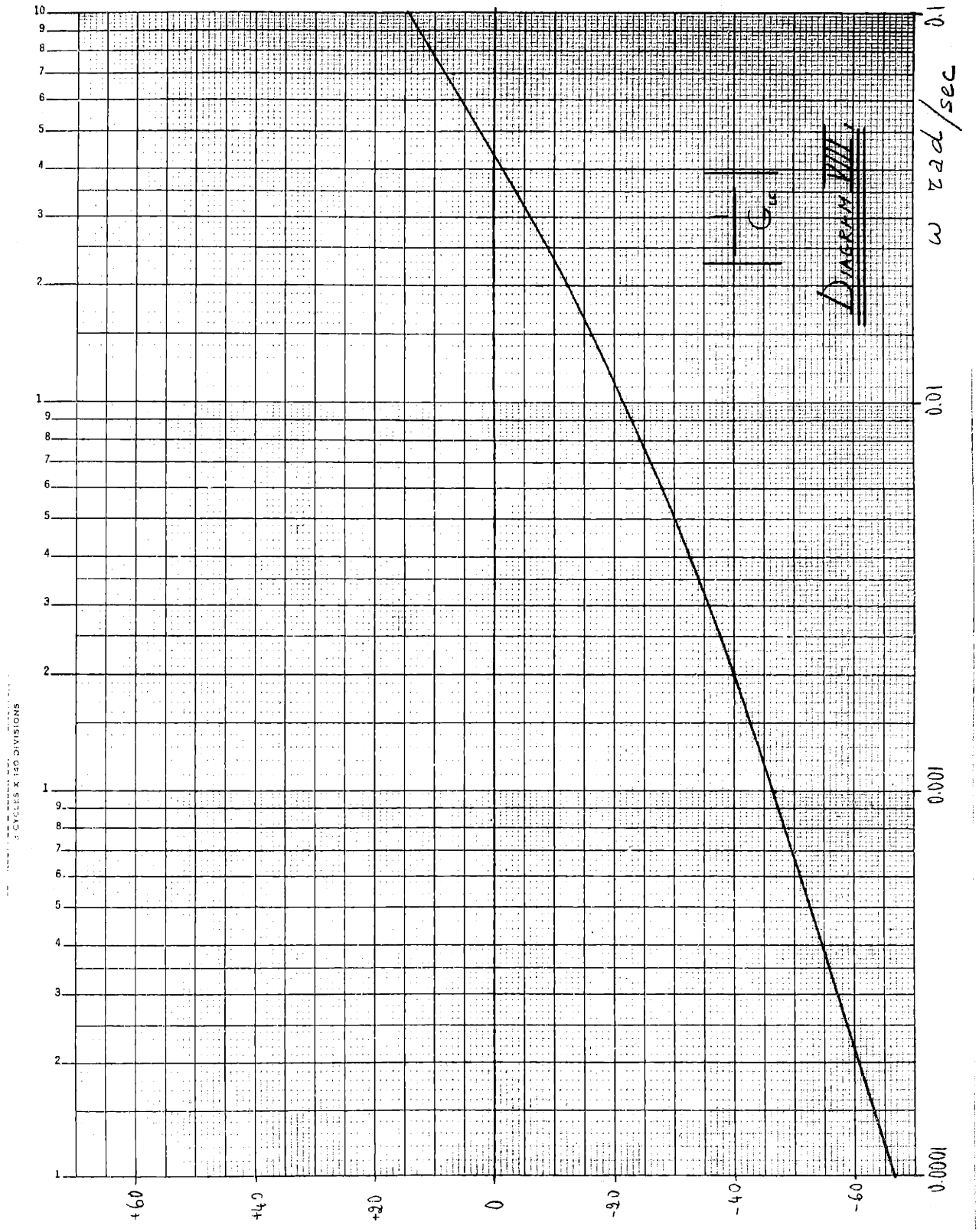
10
9
8
7
6
5
4
3
2
1
9
8
7
6
5
4
3
2
1
9
8
7
6
5
4
3
2
1
+60
+40
+20
0
-20
-40
-60
0.1
0.01
0.001
0.0001
ω rad/sec
Diagram
1 - θss
CYCLES X 140 DIVISIONS

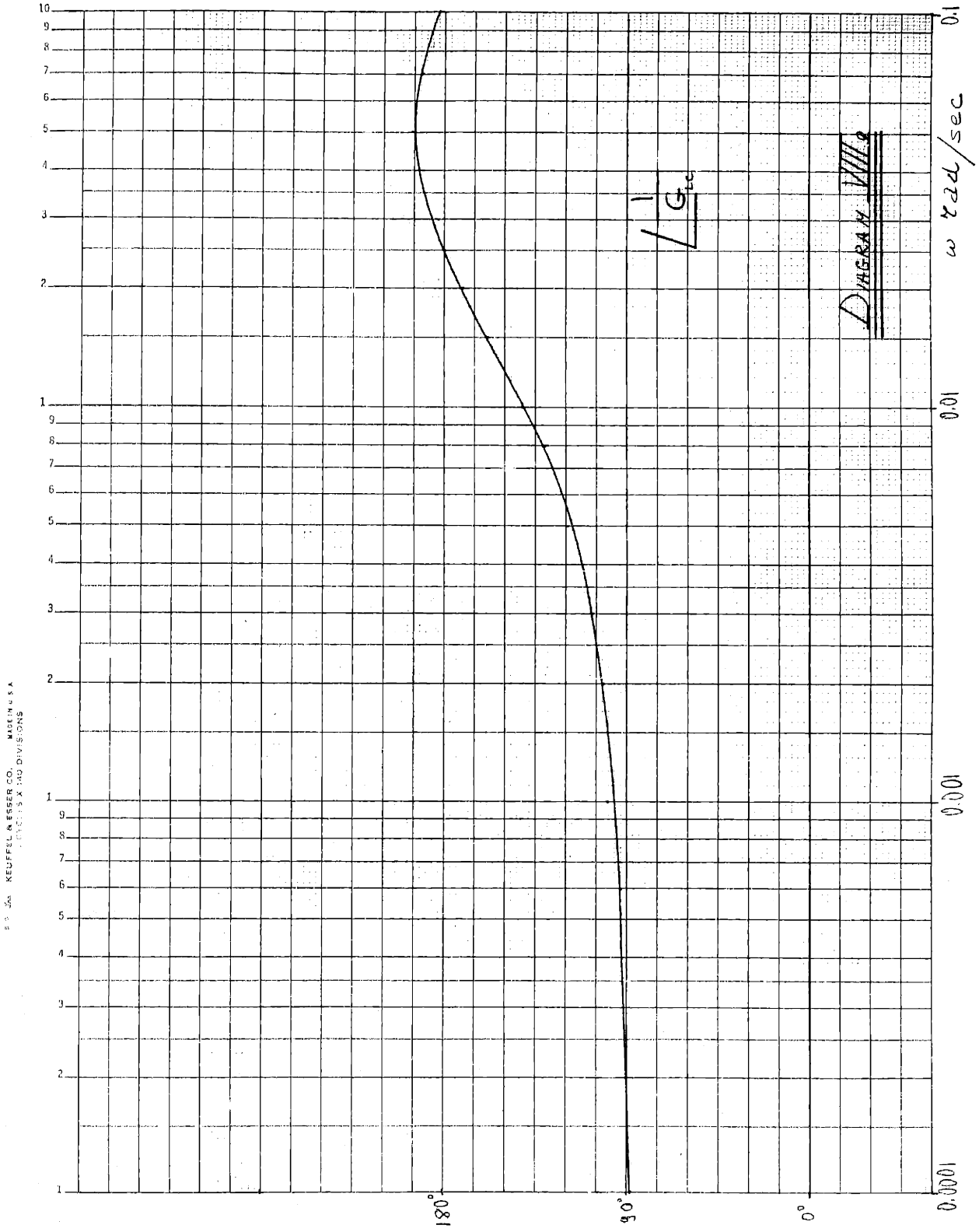
10
9
8
7
6
5
4
3
2
1
9
8
7
6
5
4
3
2
1
9
8
7
6
5
4
3
2
1
180°
90°
0°
0.1
0.01
0.001
0.0001
ω rad/sec
$\frac{1}{\sqrt{G_{tc}}}$
DIAGRAM
KEUFFEL & ESSER CO. MADE IN U.S.A.
359-15 5 X 140 DIVISIONS

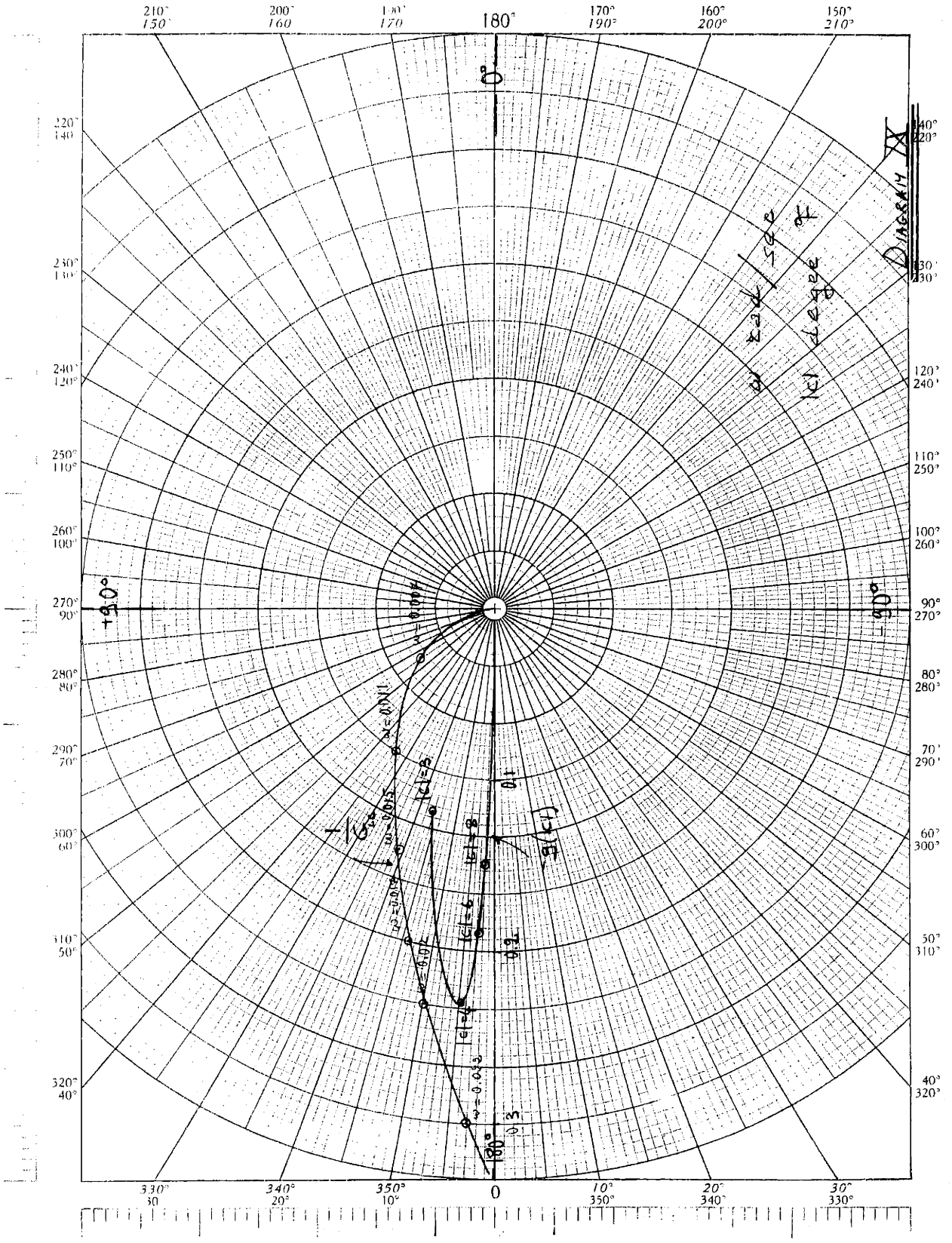
180°
0
+90°
-90°
DIAGRAM
0.1
0.2
0.3
0.4
0.5
0.6
0.8
1.0
2.0
3.0
4.0
5.0
10
20
50
100
∞

between $\omega = 0.001$ rad/sec and $\omega \geq 1.0$ rad/sec.

For a stable circuit these two conditions are obviously in opposition and a compromise should be made, observing however that it is more important to correct the phase than the magnitude.

The simplest solution consists in cascading two lead circuits through an isolating amplifier. The minimum increase in gain without losing too much in phase advance, is obtained by assuming the two circuits equal.

Using a trial and error procedure, the following value for the constants were assumed (see Fig. 19):

$$\alpha = 10, \quad \frac{1}{\alpha\tau} = 0.01, \quad \frac{1}{\tau} = 0.1, \quad \tau = 10 \text{ sec.}$$

The overall transfer function results

$$G_{CD}(s) = \frac{\left(\frac{s}{0.01} + 1\right)^2}{\left(\frac{s}{0.1} + 1\right)^2}$$

Bode's diagram of this transfer function is shown in Diagram X. The inverse of the total open loop transfer function is plotted in Diagram XI. Nyquist's plot of the compensated system is in Diagrams XII and XIII.

To have a measure of the degree of relative stability, a concept analogous to the phase margin in a linear system will be introduced.

We will define "phase margin for a non-linear system in the describing function approach" as the minimum value of the difference of the phase of any value of $1/G_L(s)$ with magnitude equal or less than the maximum amplitude of the describing function, and the phase of any value of the describing function itself.

Considering this "phase margin" on Nyquist's plot, it is the minimum angle between all the points of $1/G_L(s)$ with amplitude equal or less than the maximum amplitude of the describing function and any point of the describing function itself. This angle gives an idea of how far the two curves are from intersecting. Obviously the

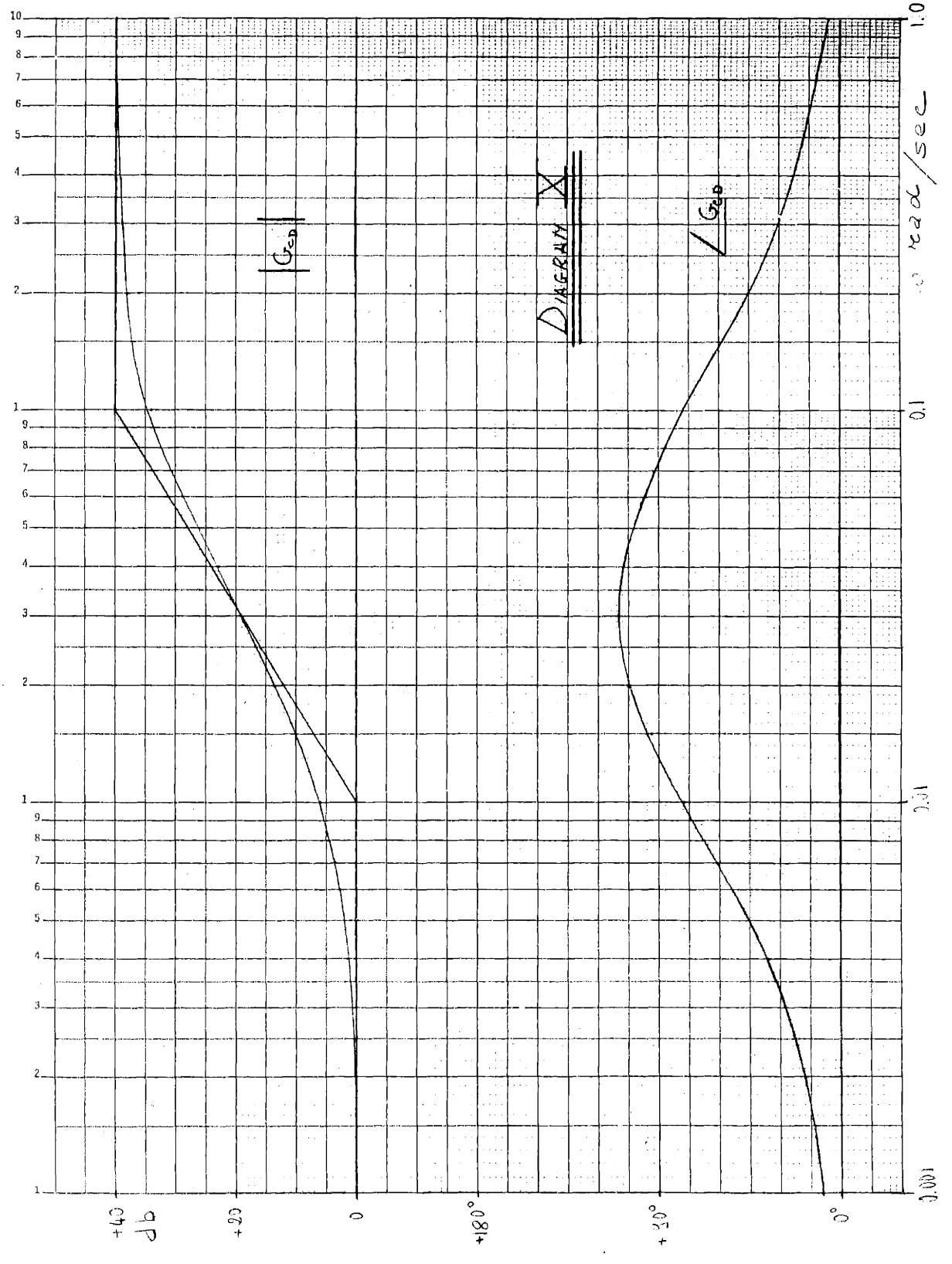
DIAGRAM X
$|G_{ED}|$
$\angle G_{ED}$
+40 db
+20
0
+180°
+20°
0°
1.0
0.1
0.01
0.001
rad/sec

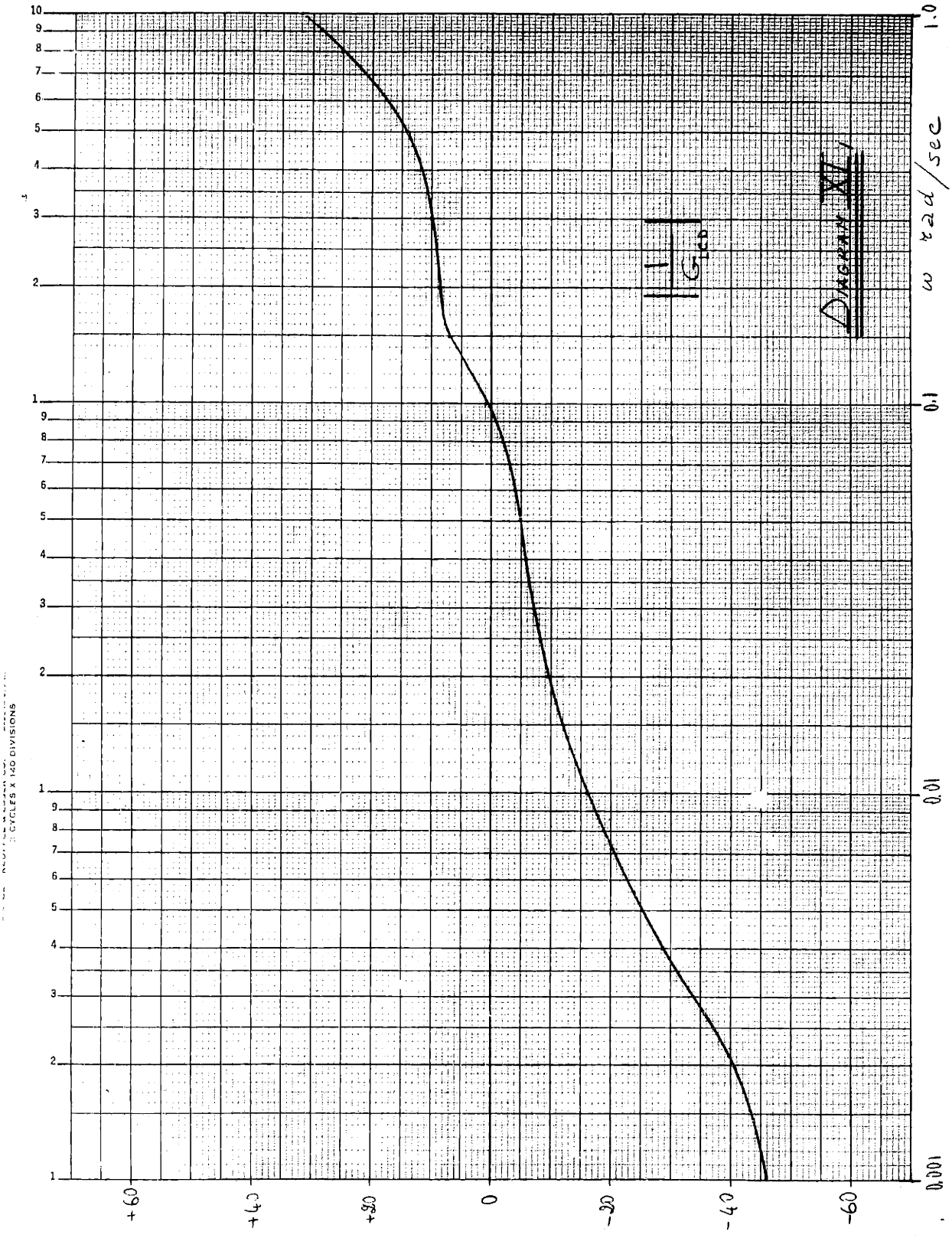
10
9
8
7
6
5
4
3
2
1
1.0
0.1
0.01
0.001
ω rad/sec
G_{cb}
Diagram XI
+90
+45
0
-45
-90
CYCLES X 140 DIVISIONS

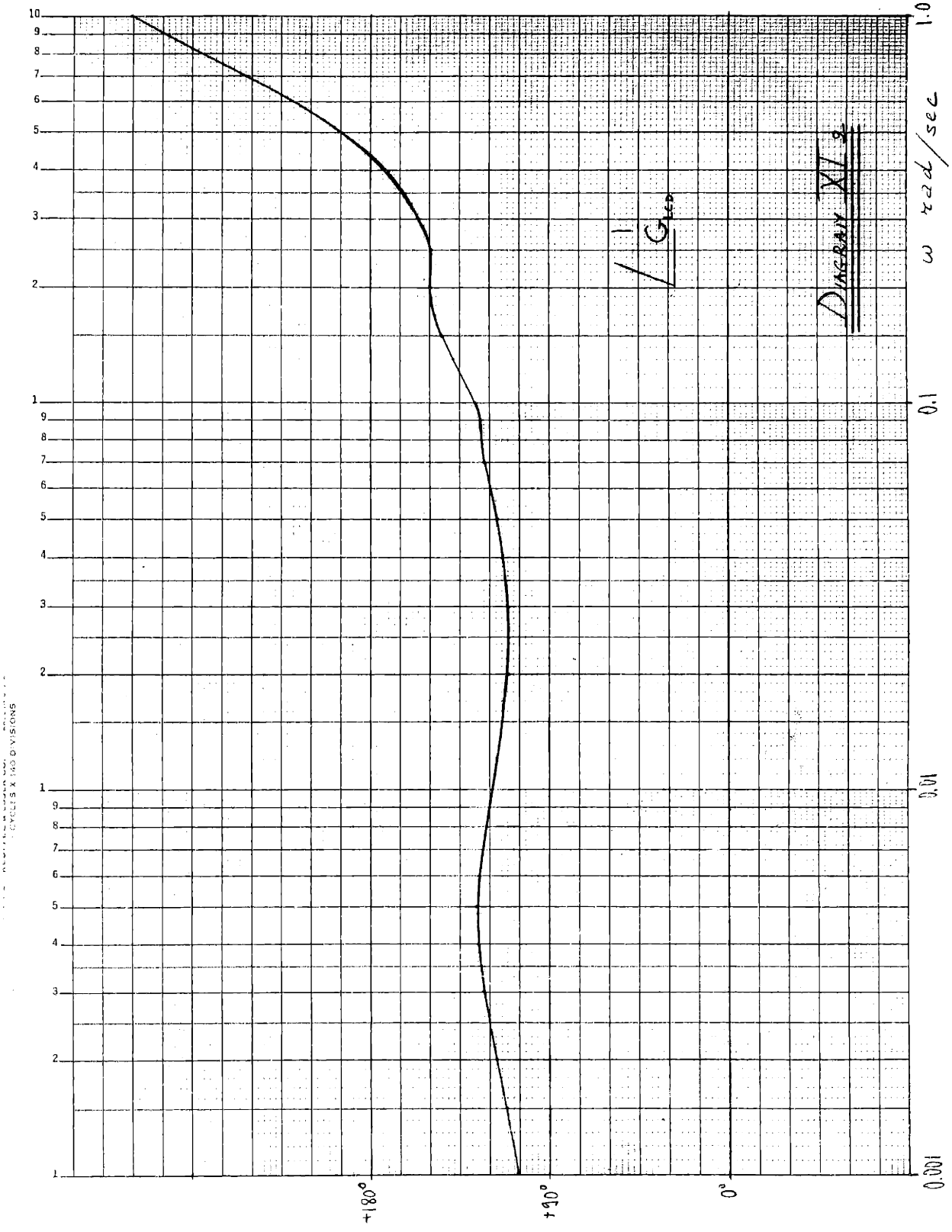
Diagram N° 2
$\frac{1}{\angle G_{(j\omega)}}$
ω rad/sec
1.0
0.1
0.01
0.001
+180°
+90°
0°

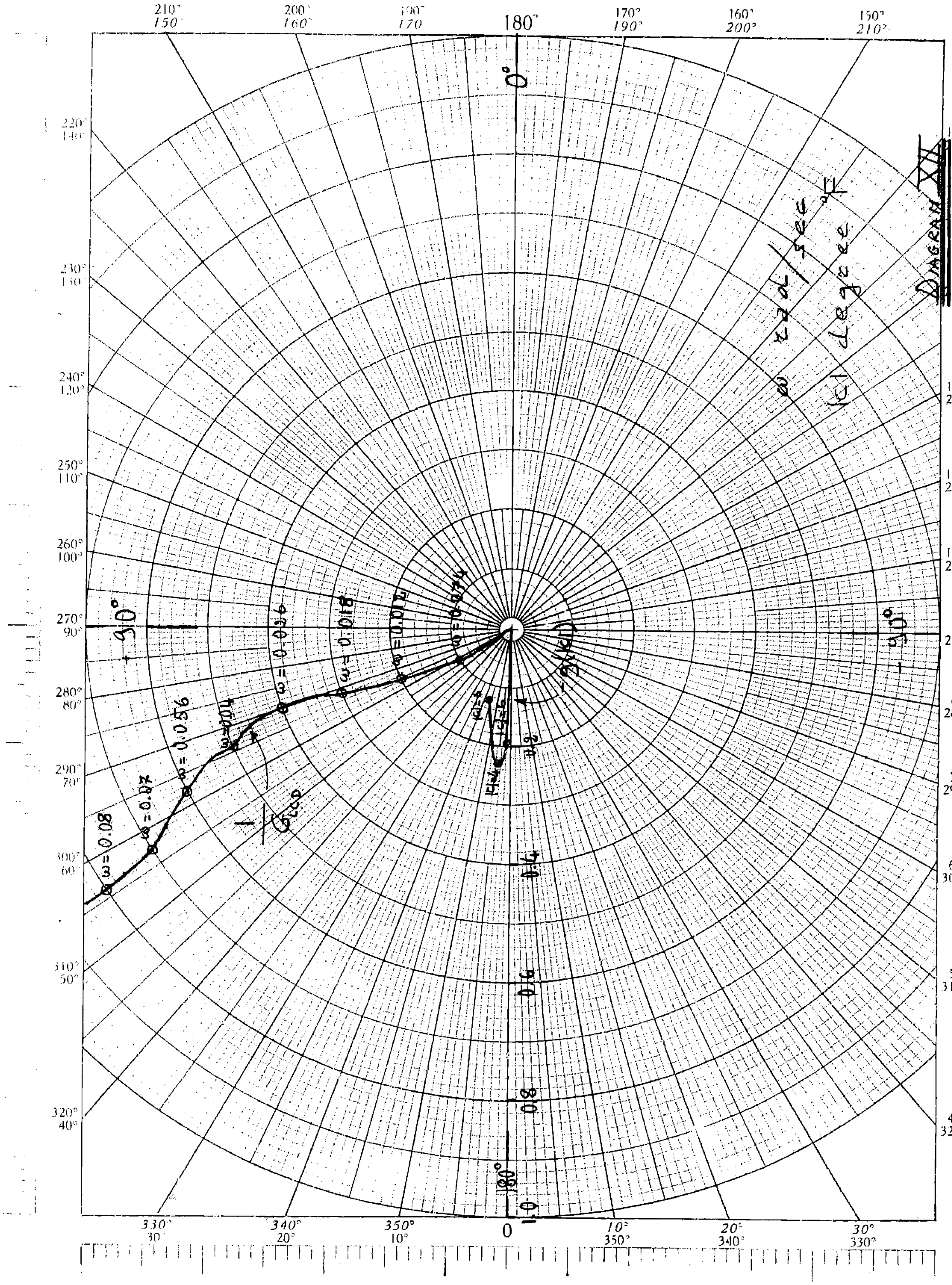
180°
0°
Diagram XII
ω rad/sec
|c| degree °F
+90°
-90°
ω = 0.08
ω = 0.07
ω = 0.056
ω = 0.044
ω = 0.036
ω = 0.018
ω = 0.012
ω = 0.004
1/G_ccD
0.4
0.6
0.8
1.0
0

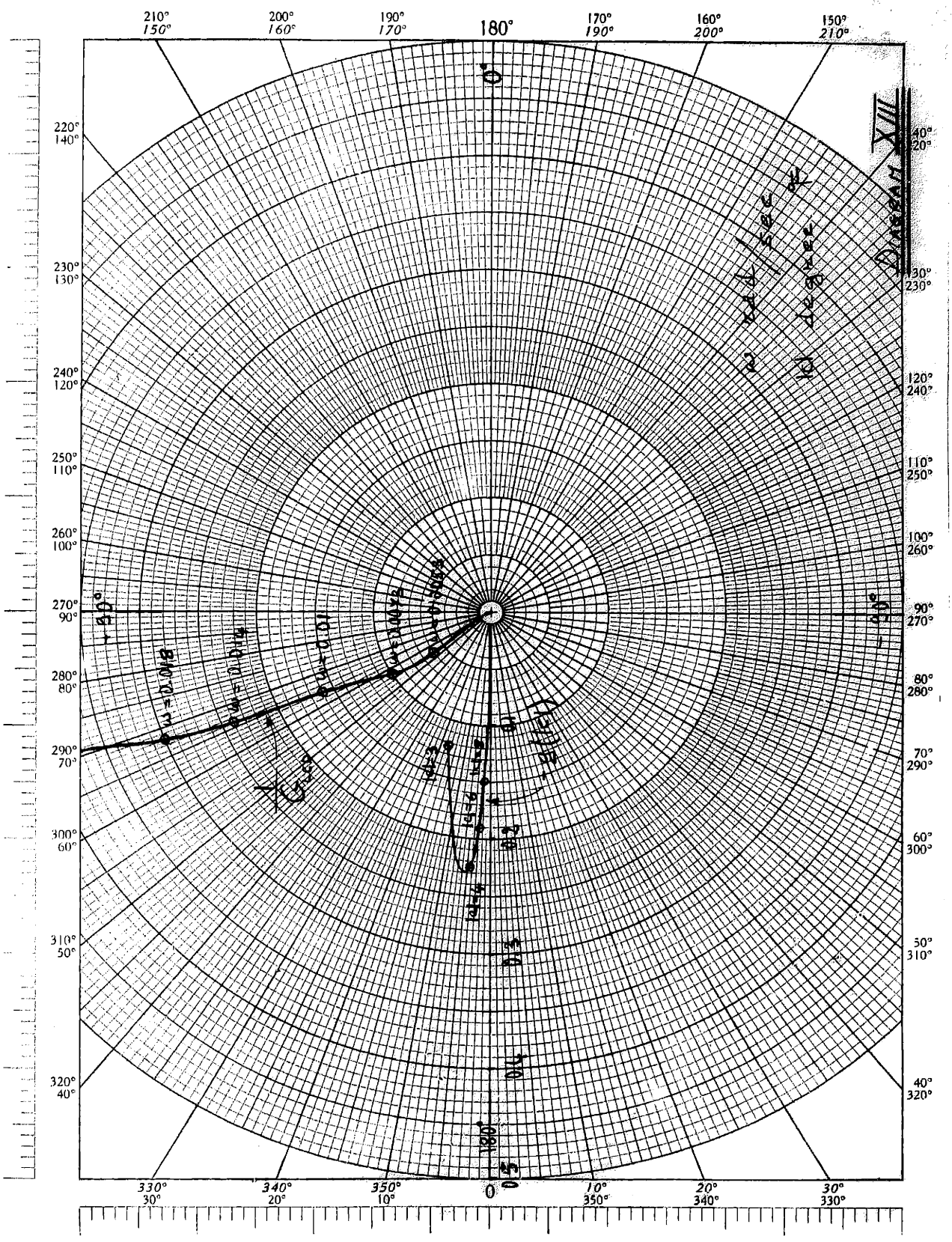
180°
0°
90°
270°
0
10
20
30
40
50
60
70
80
90
100
110
120
130
140
150
160
170
180
190
200
210
220
230
240
250
260
270
280
290
300
310
320
330
340
350
360
370
380
390
400
410
420
430
440
450
460
470
480
490
500
510
520
530
540
550
560
570
580
590
600
610
620
630
640
650
660
670
680
690
700
710
720
730
740
750
760
770
780
790
800
810
820
830
840
850
860
870
880
890
900
910
920
930
940
950
960
970
980
990
1000
1010
1020
1030
1040
1050
1060
1070
1080
1090
1100
1110
1120
1130
1140
1150
1160
1170
1180
1190
1200
1210
1220
1230
1240
1250
1260
1270
1280
1290
1300
1310
1320
1330
1340
1350
1360
1370
1380
1390
1400
1410
1420
1430
1440
1450
1460
1470
1480
1490
1500
1510
1520
1530
1540
1550
1560
1570
1580
1590
1600
1610
1620
1630
1640
1650
1660
1670
1680
1690
1700
1710
1720
1730
1740
1750
1760
1770
1780
1790
1800
1810
1820
1830
1840
1850
1860
1870
1880
1890
1900
1910
1920
1930
1940
1950
1960
1970
1980
1990
2000
2010
2020
2030
2040
2050
2060
2070
2080
2090
2100
2110
2120
2130
2140
2150
2160
2170
2180
2190
2200
2210
2220
2230
2240
2250
2260
2270
2280
2290
2300
2310
2320
2330
2340
2350
2360
2370
2380
2390
2400
2410
2420
2430
2440
2450
2460
2470
2480
2490
2500
2510
2520
2530
2540
2550
2560
2570
2580
2590
2600
2610
2620
2630
2640
2650
2660
2670
2680
2690
2700
2710
2720
2730
2740
2750
2760
2770
2780
2790
2800
2810
2820
2830
2840
2850
2860
2870
2880
2890
2900
2910
2920
2930
2940
2950
2960
2970
2980
2990
3000
3010
3020
3030
3040
3050
3060
3070
3080
3090
3100
3110
3120
3130
3140
3150
3160
3170
3180
3190
3200
3210
3220
3230
3240
3250
3260
3270
3280
3290
3300
3310
3320
3330
3340
3350
3360
3370
3380
3390
3400
3410
3420
3430
3440
3450
3460
3470
3480
3490
3500
3510
3520
3530
3540
3550
3560
3570
3580
3590
3600
3610
3620
3630
3640
3650
3660
3670
3680
3690
3700
3710
3720
3730
3740
3750
3760
3770
3780
3790
3800
3810
3820
3830
3840
3850
3860
3870
3880
3890
3900
3910
3920
3930
3940
3950
3960
3970
3980
3990
4000
4010
4020
4030
4040
4050
4060
4070
4080
4090
4100
4110
4120
4130
4140
4150
4160
4170
4180
4190
4200
4210
4220
4230
4240
4250
4260
4270
4280
4290
4300
4310
4320
4330
4340
4350
4360
4370
4380
4390
4400
4410
4420
4430
4440
4450
4460
4470
4480
4490
4500
4510
4520
4530
4540
4550
4560
4570
4580
4590
4600
4610
4620
4630
4640
4650
4660
4670
4680
4690
4700
4710
4720
4730
4740
4750
4760
4770
4780
4790
4800
4810
4820
4830
4840
4850
4860
4870
4880
4890
4900
4910
4920
4930
4940
4950
4960
4970
4980
4990
5000
5010
5020
5030
5040
5050
5060
5070
5080
5090
5100
5110
5120
5130
5140
5150
5160
5170
5180
5190
5200
5210
5220
5230
5240
5250
5260
5270
5280
5290
5300
5310
5320
5330
5340
5350
5360
5370
5380
5390
5400
5410
5420
5430
5440
5450
5460
5470
5480
5490
5500
5510
5520
5530
5540
5550
5560
5570
5580
5590
5600
5610
5620
5630
5640
5650
5660
5670
5680
5690
5700
5710
5720
5730
5740
5750
5760
5770
5780
5790
5800
5810
5820
5830
5840
5850
5860
5870
5880
5890
5900
5910
5920
5930
5940
5950
5960
5970
5980
5990
6000
6010
6020
6030
6040
6050
6060
6070
6080
6090
6100
6110
6120
6130
6140
6150
6160
6170
6180
6190
6200
6210
6220
6230
6240
6250
6260
6270
6280
6290
6300
6310
6320
6330
6340
6350
6360
6370
6380
6390
6400
6410
6420
6430
6440
6450
6460
6470
6480
6490
6500
6510
6520
6530
6540
6550
6560
6570
6580
6590
6600
6610
6620
6630
6640
6650
6660
6670
6680
6690
6700
6710
6720
6730
6740
6750
6760
6770
6780
6790
6800
6810
6820
6830
6840
6850
6860
6870
6880
6890
6900
6910
6920
6930
6940
6950
6960
6970
6980
6990
7000
7010
7020
7030
7040
7050
7060
7070
7080
7090
7100
7110
7120
7130
7140
7150
7160
7170
7180
7190
7200
7210
7220
7230
7240
7250
7260
7270
7280
7290
7300
7310
7320
7330
7340
7350
7360
7370
7380
7390
7400
7410
7420
7430
7440
7450
7460
7470
7480
7490
7500
7510
7520
7530
7540
7550
7560
7570
7580
7590
7600
7610
7620
7630
7640
7650
7660
7670
7680
7690
7700
7710
7720
7730
7740
7750
7760
7770
7780
7790
7800
7810
7820
7830
7840
7850
7860
7870
7880
7890
7900
7910
7920
7930
7940
7950
7960
7970
7980
7990
8000
8010
8020
8030
8040
8050
8060
8070
8080
8090
8100
8110
8120
8130
8140
8150
8160
8170
8180
8190
8200
8210
8220
8230
8240
8250
8260
8270
8280
8290
8300
8310
8320
8330
8340
8350
8360
8370
8380
8390
8400
8410
8420
8430
8440
8450
8460
8470
8480
8490
8500
8510
8520
8530
8540
8550
8560
8570
8580
8590
8600
8610
8620
8630
8640
8650
8660
8670
8680
8690
8700
8710
8720
8730
8740
8750
8760
8770
8780
8790
8800
8810
8820
8830
8840
8850
8860
8870
8880
8890
8900
8910
8920
8930
8940
8950
8960
8970
8980
8990
9000
9010
9020
9030
9040
9050
9060
9070
9080
9090
9100
9110
9120
9130
9140
9150
9160
9170
9180
9190
9200
9210
9220
9230
9240
9250
9260
9270
9280
9290
9300
9310
9320
9330
9340
9350
9360
9370
9380
9390
9400
9410
9420
9430
9440
9450
9460
9470
9480
9490
9500
9510
9520
9530
9540
9550
9560
9570
9580
9590
9600
9610
9620
9630
9640
9650
9660
9670
9680
9690
9700
9710
9720
9730
9740
9750
9760
9770
9780
9790
9800
9810
9820
9830
9840
9850
9860
9870
9880
9890
9900
9910
9920
9930
9940
9950
9960
9970
9980
9990
10000

points of the describing function are in the stable region.

For the compensation considered, the phase margin is 35° for values of amplitude of $1/G_{LCD}(s)$ as large as four times the maximum amplitude of $-g(|c|)$. This should also insure a good relative stability[※]. The disadvantage of this type of compensation is that it requires two circuits which have to be separated by an isolating amplifier. This could be avoided if the transfer function $G_{CD}(s)$ were synthesized with only one circuit. Since double poles are involved, the synthesis would require, if done with passive elements, resistances, capacitors, and inductances. But the values of the critical frequencies are so low that the inductances have to be extremely large and the circuit is not practical at all.

4.1.3 Single two pole phase lead circuit

The problem can be solved simply by modifying the compensating transfer function. It will be considered a transfer function for a leading circuit of the form:

$$G_{CU}(s) = k\,\frac{(s+a)^2}{(s+b)(s+c)} \qquad \text{(voltage ratio)}$$

$$k = \frac{bc}{a^2} \qquad a < b < c$$

which can be realized with an RC ladder network.

Using the trial and error method, the following values for the constants are chosen:

$$a = 0.007, \quad b = 0.07, \quad c = 0.15, \quad k = 215.$$

Bode's diagram of $G_{CD}(s)$ is plotted in Diagram XIV. The inverse of the compensated transfer function in Diagram XV and Nyquist's plot is in Diagrams XVI and XVII.

※ Since the feedback is not unity the maximum amplitude curves, as that derived by Kochenburger, cannot be easily calculated.

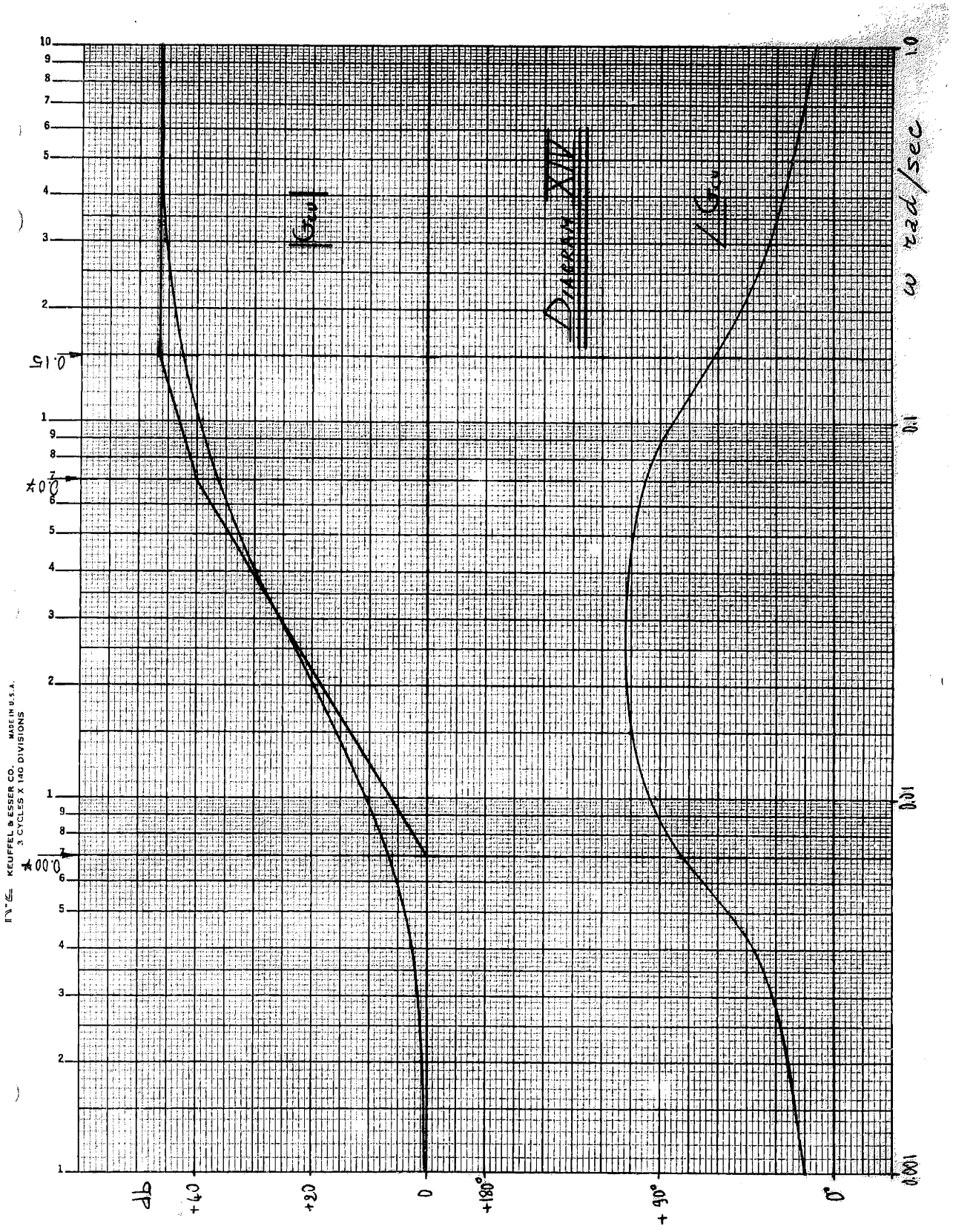
Diagram XVII
G_{ol}
G_{cl}
ω rad/sec
10
1.0
0.1
0.01
0.001
0.15
0.04
0.004
dB
+40
+20
0
+180°
+90°
0°
KEUFFEL & ESSER CO.
MADE IN U.S.A.
3 CYCLES X 140 DIVISIONS

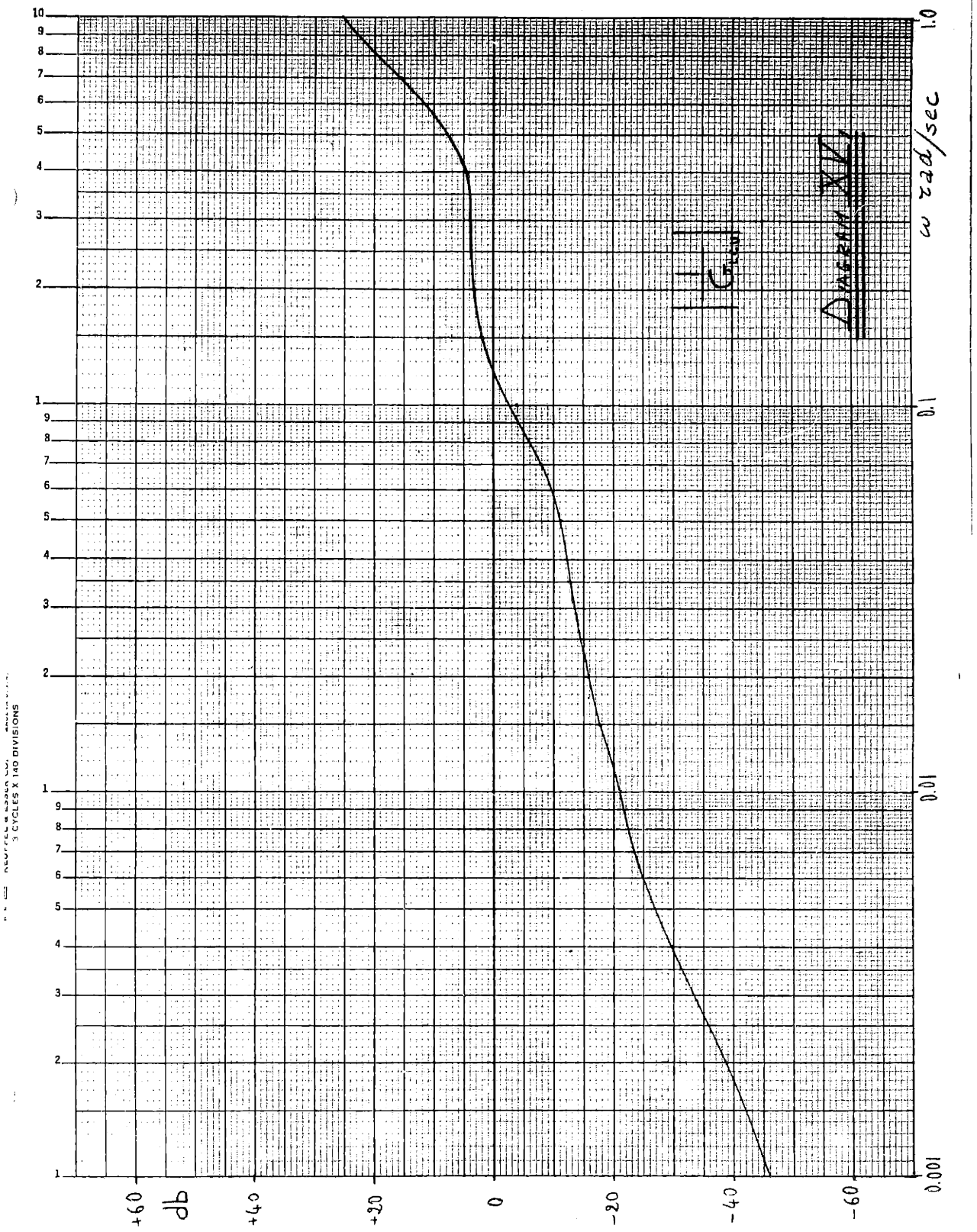
10
9
8
7
6
5
4
3
2
1
1.0
0.1
0.01
0.001
ω rad/sec
+60
+40
+20
0
-20
-40
-60
db
3 CYCLES X 140 DIVISIONS

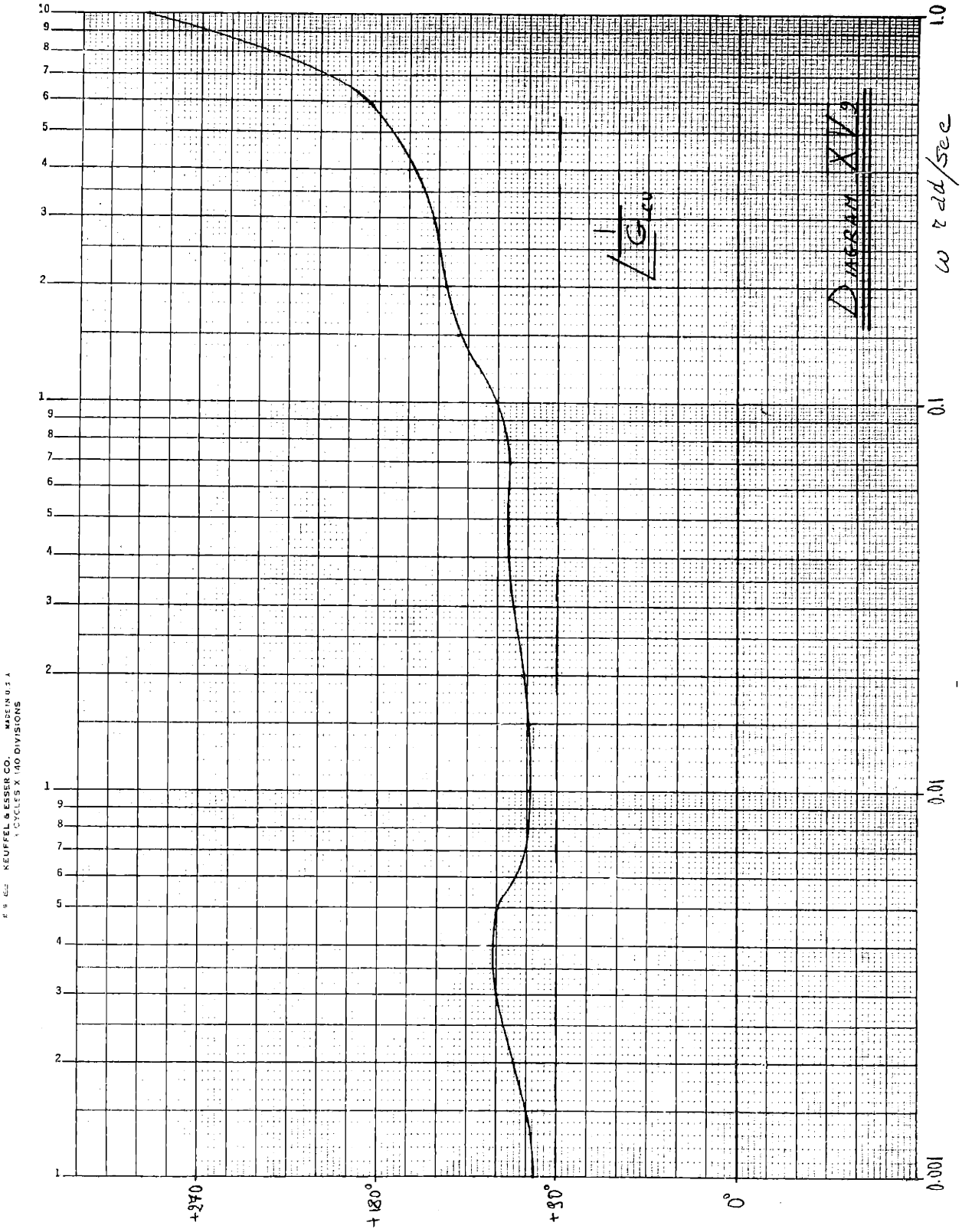
10
9
8
7
6
5
4
3
2
1
1.0
0.1
0.01
0.001
ω rad/sec
+270°
+180°
+90°
0°
KEUFFEL & ESSER CO.
MADE IN U.S.A.
4 CYCLES X 140 DIVISIONS

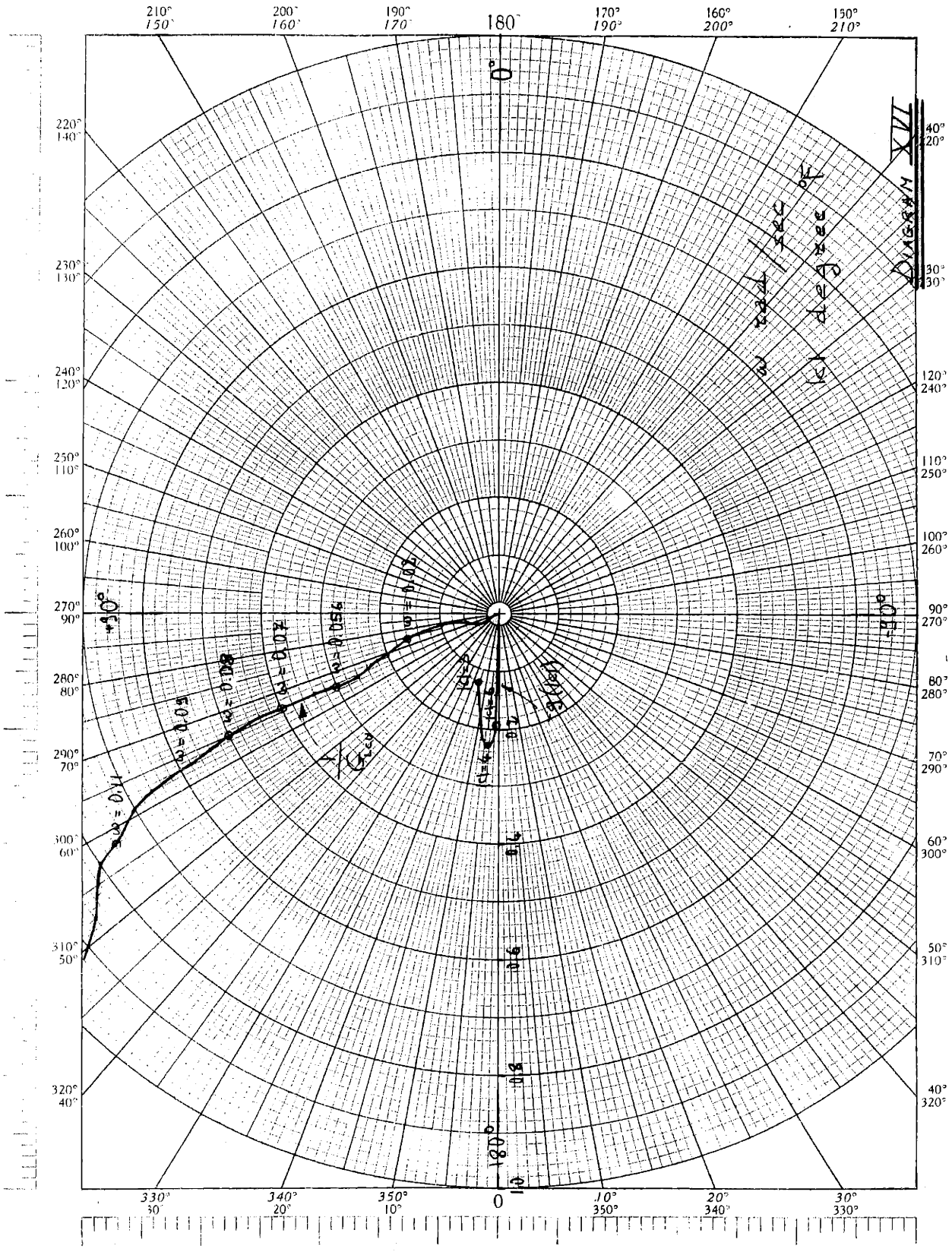
180°
0°
+90°
-90°
0
0.2
0.4
0.6
0.8
1.0
Phase
Tail Lag
Lead

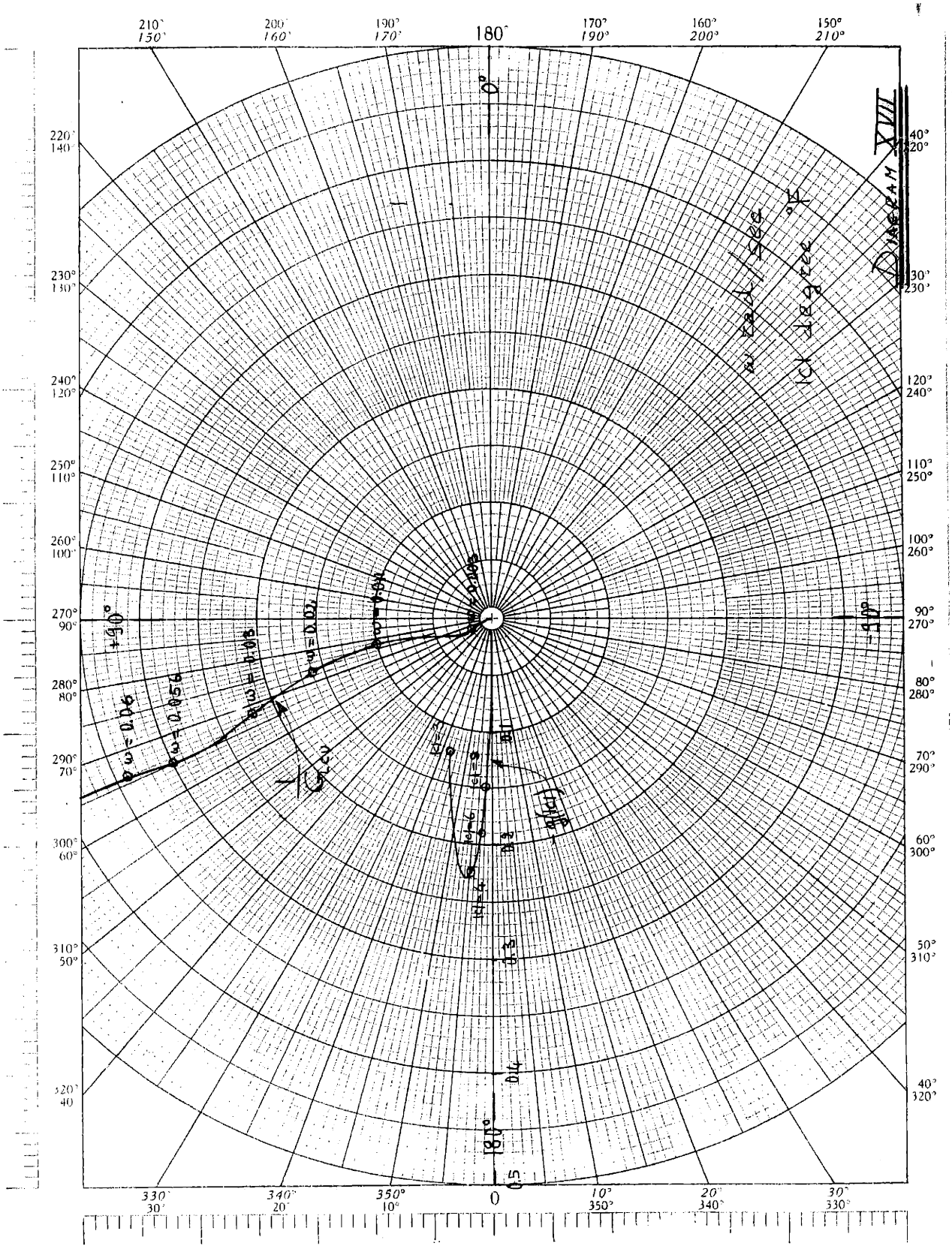
180°
0°
0
210° 150°
200° 160°
190° 170°
170° 190°
160° 200°
150° 210°
220° 140°
230° 130°
240° 120°
250° 110°
260° 100°
270° 90°
280° 80°
290° 70°
300° 60°
310° 50°
320° 40°
330° 30°
340° 20°
350° 10°
10° 350°
20° 340°
30° 330°
40° 320°
50° 310°
60° 300°
70° 290°
80° 280°
90° 270°
100° 260°
110° 250°
120° 240°
DIAGRAM XVIII

With these values of the constants, this new circuit gives, with respect to the two lead circuits in cascade, a larger phase margin for the lower value of the amplitude of $1/G_{LCU}$ (40^{*} for $1/G_{LCU} < 3\, g(|c|)_{max}$) but a little less value for the higher value (for the increase of the gain). The overall stability however appears to be improved.

4.2 Synthesis of the Compensating Network

To synthesize a ladder network with the voltage ratio:

$$\frac{E_o(s)}{E_i(s)} = \frac{(s + 0.007)^2}{(s + 0.07)(s + 0.15)}$$

we use the method suggested by Truxal[8].

The circuit as in Fig. 20a is found using the following steps.

1. Since $E_o/E_i = Y_{12}/Y_{22}$, we assume

$$Y_{22}(s) = \frac{(s + 0.07)(s + 0.15)}{(s + 0.1)}$$

$$Y_{12}(s) = \frac{(s + 0.007)^2}{(s + 0.1)}$$

so that the circuit can be realized as an RC network.

2. $Y_{22}(s)$ is synthesized in such a way that $Y_{12}(s)$ has a double zero at $s = -0.007$. These are obtained with two resistor and capacitor parallel tank circuits.

Since the values of the capacitors are not acceptable at all, the impedance level is raised by a factor of $1/3 \times 10^6$. In this way all the resistances are multiplied by $1/3 \times 10^6$ but all the capacitances are divided by the same factor.

Since through this impedance level both Y_{22} and Y_{12} are multiplied by the same factor (3×10^{-6}) the transfer ratio E_o/E_i is not altered. The final compensating network is as in Fig. 20b. Still the values of the components are very large but no further improvement can be obtained because of the very low critical frequencies.

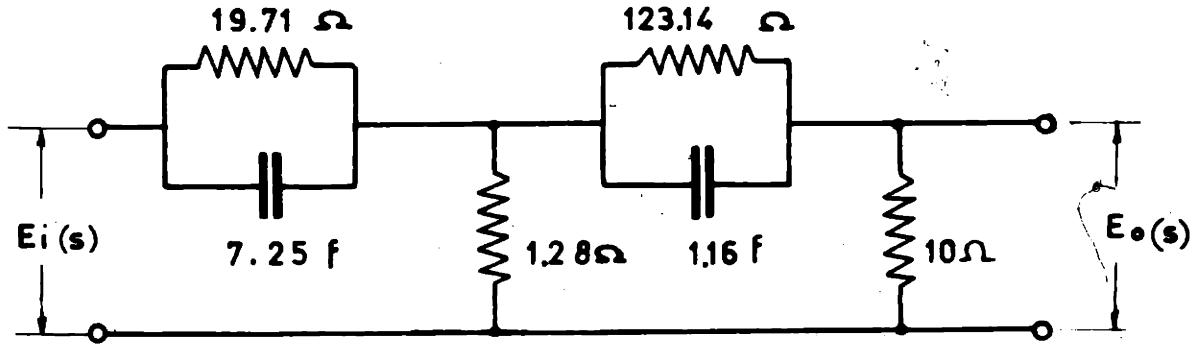

FIG 20 a

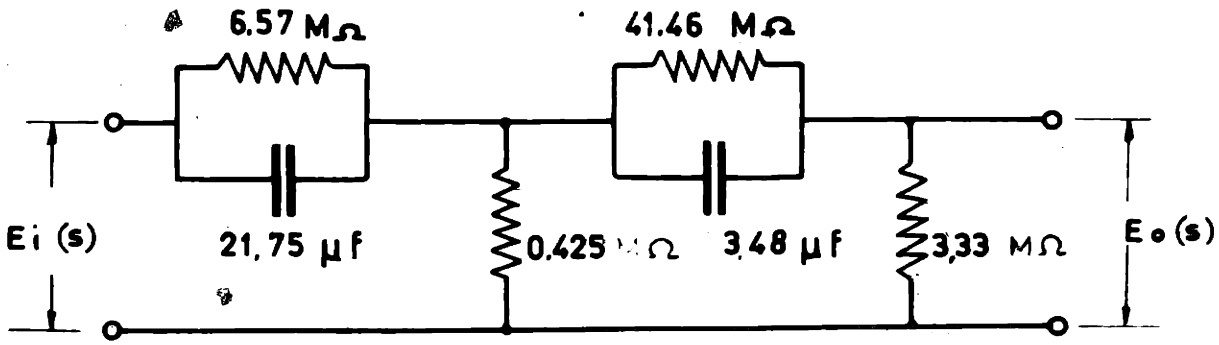

FIG. 20 b

CHAPTER V

CONCLUSIONS

To conclude the study done in this thesis, some more general considerations will be summarized.

First, we can say that, introducing reasonable approximations, an analytic study of the stability of the automatic control for a pressurized water reactor is possible, even though the system is very complex.

Second, though the results of such a method cannot be considered precise, they give us very useful information of how the system behaves, what elements have the greater influence on the stability, and in what direction we must move to improve the automatic control system.

Third, this approach gives a useful basis for more precise studies as with an analog computer or through direct measurements.

Finally, as a marginal observation, we can point out that even though the reactor and heat exchangers without control are very stable, closing a control loop around them with only the essential components makes the system unstable so that compensation is necessary.

This observation raises the question: since with a constant temperature program, which is favored by the reactor, the overall system may be unstable, is it really worth while to choose such a program or is it better to use a more efficient program, as for example, a constant output steam pressure program.

APPENDIX

Boiler Transfer Function with Variable Throttle Valve Opening

The thermal balance equations for the boilers are※:

$$Rc(T_{bi} - T_{bo}) = k_b A_b (T_b - T_s) \tag{1}$$

$$(M_m c_m + M_s c_s) \frac{dT_s}{dt} = k_b A_b (T_b - T_s) - k_a A p \tag{2}$$

$$p = f(T_s) \tag{3}$$

where

Rc = main coolant flow rate times heat capacity, BTU/sec-°F

T_{bi} and T_{bo} = coolant temperature at boiler inlet and outlet, °F

T_s = steam temperature, °F

k_b = equibalent effective heat transfer coefficient, BTU/sec-ft^2-°F

A_b = effective boiler heat transfer area, ft^2

M_m and M_s = mass of the boiler tube metal, and of the water and steam, lb.

c_m and c_s = specific heat of boiler tube metal, and of water and steam, BTU/lb-°F

k_a = throttle constant, BTU/sec-psia

A = relative throttle opening

p = saturated steam pressure, psia

T_b = $(T_{bi} + T_{bo})/2$

The system is described by a linear set of equations, but with variable coefficients. For small variation around an equilibrium condition, the equations (1), (2), and (3) can be written:

※ See Schultz[3], page 139.

$$Rc(T_{bi_o} + \delta T_{bi} - T_{bo_o} - \delta T_{bo}) = k_b A_b (T_{b_o} + \delta T_b - T_{s_o} - \delta T_s) \quad (4)$$

$$(M_m c_m + M_s c_s) \frac{d}{dt} (T_{s_o} + \delta T_s) = k_b A_b (T_{b_o} + \delta T_b - T_{s_o} - \delta T_s) -$$

$$- k_a (A_o p_o + A_o \delta p + p_o \delta A + \delta A \delta p) \quad (5)$$

$$\delta p = \left(\frac{dp}{dT_s}\right)_{sat, T_{s_o}} \cdot \delta T_s = B \delta T_s \quad (6)$$

Simplifying the equilibrium conditions and disregarding the products of increments $\delta A \cdot \delta p$, it can be written:

$$Rc(\delta T_{bi} - \delta T_{bo}) = k_b A_b (\delta T_b - \delta T_s) \quad (7)$$

$$(M_m c_m + M_s c_s) \frac{d \delta T_s}{dt} = k_b A_b (\delta T_b - \delta T_s) - k_a (A_o \delta p + p_o \delta A) \quad (8)$$

$$\delta p = B \delta T_s \quad (9)$$

$$\delta T_b = \frac{\delta T_{bi} + \delta T_{bo}}{2} \quad (10)$$

By eliminating δT_b and δp, and taking the Laplace transform we obtain:

$$\left(\frac{2Rc}{k_b A_b} + 1\right) \delta T_{bo} - \left(\frac{2Rc}{k_b A_b} - 1\right) \delta T_{bi} = 2 \delta T_s \quad (11)$$

$$\left[\frac{(M_m c_m + M_s c_s)}{k_b A_b} s + \left(1 + \frac{k_a A_o B}{k_b A_b}\right)\right] 2 \delta T_s = (\delta T_{bi} + \delta T_{bo}) - 2 \frac{k_a p_o}{k_b A_b} \delta A \quad (12)$$

By eliminating δT_s we obtain:

$$\left[\left(\frac{M_m c_m + M_s c_s}{k_b A_b}\right)\left(\frac{2Rc}{k_b A_b} + 1\right)s + \left(\frac{k_a A_o B}{k_b A_b} + 1\right)\left(\frac{2Rc}{k_b A_b} + 1\right) - 1\right]\delta T_{bo} =$$

$$= \left[\left(\frac{M_m c_m + M_s c_s}{k_b A_b}\right)\left(\frac{2Rc}{k_b A_b} - 1\right)s + \left(\frac{k_a A_o B}{k_b A_b} + 1\right)\left(\frac{2Rc}{k_b A_b} - 1\right) + 1\right]\delta T_{bi} -$$

$$- 2\,\frac{k_a p_o}{k_b A_b}\,\delta A \qquad (13)$$

With the introduction of suitable constants, relation (13) can be written in the form:

$$\delta T_{bo} = K_B \frac{1 + \tau_{bi} s}{1 + \tau_{bo} s}\,\delta T_{bi} - \frac{C}{1 + \tau_{bo} s}\,\delta A \qquad (14)$$

where

$$K_B = \frac{\left(\frac{2Rc}{k_b A_b} - 1\right)\left(\frac{k_a A_o B}{k_b A_b} + 1\right) + 1}{\left(\frac{2Rc}{k_b A_b} + 1\right)\left(\frac{k_a A_o B}{k_b A_b} + 1\right) - 1} \qquad (15)$$

$$\tau_{bi} = \frac{M_m c_m + M_s c_s}{k_b A_b\left[1 + \frac{k_a A_o B}{k_b A_b} + \frac{1}{\left(\frac{2Rc}{k_b A_b} - 1\right)}\right]} \qquad (16)$$

$$\tau_{bo} = \frac{M_m c_m + M_s c_s}{k_b A_b\left[1 + \frac{k_a A_o B}{k_b A_b} - \frac{1}{\left(\frac{2Rc}{k_b A_b} + 1\right)}\right]} \qquad (17)$$

$$C = \frac{2\,\frac{k_a p_o}{k_b A_b}}{\left(\frac{2Rc}{k_b A_b} + 1\right)\left(\frac{k_a A_o B}{k_b A_b} + 1\right) - 1} \qquad (18)$$

$$\left[\left(\frac{M_m c_m + M_s c_s}{k_b A_b}\right)\left(\frac{2Rc}{k_b A_b} + 1\right)s + \left(\frac{k_a A_o B}{k_b A_b} + 1\right)\left(\frac{2Rc}{k_b A_b} + 1\right) - 1\right] \delta T_{bo} =$$

$$= \left[\left(\frac{M_m c_m + M_s c_s}{k_b A_b}\right)\left(\frac{2Rc}{k_b A_b} - 1\right)s + \left(\frac{k_a A_o B}{k_b A_b} + 1\right)\left(\frac{2Rc}{k_b A_b} - 1\right) + 1\right] \delta T_{bi} -$$

$$- 2\,\frac{k_a p_o}{k_b A_b}\,\delta A \qquad (13)$$

With the introduction of suitable constants, relation (13) can be written in the form:

$$\delta T_{bo} = K_B \frac{1 + \tau_{bi} s}{1 + \tau_{bo} s}\,\delta T_{bi} - \frac{C}{1 + \tau_{bo} s}\,\delta A \qquad (14)$$

where

$$K_B = \frac{\left(\frac{2Rc}{k_b A_b} - 1\right)\left(\frac{k_a A_o B}{k_b A_b} + 1\right) + 1}{\left(\frac{2Rc}{k_b A_b} + 1\right)\left(\frac{k_a A_o B}{k_b A_b} + 1\right) - 1} \qquad (15)$$

$$\tau_{bi} = \frac{M_m c_m + M_s c_s}{k_b A_b\left[1 + \frac{k_a A_o B}{k_b A_b} + \frac{1}{\left(\frac{2Rc}{k_b A_b} - 1\right)}\right]} \qquad (16)$$

$$\tau_{bo} = \frac{M_m c_m + M_s c_s}{k_b A_b\left[1 + \frac{k_a A_o B}{k_b A_b} - \frac{1}{\left(\frac{2Rc}{k_b A_b} + 1\right)}\right]} \qquad (17)$$

$$C = \frac{2\,\frac{k_a p_o}{k_b A_b}}{\left(\frac{2Rc}{k_b A_b} + 1\right)\left(\frac{k_a A_o B}{k_b A_b} + 1\right) - 1} \qquad (18)$$

The block diagram is drawn in Fig. 1A.

For $\delta A = 0$, i.e., opening of the throttle valve fixed, the transfer function for the boiler becomes:

$$\frac{\delta T_{bo}}{\delta T_{bi}} = K_B \frac{1 + \tau_{bi} s}{1 + \tau_{bo} s} \tag{19}$$

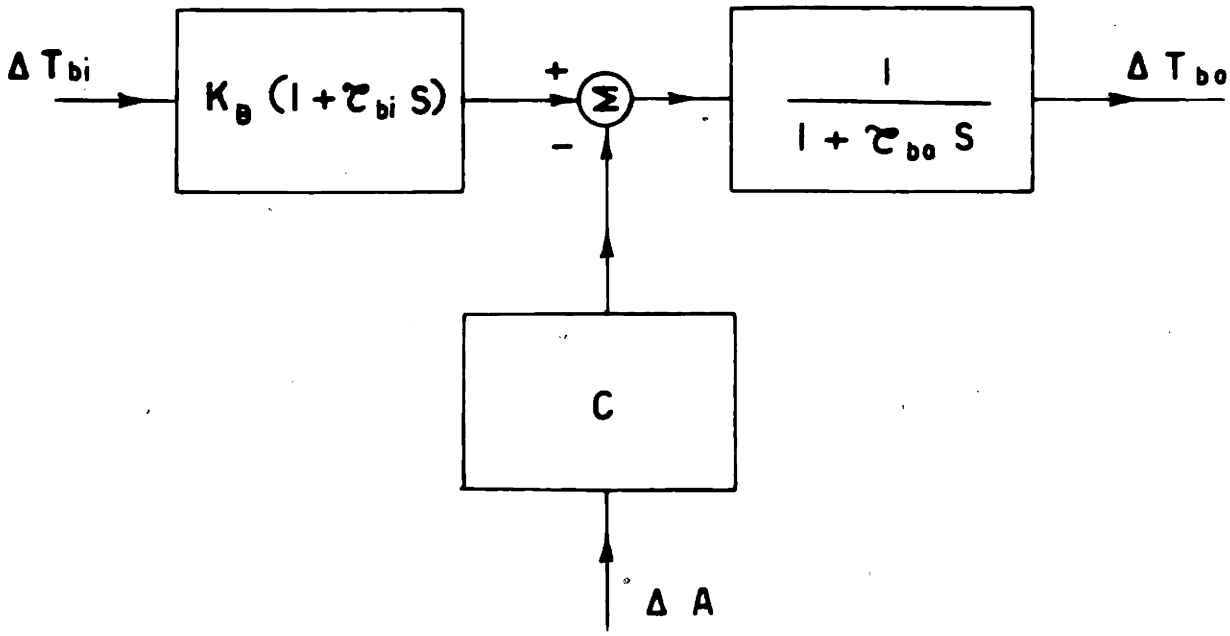

FIG. 1A

BIBLIOGRAPHY

1. "Technical Informations and Final Hazards Summary Report", USAEC – YAEC – 167, 1960.

2. Obermesser, C. F., "Thermal Stability of the Yankee Nuclear Power Plant", USAEC – YAEC – 27, May 15, 1957.

3. Schultz, M. A., "Control of Nuclear Reactors and Power Plants", McGraw-Hill, N. Y., 1955.

4. Bonilla, C. F., "Nuclear Engineering", McGraw-Hill, N. Y., 1957.

5. Balog, L. J., A. A. Bishop, and T. F. Widmer, "Design and Test Analysis of the Magnetic Jacking Positive Latch Control Rod Drive Mechanism", USAEC– YAEC – 155, July 1959.

6. Finzi, L. A. and G. C. Feth, "Magnetic Amplifiers in Bistable Operation", AIEE Trans., Vol. 74, Part I, p. 592, Nov. 1955.

7. Kochenburger, R. J., "A Frequency Response Method for Analyzing and Synthesizing Contactor Servomechanisms", AIEE Trans., Vol. 69, Part I, p. 270, 1950.

8. Truxal, J. G., Automatic Feedback Control System Synthesis, McGraw-Hill, N. Y., p. 191, 1955.